The Impact of the Stratosphere on Tropospheric Climate

Yvonne Hinssen

ISBN 978-90-393-5426-1

Institute for Marine and Atmospheric research Utrecht (IMAU)
Faculty of Science, Department of Physics and Astronomy
Utrecht University, The Netherlands

Cover: View from Laan van Vollenhove 622, Zeist, 3 August 2010.

The Impact of the Stratosphere on Tropospheric Climate

De invloed van de stratosfeer op het troposferische klimaat

(met een samenvatting in het Nederlands)

PROEFSCHRIFT

ter verkrijging van de graad van doctor aan de Universiteit Utrecht
op gezag van de rector magnificus, prof.dr. J.C. Stoof,
ingevolge het besluit van het college voor promoties
in het openbaar te verdedigen op

woensdag 15 december 2010 des middags te 12.45 uur

door

Yvonne Bernadette Louisa Hinssen

geboren op 17 september 1983 te Wageningen

Promotor: **Prof.dr.ir. J. D. Opsteegh**
Co-promotor: **Dr. A. J. van Delden**

Of het gaat goed, of ik leer.
Either it is going well, or I'm learning.

(Femke Wiersma, bron: dagelijksegedachte.net)

Contents

Samenvatting **1**

Abstract **7**

1 Introduction **9**
1.1 The stratosphere 10
1.2 Potential vorticity 21
1.3 This thesis 35

2 Stratospheric impact on tropospheric winds deduced from potential vorticity inversion in relation to the Arctic Oscillation **39**
2.1 Introduction 40
2.2 Data 41
2.3 The Arctic Oscillation and potential vorticity 42
2.4 Effect of stratospheric PV on tropospheric winds 47
2.5 Conclusion 53

3 The seasonal cycle of the potential vorticity distribution in the stratosphere **55**
3.1 Introduction 56
3.2 Data 58
3.3 Seasonal cycle of the stratospheric potential vorticity 60
3.4 Conclusions 75

4 Relation between the 100 hPa heat flux and stratospheric potential vorticity **79**
4.1 Introduction 80
4.2 Physical basis 81
4.3 Data 84
4.4 The climatological PV-flux relation 85
4.5 The PV-flux relation applied to the 2008/2009 winter 88

4.6 Sensitivity studies 91
4.7 Conclusions 94

5 Influence of the 2009 sudden stratospheric warming on the tropospheric winds 97
5.1 Introduction 98
5.2 Data 100
5.3 PV inversions 101
5.4 Conclusions 106

6 The influence of the stratosphere on the tropospheric zonal wind response to CO_2 doubling 109
6.1 Introduction 110
6.2 Data 111
6.3 Stratospheric PV changes 114
6.4 Stratospheric influence on the troposphere 118
6.5 Conclusions 124

7 General conclusions and outlook 127
7.1 General conclusions 128
7.2 Connection between the chapters 130
7.3 Remaining questions 132

Bibliography 135

Bedankt - Thank you 147

Curriculum Vitae 149

Publications 150

Samenvatting

- ⋆ -

Klimaatverandering speelt niet alleen in de troposfeer, waar het dagelijkse weer zich afspeelt, een rol, maar ook in de hoger gelegen stratosfeer. De stratosfeer is de luchtlaag tussen ongeveer 10 en 50 km hoogte. In de stratosfeer bevindt zich de ozonlaag, een laag met hoge concentraties ozon tussen zo'n 15 en 30 km hoogte, die verhindert dat schadelijke ultra violette (uv) straling van de zon het aardoppervlak bereikt. De troposfeer wordt van onderaf verwarmd, doordat het aardoppervlak zonnestraling absorbeert en deze als langgolvige warmtestraling weer uitzendt naar de atmosfeer, waar deze deels door broeikasgassen wordt geabsorbeerd. De stratosfeer, daarentegen, wordt van bovenaf verwarmd, waar uv straling van de zon wordt geabsorbeerd door ozon. Deze stralingseffecten zorgen ervoor dat de temperatuur in de stratosfeer toeneemt met de hoogte, terwijl de temperatuur in de troposfeer afneemt met de hoogte.

Een toename van het broeikasgas koolstofdioxide (CO_2) leidt in de troposfeer tot een temperatuurstijging, doordat meer infrarode straling wordt vastgehouden in de troposfeer. Een CO_2 toename in de stratosfeer leidt echter tot een afkoeling van de stratosfeer, omdat vooral de uitstraling naar de ruimte toeneemt. Ook een verandering in ozon heeft invloed op de temperatuur in de stratosfeer. Neemt de ozonconcentratie af, dan neemt de temperatuur ook af, omdat er minder zonnestraling wordt geabsorbeerd. Chemische reacties met door mensen gemaakte chloorfluorkoolstoffen (CFK's) leidden de afgelopen decennia tot ozon-afbraak. De verwachting voor de toekomst is dat de ozonconcentraties zich weer zullen herstellen, omdat de uitstoot van CFK's is teruggedrongen en deze deeltjes langzaam uit de atmosfeer verdwijnen. Veranderingen in CO_2 en in ozon zullen beide bijdragen aan veranderingen in de temperatuur en circulatie in de stratosfeer. Om deze toekomstige veranderingen te kunnen voorspellen en begrijpen is het van belang te onderzoeken welke processen in de stratosfeer belangrijk zijn en hoe deze de huidige toestand van de stratosfeer bepalen.

Als de temperatuur plaatselijk verandert, raakt de atmosfeer uit evenwicht. De atmosfeer zal proberen evenwicht te herstellen door aanpassing van de circulatie en herverdeling van de warmte. Hoewel de circulatie in de stratosfeer drie dimensionaal is, geeft de zonaal gemiddelde toestand als functie van de hoogte en de breedtegraad

een goed beeld van de grootschalige stroming in de stratosfeer. Het zonaal gemiddelde wordt bepaald door langs een breedtecirkel te middelen. De stratosferische circulatie wordt gedomineerd door de polaire vortex. Dit is een groot lagedrukgebied dat in de herfst ontstaat als het polaire gebied geen zonlicht meer ontvangt. Er is nu geen absorptie van zonnestraling door ozon, maar de uitzending van straling door broeikasgassen gaat gewoon door, waardoor de polaire stratosfeer afkoelt. In de lente breekt de polaire vortex op doordat absorptie van zonnestraling door ozon de stratosfeer opwarmt. Het grote temperatuurverschil tussen de pool en de tropen in de winter is via thermisch wind evenwicht gekoppeld aan sterke westenwinden op de gematigde breedtes rondom de pool in de stratosfeer, ook wel de polaire jet genoemd. In de zomer is de pool relatief warm en komen er oostenwinden voor in de stratosfeer rondom de pool.

In plaats van apart naar de temperatuur en de wind te kijken, is het ook mogelijk de potentiële vorticiteit (PV) te bekijken. Potentiële vorticiteit is gedefinieerd als het product van de vorticiteit en de statische stabiliteit, en een luchtpakketje volgend kan deze alleen door diabatische of wrijvingsprocessen veranderen. De vorticiteit van een luchtpakketje is gerelateerd aan de circulatie of rotatie van de lucht, welke wordt veroorzaakt door de draaiing van de aarde, en door de rotatie van de lucht ten opzichte van de aarde. De potentiële vorticiteit is een behouden grootheid voor adiabatische en wrijvingloze processen. Bij adiabatische processen vind er geen uitwisseling van warmte plaats tussen het luchtpakketje en de omgeving, terwijl dit bij diabatische processen wel het geval is. Adiabatische opwarming in de atmosfeer vindt plaats als dalende lucht wordt samengedrukt, zonder dat er warmte aan wordt toegevoegd of van onttrokken, dus bijvoorbeeld zonder dat er waterdamp condenseert (waarbij warmte vrij zou komen) of water verdampt (waar warmte voor nodig zou zijn). Onder dezelfde omstandigheden vindt adiabatische afkoeling plaats als een luchtmassa opstijgt. In het geval van een verhoging van de CO_2 concentratie van een luchtpakketje zal de absorptie en emissie van straling door dit luchtpakketje veranderen, omdat er uitwisseling van warmte met de omgeving is, is dit een diabatisch proces. De potentiële vorticiteit zal hierdoor veranderen.

Een verandering in PV is via het invertibiliteitsprincipe gerelateerd aan veranderingen in de wind. Het invertibiliteitsprincipe zegt dat, samen met een balansconditie voor de atmosfeer en geschikte randvoorwaarden, alle dynamische velden kunnen worden bepaald uit de PV. Verder kan een lokale verandering in PV het windveld over een groter gebied beïnvloeden. Met behulp van het invertibiliteitsprincipe kan er dus gekeken worden hoe veranderingen in de stratosferische PV de wind in de troposfeer beïnvloeden. Dit is niet direct uit windmetingen af te leiden, en kan informatie geven over de rol van de stratosfeer in het klimaat.

Als een toename van broeikasgassen de PV beïnvloedt, zou je hier in metingen van de afgelopen 50 jaar misschien al iets van kunnen zien. Het blijkt echter moeilijk om

iets te zeggen over de trend in de PV over de afgelopen decenia, door de grote variabiliteit van jaar tot jaar. Een groot deel van de variabiliteit in de winter op het noordelijk halfrond hangt samen met de Arctische Oscillatie (AO), welke een maat is voor het drukverschil tussen de pool en de subtropen. Is dit drukverschil groter dan normaal, dan is de AO index positief en hebben we in West-Europa te maken met extra sterke westenwinden. Deze westenwinden voeren relatief warme lucht vanaf de oceaan aan, en zorgen voor zachte winters. De variabiliteit in de winter AO index is ook groot, maar laat toch een positieve trend zien van de jaren 1960 tot de jaren 1990. Als deze trend in de toekomst doorzet, zullen januarimaanden met een gemiddeld positieve AO index meer voor gaan komen. Het is daarom interessant om naar het verschil tussen januarimaanden met een gemiddeld positieve AO index en januarimaanden met een gemiddeld negatieve AO index te kijken. Dit wordt gedaan in hoofdstuk 2 van dit proefschrift. Er blijkt een duidelijk verschil in stratosferische PV te zijn tussen deze twee gevallen, met een hogere polaire PV voor de jaren met een positieve AO index. Het invertibiliteitsprincipe is vervolgens gebruikt om te onderzoeken in hoeverre het windverschil tussen januarimaanden met een positieve AO index en januarimaanden met een negatieve AO index verklaard kan worden met de verschillen in stratosferische PV. Voor een gemiddelde januari heeft de stratosferische PV een westelijke invloed op de troposferische wind op de gematigde en hoge breedtes. Gedurende januarimaanden met een negatieve AO index is deze westelijke invloed kleiner dan gemiddeld, terwijl de westelijke invloed van de stratosfeer juist groter dan gemiddeld is voor een positieve AO index. De verschillen in stratosferische PV verklaren vooral de stratosferische windverschillen, maar ook een deel ($\sim 20\%$) van het troposferische windverschil.

Om een idee te krijgen welke processen van invloed zijn op de PV, worden in hoofdstuk 3 de seizoenscyclus en de verschillen tussen het noordelijk halfrond en het zuidelijk halfrond bestudeerd. Op basis van het invertibiliteitsprincipe kan de PV gesplitst worden in een referentietoestand, welke samenhangt met de rusttoestand, en een PV anomalie, welke samenhangt met het windveld. Het is de PV anomalie die in dit proefschrift bestudeerd wordt. Door de referentietoestand van de PV af te trekken onstaat een duidelijker beeld van de seizoenscyclus, welke sterk samenhangt met stralingseffecten. Een positieve PV anomalie vormt zich boven de pool in de herfst en winter door afkoeling in de polaire nacht en verdwijnt weer in het voorjaar door absorptie van zonnestraling door ozon. De polaire PV anomalie is negatief in de zomer.

De vorming van de polaire vortex in de herfst gaat op beide halfronden ongeveer gelijk. Door stroming over bergen en door warmteverschillen tussen land en zee kunnen in de troposfeer atmosferische golven worden opgewekt die zich in horizontale en verticale richting voortplanten. Deze golven bewegen omhoog door westelijke stromingen. In de winter is de stroming in de stratosfeer over het algemeen westelijk,

zodat golven de stratosfeer kunnen bereiken. Door de afname van de luchtdichtheid met de hoogte neemt de golfamplitude toe, en zullen de golven op een gegeven moment breken en de westelijke stroming verstoren. Door de land-zee-verdeling komen er op het noordelijk halfrond meer golven voor dan op het zuidelijk halfrond. De polaire vortex op het noordelijk halfrond wordt dan ook gedurende de hele winter verstoord door golven, wat resulteert in een zwakkere vortex op het noordelijk halfrond vergeleken met de minder verstoorde vortex op het zuidelijk halfrond. De koudere en sterkere polaire vortex op het zuidelijk halfrond zorgt voor (meer) ozonafbraak. Lagere ozonconcentraties in het polaire gebied zorgen voor een later opbreken van de polaire vortex op het zuidelijk halfrond vergeleken met het noordelijk halfrond, vooral in de lagere stratosfeer. In de zomer voorkomt de oostelijke stroming in de stratosfeer op beide halfronden dat golven de stratosfeer bereiken, waardoor de verschillen tussen de halfronden in dit seizoen klein zijn.

Door de grotere golfactiviteit is de stratosferische variabiliteit van jaar tot jaar op het noordelijk halfrond groter dan op het zuidelijk halfrond. Het blijkt dat de polaire PV anomalie sterk gerelateerd is aan de golfforcering van de stratosfeer in de periode ervoor. Hoofdstuk 4 laat zien dat gemiddeld zo'n 50% van de variabiliteit in de stratosferische polaire PV op het noordelijk halfrond verklaard kan worden met de variabiliteit in de golfforcering. Voor hele sterke verstoringen van de stratosfeer, zoals de zogenoemde 'major sudden stratospheric warming' (ofwel plotselinge stratosferische opwarming, afgekort 'SSW') in januari 2009, kan dit percentage zelfs oplopen tot boven de 80%.

Tijdens een SSW warmt de polaire stratosfeer met tientallen graden op binnen een paar dagen. Hierdoor verandert de temperatuurgradiënt tussen de gematigde breedtes en de pool van teken. Dat gaat via aanpassing aan thermisch wind evenwicht gepaard met een omdraaiing van de gemiddelde windrichting van een westelijke in een oostelijke stroming rondom de pool. De grote veranderingen in de stratosfeer rond een SSW zijn ook duidelijk zichtbaar in de PV. De PV- en windveranderingen rond de SSW in januari 2009 worden in hoofdstuk 5 bestudeerd. De PV anomalie is positief voor het optreden van de SSW, terwijl er negatieve PV anomalie waarden voorkomen na de SSW, in het bijzonder in de lagere stratosfeer. Toepassing van PV inversie volgens het invertibiliteitsprincipe op de stratosferische PV resulteert in een westelijke invloed van de stratosfeer op de troposferische winden voor de SSW en een oostelijke invloed na de SSW. De veranderingen in de stratosfeer zorgen voor een verschil van zo'n 5 m s^{-1} in de troposferische wind op de gematigde tot hoge breedtes. Deze veranderingen vormen een aanzienlijke bijdrage aan het totale troposferische windverschil dat gedurende deze periode is waargenomen. Dit geeft aan dat de stratosfeer de troposferische condities beïnvloedt en zorgt voor een verzwakking van de westelijke winden of zelfs een omslag naar oostelijke winden door het optreden van de SSW in januari 2009. Vergelijking van de winter 2008/2009 met een minder verstoorde winter

(1996/1997) laat zien dat de invloed van de SSW in de troposfeer en lagere stratosfeer weken tot maanden na de SSW nog zichtbaar is. Zo werd in maart 2009 een oostelijke invloed van de stratosfeer van zo'n 2 m s^{-1} gevonden, terwijl een westelijke invloed van dezelfde orde van grootte gevonden werd bij afwezigheid van een SSW in maart 1997. Een correcte weergave van de stratosferische variabiliteit in modellen zou dus kunnen bijdragen aan een verbetering van de weersverwachting op de langere termijn (maand- of seizoensverwachtingen).

In hoofdstuk 6, tenslotte, wordt de invloed van een toename van broeikasgassen op de stratosferische PV bekeken in twee klimaatmodellen. PV inversie wordt gebruikt om te onderzoeken in hoeverre de troposferische windrespons op CO_2-verdubbeling gerelateerd kan worden aan veranderingen in de stratosferische PV. Door CO_2-verdubbeling neemt de stratosferische PV op het zuidelijk halfrond in de winter toe, door versterkte uitstraling van warmte naar de ruimte. De PV neemt het sterkst toe rond de gematigde breedtes, aan de rand van de polaire vortex. Als gevolg hiervan versterkt de westelijke invloed van de stratosfeer op de troposferische winden op gematigde breedte in augustus, in beide klimaatmodellen. Op het noordelijk halfrond zorgt CO_2-verdubbeling juist voor een afname van de polaire PV aan het eind van de winter, gerelateerd aan een toegenomen golfforcering. Deze PV-afname zorgt voor een verzwakking van de westelijke invloed van de stratosfeer op de troposferische winden op hoge breedtegraden. In het ene model is de afname in PV echter beperkt tot hoger in de stratosfeer dan in het andere model en wordt een versterking van de westelijke invloed op gematigde breedtes in de troposfeer gevonden, samenhangend met een PV-toename op gematigde breedtes in de lagere stratosfeer. Dit laat zien dat de invloed van de stratosfeer op de troposferische respons op klimaatverandering erg gevoelig is voor de PV veranderingen in de lagere stratosfeer door zowel stralings- als dynamische effecten. De troposferische windrespons als gevolg van de stratosferische PV veranderingen is van de orde van 0.5 tot 1 m s^{-1}. De totale troposferische respons heeft een andere structuur, maar is van dezelfde grootte. Dit laat zien dat de veranderingen in de stratosfeer effect kunnen hebben op de troposferische respons op CO_2-verdubbeling en dat het van belang is de stratosferische veranderingen in klimaatmodellen mee te nemen.

Abstract

The stratospheric potential vorticity (PV) field in the current climate, its variations around the occurrence of a sudden stratospheric warming, and possible future changes are examined.

The PV presents a compact way to describe the state of the atmosphere, and is linked to all other dynamical fields through the invertibility principle. Local changes in the PV have a nonlocal effect on the wind field, so that changes in the stratospheric PV can be related to circulation changes in the troposphere, making it possible to study the role of the stratosphere in climate.

The seasonal cycle of the stratospheric polar cap PV anomaly (the PV anomaly is defined as that part of the PV that induces a wind field according to the PV inversion equation) is related to radiative effects. A positive polar PV anomaly forms in autumn and winter due to radiative cooling in the polar night, and vanishes in spring due to absorption of solar radiation by ozone.

The formation of the vortex in autumn is similar for the Northern Hemisphere (NH) and the Southern Hemisphere (SH), but atmospheric waves affect the NH stratosphere throughout winter, weakening the vortex compared to the less disturbed SH vortex. The stronger and colder SH vortex allows for (more) ozone depletion in spring, leading to a delayed break up of the SH vortex. In summer, the easterly stratospheric flow prohibits wave propagation to the stratosphere in both hemispheres, resulting in small interhemispheric differences.

Wave forcing of the stratosphere from below can not only explain interhemispheric differences, but also the interannual variability of the winter stratosphere. On average, about 50% of the interannual variability in the state of the stratosphere that is observed in the NH can be explained by the interannual variations in the 100 hPa heat flux, which is a measure of the wave forcing of the stratosphere.

For the monthly mean climatology, the influence of the stratosphere on the tropospheric winds is small, but for individual winters the influence can be substantial, on monthly as well as daily timescales. The stratospheric changes that accompanied the major sudden stratospheric warming in January 2009, for example, resulted in an easterly wind forcing of about 5 m s^{-1} on the tropospheric winds. Furthermore, the

influence of the stratosphere on the tropospheric winds was felt until months after the warming event, indicating that inclusion of stratospheric processes in models might improve extended range weather forecasts.

Due to CO_2 increases, the SH stratospheric PV increases in winter, related to enhanced stratospheric emission of longwave radiation to space. In the NH, CO_2 increases are associated with a decrease in the stratospheric polar PV in winter, related to an increased stratospheric wave forcing.

The stratospheric changes that result from CO_2 increases in a climate model also influence the tropospheric winds. Although the magnitude of the tropospheric response related to stratospheric changes is small, it is of the same order of magnitude as the total tropospheric response, indicating that changes in the stratosphere can certainly modify the tropospheric response to climate change.

1

Introduction

- ⋆ -

The stratosphere contains only a fraction (about 15%) of the mass of the underlying troposphere. Therefore, it was long believed that the coupling between the troposphere and the stratosphere was a one way effect of the troposphere influencing the stratosphere. However, over the last few decades, confidence grew that this is in fact a two way interaction, where changes in the stratosphere can feed back on the state of the troposphere. Improved understanding of the stratosphere can then lead to improved forecasts of the tropospheric weather and climate. For this, it is important to determine which processes affect the state of the stratosphere, and on what timescales. In this chapter, the stratosphere, its climate, and the coupling between the stratosphere and the troposphere are described. An introduction is presented on the dynamical, chemical and radiative processes that together determine the state of the stratosphere. Furthermore, an outline of the thesis is presented.

1.1 The stratosphere

1.1.1 What is the stratosphere?

The stratosphere is the atmospheric layer between approximately 10 and 50 km height (or 100 - 1 hPa in pressure), and it is located between the troposphere below and the mesosphere above. The boundary between the troposphere and the stratosphere is called the tropopause and the stratosphere and mesosphere are separated by the stratopause. The height of the tropopause varies from about 8 km near the poles to about 15 km in the tropics.

An important characteristic of the stratosphere is the increase of temperature with height, which is illustrated in Fig. 1.1 for the January mean, global mean temperature. This temperature increase is related to the absorption of solar ultra violet (uv) radiation by ozone, which has its highest mixing ratio in the stratosphere. In the troposphere, on the other hand, temperature decreases with height, and the change in vertical temperature gradient is a way to define the tropopause.

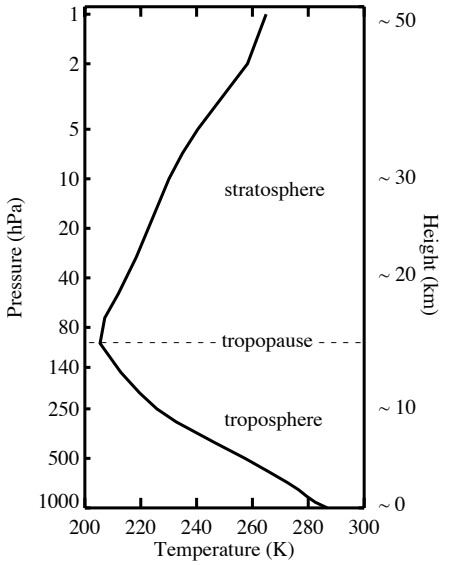

Figure 1.1: *January mean, global mean temperature (K) as a function of height, derived from the European Centre for Medium-range Weather Forecasts (ECMWF) ERA-40 reanalysis monthly mean temperature data, averaged over the years 1958-2002.*

The stratospheric climate is mainly controlled by the radiative balance between heating through absorption of solar radiation by ozone and cooling through emission of thermal radiation by greenhouse gases like carbon dioxide (*Schoeberl and Hart-*

mann, 1991).

1.1.2 Why is the stratosphere important in climate research?

The stratosphere is important in climate, since it contains the ozone layer, which is a layer with high ozone concentrations. Maximum ozone concentrations are found in the lower to middle stratosphere, between about 15 and 30 km height. The ozone layer is important for life on Earth, because it absorbs harmful solar uv radiation before it can reach the surface. However, chemical reactions with chlorofluorocarbons (CFCs) can lead to depletion of ozone. An ozone hole, meaning substantially reduced ozone concentrations, is indeed observed since the 1980s, especially over the south pole in spring. The ozone hole is clearest over the south pole, since the ozone depleting chemical reactions occur on polar stratospheric clouds (e.g., *Brune et al.*, 1991; *Schoeberl and Hartmann*, 1991). These polar stratospheric clouds form at very low temperatures, which are observed over the south pole much more frequent than over the north pole. Furthermore, sunlight is needed for the reaction, which is why the ozone hole is present in spring, and not in winter. CFCs were used, for example, as refrigerants or solvents, but due to the Montreal Protocol that entered into force in 1989, the manufacture of such compounds is being phased out, and the ozone layer is expected to recover this century. Dynamical, chemical and radiative processes affect the distribution and depletion of ozone. Additionally, changes in climate over the coming century will affect the recovery of ozone (*Shepherd*, 2008). It is therefore important to understand the current climate of the stratosphere and how this might change due to increases in greenhouse gases.

More recently, it has also been recognized that the stratosphere can influence weather and climate in the troposphere, and even at the surface (this is further discussed in section 1.1.6). When considering the effect of an increase in greenhouse gases on the climate, it is thus important to take the stratosphere into account.

1.1.3 What is the global circulation in the stratosphere?

Only the combination of low temperatures and solar radiation can lead to substantial ozone depletion, which highlights the importance of understanding the state of the stratosphere and its seasonal cycle. The circulation in the stratosphere varies with height, latitude and longitude, but the largest variations are in height and latitude (*Haynes*, 2005). A way to examine the variations in height and latitude is by examining the zonal mean. The zonal mean is obtained by calculating the average over all longitudes along a certain latitude circle. It is interpreted as if the zonal mean wind at each latitude is flowing symmetrically around the pole. The January mean, zonal mean, zonal wind in the Northern Hemisphere is shown in Fig. 1.2, clearly showing the subtropical jet in the upper troposphere, and the polar jet in the stratosphere.

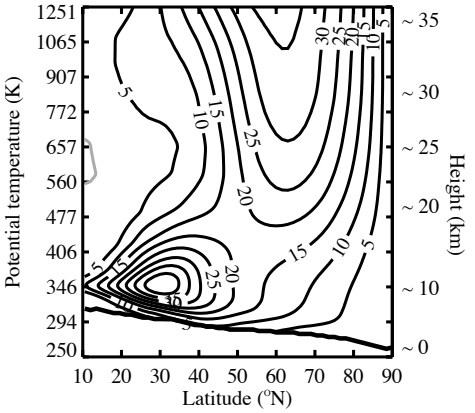

Figure 1.2: *January mean, zonal mean, zonal wind (m s^{-1}) as a function of height and latitude for the Northern Hemisphere, derived from the European Centre for Medium-range Weather Forecasts (ECMWF) ERA-Interim reanalysis daily wind data, averaged over the years 1989-2008. The potential temperature is the temperature an air parcel would have if it was adiabatically brought to sea level, without exchange of heat with the surroundings. The potential temperature can be used as a vertical coordinate when it increases monotonically with height, which is the case in the stratosphere due to the increase of temperature with height. Logarithmic scaling is used for the potential temperature axis in this and following figures. Contours are shown every 5 m s^{-1} with the zero line omitted and negative values indicated by grey lines. The thick line near the bottom represents the surface. The slope of the surface with latitude is due to the temperature increase from around 250 K near the pole to 300 K in the tropics.*

The state of the stratosphere and its seasonal cycle are largely driven by radiation. The seasonal cycle is greatly influenced by the occurrence of the polar night, when the winter pole does not receive solar radiation, but there is still emission of longwave radiation to space. This leads to cooling of the polar cap, and an increased horizontal temperature gradient between the pole and the tropics. A balance that is found in the stratosphere is thermal wind balance, which relates the horizontal temperature gradient to the vertical gradient in zonal wind. Through the thermal wind relation an increased horizontal temperature gradient is related to a band of increased westerly winds (meaning from the west, or eastward) around the pole in the midlatitudes. These winds are also referred to as the polar jet, and the whole cyclone system centered over the pole is called the polar vortex, illustrated for both hemispheres in Fig. 1.3. In spring, absorption of solar radiation by ozone heats the polar stratosphere, reducing the horizontal temperature gradient. The polar vortex vanishes, and weak easterly winds are found in the stratosphere in summer.

The large scale meridional (north-south) circulation in the stratosphere, referred to as the Brewer-Dobson circulation, consists of a hemispheric-scale cell, with rising air in the tropics, and sinking air over the winter pole. Tropospheric air thus enters

the stratosphere mainly in the tropics, and then moves poleward in the stratosphere (*Shepherd*, 2000). As explained below, this circulation is driven by wave motions in the atmosphere. Due to this meridional overturning circulation, temperatures over the winter pole are much higher than the radiative equilibrium temperatures that would be obtained if the polar atmosphere was free to cool radiatively during the winter season (*Schoeberl and Hartmann*, 1991).

1.1.4 What is the difference between the Northern and the Southern Hemisphere?

There are large differences between the polar stratosphere in the Northern Hemisphere (NH) and in the Southern Hemisphere (SH). The SH polar vortex is much less disturbed than its NH counterpart. The SH vortex is therefore larger and more zonally symmetric (see Fig. 1.3), with higher wind speeds in the polar jet at the edge of the polar vortex. As noted above, the large-scale circulation in the stratosphere is dominated by a zonally symmetric mean flow that is westerly in winter and easterly in summer. Superposed on this zonal mean flow are longitudinally varying wave perturbations, referred to as Rossby waves or planetary waves. Planetary waves are primarily forced by topography and land-sea contrast, and these are much stronger in the NH than in the SH.

Planetary waves can only propagate vertically if the waves propagate westward relative to the mean wind (*Charney and Drazin*, 1961; *Holton*, 1980). Planetary waves tend to be quasi-stationary, because their main forcing mechanisms are stationary (*Shepherd*, 2002). Stationary waves can thus only propagate upward when the mean wind is westerly. Upward propagating planetary waves have westward phase speeds relative to the local wind, and carry westward angular momentum. As waves propagate upward they grow in amplitude due to the decrease of density with height, and eventually they break down. The waves deposit the angular momentum that they are carrying where they break (*Shepherd*, 2000). This implies a westward force on the large-scale flow where the breaking takes place (*Haynes*, 2005), resulting in a deceleration of the westerly zonal wind. Change of just the zonal wind by the wave drag would violate thermal wind balance. Therefore, also a meridional circulation is induced, with rising motion in the tropics and sinking motion over the pole, thereby adiabatically warming the pole to maintain thermal wind balance (*Shepherd*, 2002). Relative to the SH winter, the NH winter has a greater angular momentum deposition, and consequently a stronger poleward branch of the Brewer-Dobson circulation (*Shepherd*, 2000). This leads to stronger downwelling over the pole, a warmer polar stratosphere and a weaker polar vortex in the NH winter than in the SH winter. Since the meridional overturning circulation in the stratosphere is wave-driven, it is mainly restricted to the winter season, when upward propagation of waves is permitted by the

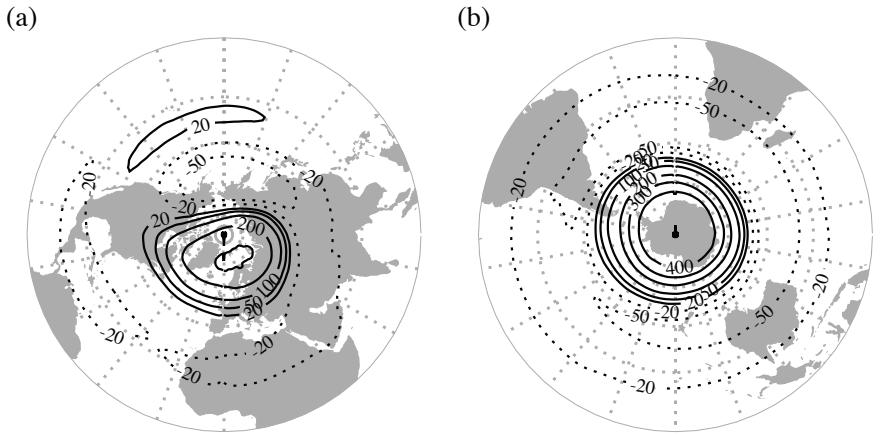

Figure 1.3: *Climatological polar vortex for (a) January in the Northern Hemisphere and (b) July in the Southern Hemisphere, in the mid-stratosphere at the 800 K level (∼ 30 km), derived from the daily ECMWF ERA-Interim reanalysis data, averaged over the years 1989-2008. Shown are the potential vorticity anomaly values (explained in section 1.2.2, minus the SH values are shown for comparison with the NH), with a contour interval of 100 potential vorticity units (PVU, 1 PVU = 10^{-6} K m^2 kg^{-1} s^{-1}), with the ± 20 and 50 PVU contours added, the zero contour omitted and negative values indicated by dashed lines. The positive potential vorticity anomaly values over the pole can be associated with the polar vortex. A positive potential vorticity anomaly at the pole is associated with westerly winds around the pole, where the wind maximum, also referred to as the polar jet, is found near the edge of the positive potential vorticity anomaly.*

westerly flow (*Shepherd*, 2002).

The Brewer-Dobson circulation transports more ozone from the tropics to the polar stratosphere in the NH winter, leading to interhemispheric ozone differences. Even before the occurrence of the ozone hole, this resulted in springtime ozone concentrations that were lower in the Antarctic than in the Arctic (*Shepherd*, 2000). These interhemispheric differences are enhanced by radiative and chemical feedbacks, since more ozone leads to more heating in spring, and higher temperatures lead to less ozone depletion. Ozone depletion is therefore more likely to occur in the colder SH polar stratosphere, which leads to lower spring ozone concentations and a delayed break up of the polar vortex in the SH compared to the NH. The difference in planetary wave generation can thus explain a large part of the asymmetry between the hemispheres in the stratosphere.

1.1.5 What is the variability in the stratospheric circulation?

Besides causing interhemispheric differences, wave effects are also responsible for the interannual variability in the polar vortices. The land-sea configuration is not only more favourable of wave excitation in the NH than in the SH, but also leads to a much

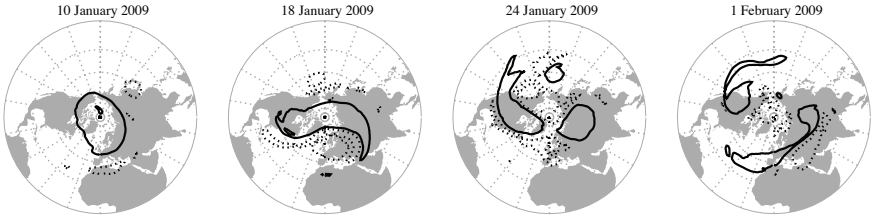

Figure 1.4: *Daily polar vortex on 10 January, 18 January, 24 January and 1 February 2009 in the Northern Hemisphere, at the 800 K level (∼ 30 km), as indicated by the potential vorticity anomaly values (see section 1.2.2), derived from the ECMWF ERA-Interim reanalysis daily data. Only the ± 100 PVU contour are plotted (negative values indicated by dashed lines), to indicate the structure and variability of the polar vortex around the occurrence of a major sudden stratospheric warming in January 2009. On 10 January the vortex is centred at the pole, on 18 January the vortex is strongly elongated and by 24 January the vortex has split, with two main vortex centres with positive potential vorticity anomaly values. These two centres are still visible on 1 February.*

larger interannual variability in waves in the NH.

A wave event that distorts the vortex in such a way that at a latitude of 60° and a height of 10 hPa the zonal winds switch from westerlies to easterlies and the meridional temperature gradient is reversed (with temperature increasing toward the pole), is called a major Sudden Stratospheric Warming (SSW). It is associated with a large increase in the polar stratospheric temperature of tens of kelvins within a few days. As illustrated in Fig. 1.4, the polar vortex is highly deformed during an SSW. Two types of SSWs are distinguished: vortex displacements, where the vortex is displaced from the pole, and vortex splits, where the vortex splits in two, which is the case in the example shown in Fig. 1.4 for January 2009. On average SSWs occur every other winter, but there are winters during which two SSWs occur. In the early 1990s there was a nine year period without SSWs (*Charlton and Polvani*, 2007), while there were seven SSWs in the six year period including the winters of 1998/1999 to 2003/2004 (*Manney et al.*, 2005), so the variability is large.

SSWs do not occur during summer, since waves only propagate up through westerly flow, and in summer the stratospheric flow is easterly (*Charney and Drazin*, 1961). Upward wave propagation is also prohibited for small scale waves, so only large scale waves can propagate into the stratosphere. Disturbances in the winter stratosphere are therefore of much larger scale than, for example, high and low pressure systems in the troposphere (*Haynes*, 2005).

In general, the Arctic polar stratosphere is frequently disturbed by SSWs, while the Antarctic vortex is much more stable and the vortex air well isolated (*Shepherd*, 2000). In 2002, however, the first SH SSW was observed (*Charlton et al.*, 2005b), so the occurrence of SSWs is not necessarily restricted to the NH.

SSWs are believed to be forced from the troposphere, by upward propagating

waves. Enhanced upward propagation of planetary scale waves before SSWs is found in observations (*Charlton and Polvani*, 2007) as well as in model studies (*Yoden et al.*, 1999). However, the effect of an SSW might feed back on the tropospheric circulation. An SSW is related to large changes in the stratosphere, leading to a deviation from thermal wind balance, and adjustment of the atmosphere to thermal wind balance leads to nonlocal wind changes. The effect of changes in the stratosphere on the wind in the troposphere, for an SSW that occurred in January 2009, is studied in this thesis (Chapter 5).

1.1.6 What is the connection between the stratosphere and the troposphere?

In the past decades, Western Europe has experienced rather warm winters. This was partly caused by an increase in the frequency of westerly winds in winter (*Hartmann et al.*, 2000), advecting relatively mild air from the Atlantic Ocean over Europe. A change in surface winds over Western Europe might be related to changes in the Arctic Oscillation (AO) or the North Atlantic Oscillation (NAO). The AO is a dominant pattern of natural climate variability in the mid- to high latitudes of the NH in winter (*Thompson and Wallace*, 1998). A positive AO index is associated with a larger north-south pressure difference leading to stronger than normal westerly winds and warm winters over Europe. A negative AO index has the opposite effect. The NAO index is strongly related to the AO index, but based on the North Atlantic region rather than the hemispheric scale surface pressure distribution (*Thompson and Wallace*, 1998; *Greatbatch*, 2000). The (N)AO index is a quantitative measure of the strength of the surface westerlies at midlatitudes (*Hurrell*, 1995; *Greatbatch*, 2000).

Studies of the time-series of the (N)AO index indicate a positive trend from the 1970s to the mid 1990s (*Hurrell*, 1995; *Hurrell et al.*, 2001; *Thompson and Wallace*, 1998; *Uppenbrink*, 1999; *Visbeck et al.*, 2001; *Thompson et al.*, 2000). The variability of the winter mean AO index from the 1960s to 2002 is shown in Fig. 1.5. A more positive (N)AO index is consistent with the occurrence of mild winters in Europe. Despite the large natural variability of the (N)AO, external forcings like increasing greenhouse gas concentrations, stratospheric ozone depletion, natural changes in volcanic activity and solar irradiance are also believed to have affected the (N)AO index during recent decades (*Fyfe et al.*, 1999; *Shindell et al.*, 1999, 2001; *Osborn*, 2004, 2006; *Rind et al.*, 2005). However, several studies find that the late twentieth century (N)AO extremes are within the range of variability during earlier centuries (*Luterbacher et al.*, 2002), and can be internally generated within the coupled atmosphere-ocean system without external forcing (*Semenov et al.*, 2008). Furthermore, the positive trend in the (N)AO index from the 1960s to the early 1990s has not continued into the 21st century (*Osborn*, 2004, 2006; *Overland and Wang*, 2005). So whether or not anthropogenic effects lead to a change in the (N)AO state remains to be seen, when longer time series

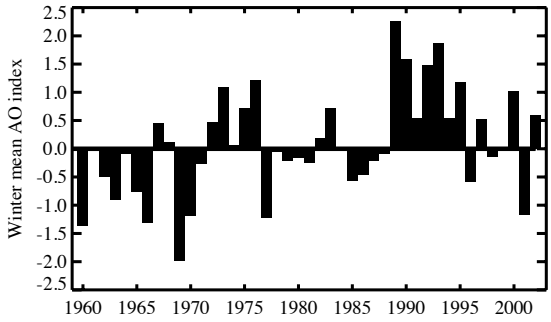

Figure 1.5: *Winter mean (November to March) AO index as a function of time (years), based on the monthly AO index from the National Centers for Environmental Prediction/National Center for Atmospheric Research (NCEP/NCAR) reanalysis.*

become available and the trend might eventually exceed the natural variability.

Recent research has shown that the stratosphere can have an important influence on surface climate (e.g., *Baldwin and Dunkerton*, 1999, 2001; *Scaife et al.*, 2005; *Haynes*, 2005; *Shaw and Shepherd*, 2008), especially in the mid- to high latitudes. Even though the (N)AO is defined on the basis of tropospheric variables, many studies indicate a relation between the phase of the (N)AO and the strength of the stratospheric polar vortex. A positive (N)AO index is in general positively correlated with a stronger stratospheric polar vortex (e.g., *Perlwitz and Graf*, 1995; *Thompson and Wallace*, 1998; *Kodera et al.*, 1999; *Hartmann et al.*, 2000; *Thompson and Wallace*, 2000; *Ambaum and Hoskins*, 2002; *Thompson et al.*, 2003). A negative winter NAO response is, on the other hand, found in connection to tropical sea surface temperature anomalies in the Pacific related to El Niño, but only when the stratosphere, which shows a weakened polar vortex during El Niño years, is taken into account (*Bell et al.*, 2009).

Studies in the early 1990s showed that the influence of changes in the upper stratospheric zonal wind appear to gradually penetrate downward, affecting the circulation in the lower atmosphere (*Kodera et al.*, 1990). A decade later this was related to the AO index. It was found that a stratospheric AO signature often precedes a tropospheric AO signature (*Baldwin and Dunkerton*, 1999, 2001), providing observational evidence on the coupling between the stratosphere and the troposphere. This triggered an increased interest in the stratosphere, as information from the stratosphere might be used to improve and/or extend weather forecasts (*Thompson et al.*, 2002; *Baldwin et al.*, 2003; *Siegmund*, 2005).

Studies that examine the influence of the stratosphere on the troposphere often use numerical models of the atmosphere. In initial condition experiments, a change is

made to the initial conditions in the stratosphere, while keeping the tropospheric initial conditions constant, and the transient response of the troposphere to an imposed stratospheric change is studied (*Charlton et al.*, 2004; *Simpson et al.*, 2009). This type of experiment is, for example, suitable to examine the influence of the stratosphere on weather prediction (*Charlton et al.*, 2004). Another option is to perform boundary condition experiments, in which a change is made to the dynamics of the stratosphere, by adjusting, for example, the height of the upper boundary, the equilibrium temperature profile, or the damping in the stratosphere. In these experiments the time mean stratospheric flow is changed, and the impact on the time mean flow in the troposphere is examined (*Boville*, 1984; *Polvani and Kushner*, 2002; *Norton*, 2003; *Kushner and Polvani*, 2004). These type of experiments are suitable to study, for example, the response of the troposphere to changes in the stratosphere under climate change. Imposing observed wind trends in the lower stratosphere in a model, it was shown that changes in the stratosphere could account for a large part of the regional surface climate change over Europe and Northern America between 1965 and 1995, and that the imposed wind changes are positively correlated with the NAO index (*Scaife et al.*, 2005).

Stratospheric changes can affect the tropospheric circulation directly through hydrostatic and geostrophic adjustment, or indirectly due to changes in the reflection and propagation of planetary waves. The term 'direct' is used to indicate that adjustment to a change in the stratosphere directly results in changes in the troposphere, but the cause of the change in the stratosphere might still be located in the troposphere. The term 'indirect', on the other hand, is used to indicate that beside the tropospheric adjustment to the stratospheric changes, additionally the propagation of waves changes. Tropospheric dynamics can then amplify and modify the response to stratospheric forcing (*Song and Robinson*, 2004).

The direct pathway is examined by means of piecewise potential vorticity (PV) inversion (*Davis*, 1992), which makes use of the relation between the PV and other dynamical fields. Previous PV inversion studies (e.g., *Hartley et al.*, 1998; *Black*, 2002; *Black and McDaniel*, 2004) showed that changes in the stratospheric PV influence the winds in the troposphere. The PV is discussed in more detail in section 1.2.

As an example of the indirect effect, it was shown that the propagation of waves depends on the strength of the stratospheric vortex (*Perlwitz and Graf*, 2001), and that the amount of reflection of waves in the stratosphere back to the troposphere also depends on the wind speeds in the lower stratosphere (*Perlwitz and Harnik*, 2003, 2004). Furthermore, wave propagation within the troposphere is influenced by changes in the zonal wind, providing a feedback mechanism for further affecting the tropospheric flow (*Simpson et al.*, 2009).

The stratosphere-troposphere coupling is, however, still not completely under-

stood, and a subject of ongoing research.

1.1.7 Will the state of the stratosphere change due to climate change?

Future climate change will not only affect the troposphere, but also initiate changes in the state of the stratosphere. Radiative processes like changes in the absorption of solar radiation by ozone, or in the emission of thermal radiation by carbon dioxide (CO_2) affect stratospheric climate (*Fels et al.*, 1980; *Schoeberl and Hartmann*, 1991).

An increase in greenhouse gas concentrations leads to tropospheric warming, due to the trapping of longwave radiation, but additionally to stratospheric cooling, due to increased emission of longwave radiation to space (*Butchart et al.*, 2000; *Shindell et al.*, 2001). Enhanced greenhouse gas concentrations also enhance the stratospheric absorption of thermal radiation, but due to the increase in tropospheric opacity the increased emission dominates over the increased absorption of upwelling radiation and increased greenhouse gas concentrations lead to stratospheric cooling. The January mean temperature change related to CO_2 doubling in a climate model is presented in Fig. 1.6. In general, the stratosphere cools and the troposphere warms, but a warming of the Arctic lower stratosphere is found, indicating that dynamical processes might modify the radiative response to climate change.

A decrease in ozone concentrations in the polar stratosphere also leads to stratospheric cooling (*Graf et al.*, 1998; *Randel and Wu*, 1999; *Langematz et al.*, 2003; *Manzini et al.*, 2003). In the future, ozone recovery will lead to increases in ozone, with a stratospheric warming contribution, while cooling due to increasing greenhouse gases is expected to continue (*Schnadt et al.*, 2002; *Stolarski et al.*, 2010). The timing of these effects could, however, differ, as ozone recovery will mainly affect the spring and summer warming of the stratosphere, while CO_2 cooling can act throughout the whole year. From these radiative arguments, a decrease in the stratospheric cooling rate is expected in spring and summer over the coming decades, while autumn and winter cooling rates might increase.

The state of the stratosphere strongly depends on the wave forcing from the troposphere, and the wave-driven stratospheric overturning circulation. With respect to wave forcing from the troposphere to the stratosphere, a decrease has been noted in the NH winter in the 1990s, resulting in a weaker Brewer-Dobson circulation and a stronger Arctic vortex in that period (*Langematz et al.*, 2003; *Langematz and Kunze*, 2006). The reduction in planetary wave activity propagating from the troposphere into the lower stratosphere in the Arctic in February and March during the 1980s and 1990s might be related to ozone reduction. The cooling due to reduced ozone concentrations strengthens the polar vortex, with stronger zonal mean zonal winds in the lower stratosphere increasing the refraction of planetary waves into low latitudes and decreasing the wave activity in the polar lower stratospere (*Cagnazzo et al.*, 2006).

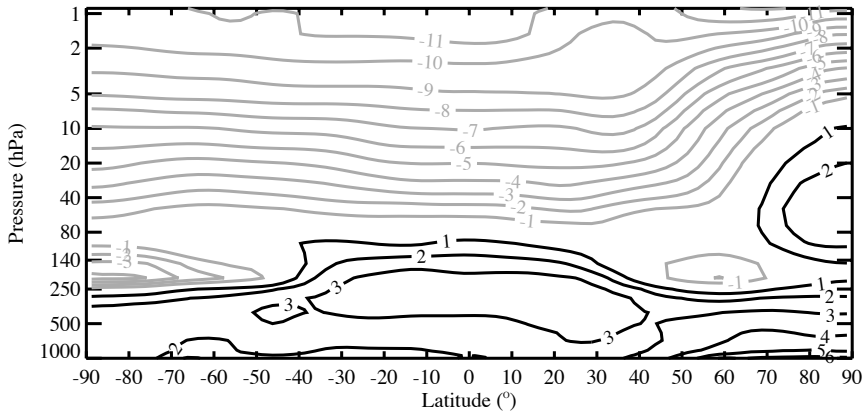

Figure 1.6: *January mean temperature change (K) due to CO_2 doubling in the Unified Model, based on the Hadley Centre Atmosphere Model coupled to a thermodynamic slab ocean model (Gillett et al., 2003; Bell et al., 2010, see also chapter 6) as a function of pressure and latitude (negative latitude values represent the Southern Hemisphere). The contour interval is 1 K, with the zero line omitted and negative values indicated by grey lines.*

For the future climate, however, most climate models with well-represented stratospheres indicate that the Brewer-Dobson circulation will accelerate (*Baldwin et al.*, 2007; *Shaw and Shepherd*, 2008). This dynamical response could explain the warming of the Arctic lower stratosphere, seen in Fig. 1.6 as a response to CO_2 doubling, since enhanced downwelling over the pole will lead to adiabatic warming as air is compressed. An increased Brewer-Dobson circulation is consistent with climate change experiments that find an increase in the wave driving of the polar stratosphere in the future (*Rind et al.*, 1998; *Butchart and Scaife*, 2001; *Eichelberger and Hartmann*, 2005; *Li et al.*, 2008; *Haklander et al.*, 2008; *Shepherd*, 2008). Observational support is limited, but indications have been found that the Brewer-Dobson circulation has increased in recent years (*Thompson and Solomon*, 2009; *Lin et al.*, 2009). This is in line with model projections for the future, suggesting that the decreases in wave forcing that were found in the 1990s have not continued into the 21st century. An increase in the wave driving of the stratosphere can lead to a change in the mean state, but also to increased stratospheric variability. A model study has shown that the number of days with SSWs increases due to CO_2 doubling, while days with cold polar stratospheric temperatures are also still possible under increased greenhouse gas concentrations (*Bell et al.*, 2010). Uncertainties remain with respect to the dynamical response of the stratosphere to climate change, and this subject is part of ongoing research.

In the future, the springtime ozone hole is expected to recover, due to a decrease in

ozone depleting substances. This will result in a change in the stratospheric climate. However, besides ozone recovery, an increase in greenhouse gases also affects the climate of the stratosphere. Climate change affects the stratospheric ozone mainly in two ways. The first is through radiative-chemical processes in the stratosphere. Since the stratosphere cools due to increases in greenhouse gases, the possibility for springtime ozone depletion is increased in the near future when ozone depleting substances are still high. The second is dynamical, through changes in the stratospheric wave forcing and the Brewer-Dobson circulation, resulting from tropospheric climate change (*Shepherd*, 2008). An increase in wave forcing will increase polar stratospheric temperatures, decreasing the possibility for the formation of polar stratospheric clouds and springtime ozone depletion. Furthermore, an increased Brewer-Dobson circulation will transport more ozone from the tropics to the polar lower stratosphere, providing a positive feedback, since this increases heating due to absorption of solar radiation which further reduces ozone depletion.

The eventual stratospheric climate change will depend on the balance between these dynamical, chemical and radiative processes. Confidence in future predictions of the stratospheric climate can be gained by understanding what determines the current state of the stratosphere. This is examined in this thesis by studying the potential vorticity distribution of the stratosphere. The definition of potential vorticity and its use are explained in the next section.

1.2 Potential vorticity

As noted in the previous section, important radiative effects in the stratosphere are absorption of solar radiation by ozone and emission of longwave radiation by greenhouse gases. These radiative effects will likely change in the future due to emissions of greenhouse gases and increases in ozone due to reduced ozone depletion (related to the ban of CFCs), affecting the temperature gradients in the stratosphere. To maintain thermal wind balance, the atmospheric circulation will also change. Instead of examining the temperature, pressure and wind anomalies separately, it is also possible to examine the isentropic potential vorticity (PV) anomaly. The PV is a useful variable to represent the state of the stratosphere, since it presents a compact way to describe the dynamics of the atmosphere.

The potential vorticity is proportional to the product of absolute vorticity and static stability. Following an air parcel, the PV can only be changed through diabatic processes or friction. The vorticity of an air parcel is related to the rotation of the air. The absolute vorticity is the sum of the planetary vorticity, related to the rotation of the Earth, and the relative vorticity, related to the rotation of air relative to the Earth. The static stability represents the variation of pressure with potential temperature. The isentropic PV is determined on levels of equal potential temperature. The

potential temperature is the temperature an air parcel would have if it were brought adiabatically to the surface. The stratosphere is stably stratified due to the increase of temperature with height. The potential temperature increases monotonically with height when the stratification is stable (*Haynes*, 2005), making it suitable to use as a vertical coordinate in the stratosphere.

The PV is a conserved quantity for adiabatic and frictionless processes. For adiabatic processes, there is no heat exchange between the air parcel and the environment. Adiabatic warming in the atmosphere takes place in, for example, the descending branch of the Brewer-Dobson circulation, when air compresses without exchange of heat with the surrounding air, while adiabatic cooling takes place as ascending air expands. Latent heat release due to condensation of water vapour in an air parcel or absorption of solar radiation by ozone are examples of diabatic processes. The radiative effect associated with an increase in greenhouse gas concentrations is also a diabatic process, since an air parcel will emit more longwave radiation when the greenhouse gas concentrations are increased. This will lead to a change in the potential vorticity.

The PV can be linked to the wind field through the invertibility principle, which states that together with a balance condition and boundary conditions, the PV determines all other dynamical variables. Through diabatic processes, a change in stratospheric ozone or greenhouse gas concentrations can possibly affect the tropospheric winds by changing the stratospheric PV, since a local change in PV can have a nonlocal effect on the wind field. The influence of climate change on the global circulation of the atmosphere can thus be studied through examination of the PV distribution and its changes. Knowledge of processes that determine the current PV distribution can help to understand changes in the PV field due to greenhouse gas increases. The invertibility principle relates changes in the PV to changes in the wind field, and can be used to examine the influence of the stratosphere on the troposphere.

1.2.1 PV inversion

The isentropic potential vorticity Z_θ (*Hoskins et al.*, 1985) is defined as:

$$Z_\theta = \frac{\zeta_\theta + f}{\sigma} \tag{1.1}$$

Here ζ_θ is the zonal mean isentropic relative vorticity, f is the Coriolis parameter and σ is the zonal mean isentropic density (σ is the inverse of the static stability):

$$\zeta_\theta = -\frac{1}{a}\frac{\partial u}{\partial \phi} + \frac{u \tan \phi}{a} \tag{1.2}$$

$$\sigma = -\frac{1}{g}\frac{\partial p}{\partial \theta} \tag{1.3}$$

Here u is the zonal mean zonal wind, a is the radius of the Earth, ϕ is the latitude, p is the pressure, θ the potential temperature and g is the gravitational acceleration.

To study the relation between the potential vorticity and the zonal wind, we derive a PV inversion equation that is based on the invertibility principle (*Kleinschmidt*, 1950; *Hoskins et al.*, 1985). We assume axi-symmetry about the North Pole. The PV inversion equation is derived from a balance condition and the definition of the isentropic potential vorticity (Eq. 1.1). The zonal mean zonal wind is assumed to be in hydrostatic balance and in gradient wind balance with the zonal mean temperature and pressure (neglecting deviations from the zonal average), i.e.

$$\frac{\partial \Psi}{\partial \theta} = \Pi \tag{1.4}$$

and

$$u\left(f + \frac{u \tan\phi}{a}\right) = -\frac{1}{a}\frac{\partial \Psi}{\partial \phi} \tag{1.5}$$

In these equations Π is the Exner function ($= c_p T/\theta$, with c_p the heat capacity of dry air at constant pressure and T the temperature) and Ψ is the isentropic stream function ($\Psi = c_p T + gz$, with z the height).

Differentiation of Eq. 1.1 with respect to ϕ, using Eqs. 1.4 and 1.5 and the equation of state ($p = \rho R T$, with ρ the density and R the gas constant for dry air), leads to the PV inversion equation

$$\frac{Z_\theta}{g}\frac{\partial}{\partial \theta}\left(\rho\theta f_{loc}\frac{\partial u}{\partial \theta}\right) + \frac{\partial^2 u}{\partial r^2} + \frac{\tan\phi}{a}\frac{\partial u}{\partial r} - \frac{u}{a^2\cos^2\phi} = \sigma\frac{\partial Z_\theta}{\partial r} - \frac{\partial f}{\partial r} \tag{1.6}$$

with

$$f_{loc} = f(r) + \frac{2\tan\phi}{a}u;\, r = a\left(\frac{\pi}{2} - \phi\right);\quad f(r) = 2\Omega\sin\phi = 2\Omega\cos\left(\frac{r}{a}\right) \tag{1.7}$$

Here, r is the distance from the pole measured along the surface of the Earth and Ω is the rotation rate of the Earth.

The PV inversion equation (Eq. 1.6) can be seen as the formulation of thermal wind balance in terms of potential vorticity. It describes the flow pattern that is associated with a specific pattern of the potential vorticity in a balanced axi-symmetric vortex centred at the pole.

1.2.2 Reference PV and PV anomaly

Equation 1.6 shows that a horizontal gradient in the PV will result in a wind field, except when this gradient term is exactly cancelled by the horizontal gradient in the Coriolis parameter. In the latter case, the right hand side of Eq. 1.6 vanishes and a zero wind field is found as a solution, since there is no longer a forcing term to induce a wind field. On the basis of this equation we can thus split the PV into a reference PV and a PV anomaly in such a way that the reference PV represents that part of the PV field that does not induce a wind field. The remaining PV anomaly then represents the part of the PV field that does induce a wind field, according to the PV inversion equation (Eq. 1.6). The PV anomaly field can be studied to gain insight into the large scale circulation in the atmosphere.

The zonal mean PV and the isentropic density are split into a reference state and an anomaly as follows:

$$Z_\theta \equiv Z_{\theta,\text{ref}} + Z'_\theta; \sigma \equiv \sigma_{\text{ref}} + \sigma' \tag{1.8}$$

with

$$Z_{\theta,\text{ref}} = \frac{f}{\sigma_{\text{ref}}} \tag{1.9}$$

and

$$\sigma_{\text{ref}} = \frac{\int \sigma a \cos(\phi) d\phi}{\int a \cos(\phi) d\phi} \tag{1.10}$$

In other words, the reference isentropic density σ_{ref} is the area-weighted average of σ over the domain in question. In our case we choose the area poleward of 10° north (south), for the NH (SH). Therefore, σ_{ref} only depends on the height (θ) and the hemisphere.

As an example, the January mean reference PV and PV anomaly are shown in Fig. 1.7 for the NH. Two clear PV anomalies are visible in Fig. 1.7b: a broad, flat PV anomaly in the upper troposphere/lower stratosphere region and a tall PV anomaly in the polar stratosphere. Comparison with Fig. 1.2 shows that the subtropical jet and the stratospheric polar jet are found near the edge of these PV anomalies.

The response in the wind field, induced by thermal wind adjustment to a PV anomaly, is not restricted to the area of the PV anomaly, but has a characteristic vertical scale, referred to as the Rossby height H (*Hoskins et al.*, 1985):

$$H \sim \frac{\sqrt{f(f+\zeta)}L}{N} \tag{1.11}$$

with N the Brunt-Väisälä frequency ($= \sqrt{g\rho/(\theta\sigma)}$ in isentropic coordinates) and L the horizontal scale of the flow. It measures the vertical penetration of the flow struc-

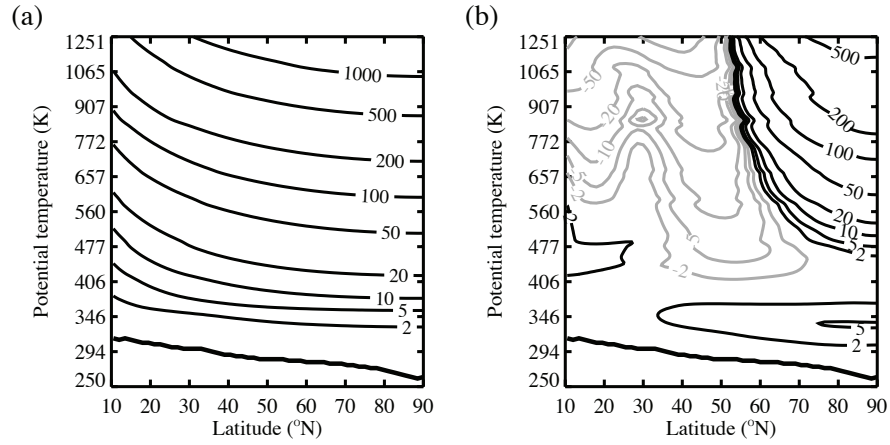

Figure 1.7: *January mean, zonal mean (a) reference PV and (b) PV anomaly (PVU) as a function of potential temperature and latitude for the Northern Hemisphere, derived from the ERA-Interim reanalysis daily data, averaged over the years 1989-2008. Contours at ± 2, 5, 10, 20, 50, 100, 200, 500, 1000, 2000 and 3000 PVU, with negative values indicated by grey lines. The thick line near the bottom represents the surface.*

ture above and below the location of the PV anomaly, where the response approximately decays by a factor $1/e$ over the Rossby height. The Rossby height hardly varies in the stratosphere, since N is nearly constant with height there ($N \sim 2 \cdot 10^{-2}$ s^{-1}). Lower values of N ($\sim 1 \cdot 10^{-2}$ s^{-1}) are found in the troposphere, corresponding to larger values of the Rossby height in the troposphere than in the stratosphere. The Rossby height is about four times as large for the upper troposphere/lower stratosphere PV anomaly in Fig. 1.7b as for the polar stratospheric PV anomaly, since $f \sim 10^{-4}$ s^{-1} for both PV anomalies, while N is twice as large for the polar stratospheric PV anomaly, and L is about twice as large for the upper troposphere/lower stratosphere PV anomaly (assuming L is proportional to the horizontal scale of the PV anomaly). This illustrates that PV anomalies in the tropopause region have a larger chance of affecting the surface winds than PV anomalies higher in the stratosphere. However, the influence of stratospheric PV anomalies of large amplitude might be felt in the tropospheric winds, since these PV anomalies will have a large response in ζ, increasing the Rossby height associated with these anomalies.

1.2.3 Method of solution of the PV inversion equation

The method of solution is in line with the method used by *Thorpe* (1985, 1986). Equation 1.6 is solved by successive relaxation. In the horizontal direction, the domain of the inversion ranges from the pole to 10°. By putting the boundary well poleward of the equator, we avoid problems associated with the inversion of negative (positive)

values of the potential vorticity that are found near the equator in the NH (SH). In the vertical direction, the inversion domain ranges from the lower boundary near the Earth's surface to the mid-stratosphere. The lower boundary is a sloping surface in isentropic coordinates, since the surface temperature decreases from the equator toward the pole. The horizontal and vertical resolution depend on the dataset to which the PV inversion is applied, and are described in each chapter separately.

The boundary condition at the pole is simply that u =0, because the vortex is assumed to be axi-symmetric and centred at the pole. At the outer boundary at 10° we prescribe the wind according to the circulation theorem (*Hoskins et al.*, 1985, p 897), which relates the surface integral of the vorticity on each isentropic surface to the circulation at the horizontal boundary of that surface. At the upper boundary we impose the zonal wind that was used to calculate the PV distribution we are considering. At the lower boundary, thermal wind balance is imposed, which is approximated in isentropic coordinates by:

$$\frac{\partial u}{\partial \theta} = \frac{c_p}{f\theta}\left(\frac{\partial T}{\partial r}\right)_\theta \tag{1.12}$$

with T the temperature averaged over the lowest layer between two isentropic surfaces. The temperature at the lower boundary is derived from the zonal mean pressure at isentropic levels ($T = \theta(p/p_0)^{R/c_p}$, with p_0=1000 hPa).

Since the potential temperature quickly increases with height in the stratosphere, a stretched grid in the vertical direction is employed:

$$\theta = \theta_s e^{z^*/H} \tag{1.13}$$

with θ_s=250 K and H ($= R\theta_s/g$) a vertical scale height. This way, a higher vertical resolution in terms of θ can be obtained in the lower part of the domain than in the upper stratosphere. Since levels are spaced at equal distances in z^*, the derivatives with respect to θ are redefined:

$$\frac{\partial}{\partial \theta} = \frac{\partial z^*}{\partial \theta}\frac{\partial}{\partial z^*} = \frac{H}{\theta}\frac{\partial}{\partial z^*} \tag{1.14}$$

The inversion equation is now rewritten as:

$$\frac{Z_\theta H}{g\theta}\frac{\partial}{\partial z^*}\left(\rho f_{loc} H \frac{\partial u}{\partial z^*}\right) + \frac{\partial^2 u}{\partial r^2} + \frac{\tan\phi}{a}\frac{\partial u}{\partial r} - \frac{u}{a^2\cos^2\phi} = \sigma\frac{\partial Z_\theta}{\partial r} - \frac{\partial f}{\partial r} \tag{1.15}$$

To solve this equation, given the PV distribution, the terms in Eq. 1.15 are approxi-

mated by finite differences on the grid in $r - z^*$ space. The result is of the following form, where the indices i and j represent the vertical (z^*) and horizontal (r) direction, respectively:

$$X_{i,j} \cdot u_{i,j} + S_{i,j} = D_{i,j} \tag{1.16}$$

where

$$X_{i,j} = -\left(\frac{2}{\Delta r^2} + \frac{1}{a^2 \cos^2 \phi_j} + F^+_{i,j} + F^-_{i,j}\right) \tag{1.17}$$

$$S_{i,j} = \left(\frac{1}{\Delta r^2} + \frac{\tan \phi_j}{2a\Delta r}\right) u_{i,j+1} + F^+_{i,j} u_{i+1,j} + \left(\frac{1}{\Delta r^2} - \frac{\tan \phi_j}{2a\Delta r}\right) u_{i,j-1} + F^-_{i,j} u_{i-1,j} \tag{1.18}$$

$$D_{i,j} = \frac{\sigma_{i,j}}{2\Delta r} \left(Z_{\theta,i,j+1} - Z_{\theta,i,j-1}\right) + \frac{2\Omega}{a} \sin \frac{r_j}{a} \tag{1.19}$$

$$F^+_{i,j} = \frac{1}{4} \frac{Z_{\theta,i,j} H^2}{g\theta_i} \frac{1}{\left(\Delta z^*\right)^2} \left(\rho_{i+1,j} + \rho_{i,j}\right) \left(f_{loc,i+1,j} + f_{loc,i,j}\right) \tag{1.20}$$

$$F^-_{i,j} = \frac{1}{4} \frac{Z_{\theta,i,j} H^2}{g\theta_i} \frac{1}{\left(\Delta z^*\right)^2} \left(\rho_{i,j} + \rho_{i-1,j}\right) \left(f_{loc,i,j} + f_{loc,i-1,j}\right) \tag{1.21}$$

Rearranging shows that the solution for u should satisfy:

$$u_{i,j} + \frac{S_{i,j} - D_{i,j}}{X_{i,j}} = 0 \tag{1.22}$$

This equation is solved iteratively for all interior gridpoints. The iteration is started by inserting $u = 0$ into Eq. 1.22 and evaluating the residue:

$$\text{residue}_{i,j} = u_{i,j} + \frac{S_{i,j} - D_{i,j}}{X_{i,j}} \tag{1.23}$$

The residue is subtracted from u to make a new guess for u. This is done for all gridpoints, after which the value of f_{loc} is updated and u at the lower boundary is determined from u in the interior and the wind shear over the lowest layer as determined from the lower boundary condition (Eq. 1.12, rewritten in terms of z^* with Eq. 1.14). The procedure is repeated until the residue becomes less than some prescribed value (taken to be $1 \cdot 10^{-5}$ m s^{-1}) at all gridpoints. Next, σ is adjusted. Since the PV is

fixed, and a change in u will give a change in ζ, σ will also change. A constraint that is put on the changes in σ is that the mass between two isentropic surfaces does not change during the inversion, and remains the same as in the reference state (*Hoskins et al.*, 1985, p 897). After adjusting σ, the pressure and density are updated (using the definition of σ and the equation of state) and the inner loop is repeated with σ again held fixed. The solution is thus found in two embedded iteration loops. The final solution for u is found when only one iteration of the inner loop is needed to find a new solution for u after σ has been adjusted.

1.2.4 Examples of PV inversion

In this section several examples are shown of simple zonal mean PV anomalies and the zonal mean zonal wind field which they induce. The PV anomalies studied have their maximum value at the pole, falling off sinusoidally to zero at 60°N or 30°N. In the vertical, the PV anomaly is placed at a certain height, for example between 400 K and 600 K or between 600 K and 800 K, with the maximum values in the middle of the layer, falling off sinusoidally to zero at the top and bottom of the PV anomaly.

It is not possible to invert just a PV anomaly with the inversion equation used here (Eq. 1.6). Therefore the PV anomalies are combined with a reference PV field. The wind fields obtained from the PV inversion will however correspond to the PV anomalies, since the reference PV alone does not induce a wind field. The reference PV field is derived from the climatological (averaged over 1989-2008) monthly mean ERA-Interim PV for January, which is calculated from the European Centre for Medium-Range Weather Forecasts (ECMWF) ERA-Interim reanalysis velocity and temperature data. The horizontal resolution of this dataset is 1.5°, and the vertical resolution varies from about 2 K in the troposphere to 10 K in the upper layers. Further, zero thermal wind is imposed at the lower boundary, allowing a different wind at the lower boundary for different PV anomalies (which would not be the case if $u = 0$ is imposed as boundary condition). At the other boundaries zero wind is imposed. Although this is a rather strong constraint, these are suitable boundary conditions for the current purpose, of examining the relation between simple PV anomalies and their corresponding wind fields.

Figure 1.8 presents two different PV anomalies and their accompanying inverted wind fields, where the PV anomalies have been chosen positive. The PV anomalies are given in PV units, where 1 PVU = 10^{-6} K m^2 kg^{-1} s^{-1}. It should be noted that the vertical axis is plotted logarithmic, to stretch the lower stratospheric area, since the potential temperature increases faster with height in the upper stratosphere (340 K $\sim$ 10 km, 500 K $\sim$ 20 km, 850 K $\sim$ 30 km).

Figure 1.8 shows that a local PV anomaly has a nonlocal effect on the wind. A PV anomaly in the (lower) stratosphere can affect the wind in the troposphere, and

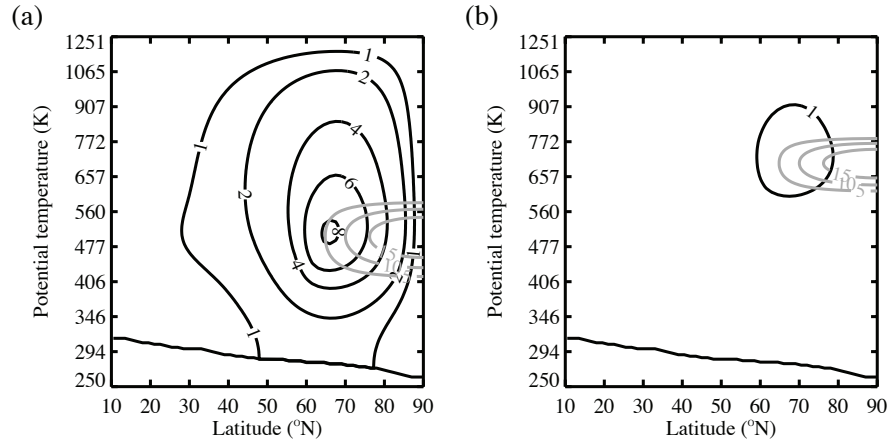

Figure 1.8: *PV anomaly (grey lines, in PVU) and accompanying inverted zonal wind (black lines, in m s^{-1}) for a PV anomaly between (a) 60° N - 90° N, 400 K - 600 K and (b) 60° N - 90° N, 600 K - 800 K, as a function of potential temperature (K) and latitude (° N). The solid line near the bottom represents the lower boundary of the inversion domain. Contours every 5 PVU for the PV anomaly and at ± 1 m s^{-1} and then every 2 m s^{-1} for the wind field, with negative values represented by dashed lines and zero contours omitted. A positive wind corresponds to westerlies, while negative values are associated with easterly winds.*

changes in the PV over the pole might affect the wind at midlatitudes. It is clear from this figure that the same PV anomaly at a different location in the atmosphere has a different effect on the wind field. If the PV anomaly is put at higher levels, the effect on the wind field is much smaller. Furthermore, it can be noted from Fig. 1.8a that the wind response to a PV anomaly is not symmetric with respect to height, as the response penetrates farther upward than downward. The extent of the response downward is of course limited by the surface of the Earth, but the wind speeds also decrease faster in downward direction (340 K and 850 K are, for example, both about 10 km away from 500 K, but the wind speeds at 850 K are higher than those at 340 K in Figs. 1.8a). To understand the variation of the wind response with height, the definition of the PV (Eq. 1.1) and reference state (Eqs. 1.8 and 1.9) are used to express ζ in terms of the PV:

$$\zeta = \frac{1}{\alpha_{\text{ref}}} \left(Z'_\theta - Z_\theta \frac{\alpha'}{\alpha} \right) \tag{1.24}$$

with $\alpha = 1/\sigma$ the static stability ($\alpha = \alpha_{\text{ref}} + \alpha'$, and $\sigma_{\text{ref}} = 1/\alpha_{\text{ref}}$).

The first term on the right hand side in Eq. 1.24 is only nonzero when the PV anomaly is nonzero. For a positive PV anomaly, this term gives a positive contribution to the relative vorticity field in the area of the PV anomaly. Since the static stability increases with height, this term will be larger for a PV anomaly in the lower stratosphere, than for a PV anomaly of similar size at higher levels. A similar sized

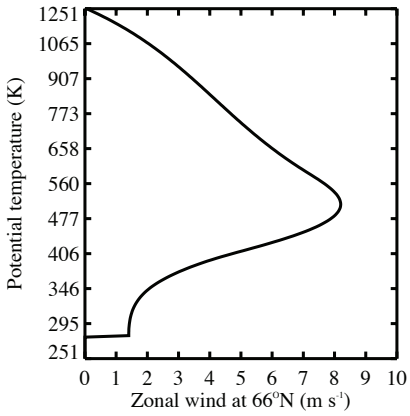

Figure 1.9: *Zonal wind (in m s^{-1}) at 66°N as a function of potential temperature (K), corresponding to the PV anomaly in Fig. 1.8a.*

PV anomaly in the lower stratosphere will therefore lead to a larger response in ζ, and therefore also in the wind field, explaining the different wind fields in Figs. 1.8a and 1.8b.

Outside the region of the PV anomaly, the response in ζ is determined by the fraction α'/α. For a positive PV anomaly, the static stability increases in the region of the PV anomaly, while it decreases above and below the anomaly (*Hoskins et al.*, 1985). Away from the PV anomaly α' will therefore be negative, corresponding to a positive ζ. The fraction α'/α decreases in magnitude when you move away from the PV anomaly region, but the damping is less strong in upward direction than in downward direction, resulting in a stronger response in the wind above the PV anomaly than below. This asymmetry in damping is likely related to the upper boundary condition, which forces the wind to zero at the top of the domain. An exponential decay of the response is expected away from the PV anomaly, where the Rossby height represents the typical penetration depth of the flow above and below the PV anomaly (see section 1.2.1). The zonal wind response at 66°N for the PV anomaly shown in Fig. 1.8a (66°N is the latitude of the maximum wind response for this PV anomaly) is presented in Fig. 1.9. This figure indeed indicates an exponential decay of the response in the wind field below the PV anomaly, but a much more linear decay of the wind field above the PV anomaly, to zero wind at the upper boundary. It should thus be noted that the boundary condition affects the wind field. In the following chapters, a more realistic upper boundary condition is therefore used, applying the observed wind at the upper boundary when the stratospheric PV is inverted.

It is interesting to change the sign of the PV anomaly (Fig. 1.10a) or to double its

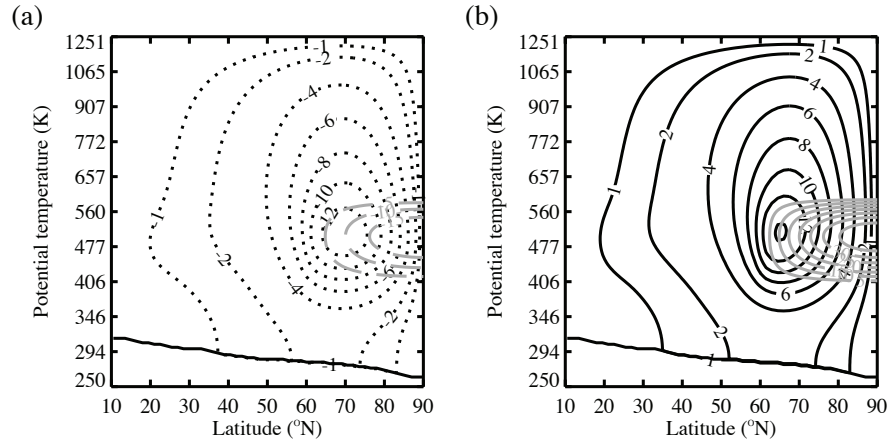

Figure 1.10: *PV anomaly (grey lines, in PVU) and accompanying inverted zonal wind (black lines, in m s^{-1}) for the same PV anomaly as in Fig. 1.8a, but (a) of opposite sign and (b) with the amplitude doubled, as a function of potential temperature (K) and latitude (° N). Contours as in Fig. 1.8.*

strength (Fig. 1.10b), compared to the PV anomaly in Fig. 1.8a. Changing the sign of the PV anomaly, results in a change in the sign of the inverted wind field, as expected. However, the easterlies that accompany the negative PV anomaly are much stronger than the westerlies that accompany the positive PV anomaly. This can be related to the second term on the right hand side of Eq. 1.24, which represents the nonlinearity of the response with respect to the PV anomaly strength. In the region of the PV anomaly, this term acts to damp the response in ζ that is forced by the first term. Changing the sign of the PV anomaly results in a change in the sign of α' and ζ, but the PV itself remains positive. Compared to a positive PV anomaly, the PV decreases for a negative PV anomaly, so that the damping influence of the second term in Eq. 1.24 on ζ decreases. This results in a larger response in ζ, and therefore also in u, for a negative PV anomaly than for a positive PV anomaly.

Doubling the strength of the PV anomaly increases the strength of the induced wind field, although by slightly less than a factor of two. Again Eq. 1.24 can be used to understand this nonlinearity. If only the first term on the right hand side of Eq. 1.24 would change due to a doubling of the PV anomaly, this would result in a doubling of ζ. However, the second term on the right hand side of Eq. 1.24 increases as the PV increases, damping the response in ζ that would result from the first term alone. These examples show that the PV inversion is nonlinear, which is expected, since Eq. 1.6 is a nonlinear equation.

Hoskins et al. (1985) note that a broad, shallow PV anomaly tends to have a larger effect on the isentropic density, while a tall PV anomaly tends to have a larger effect

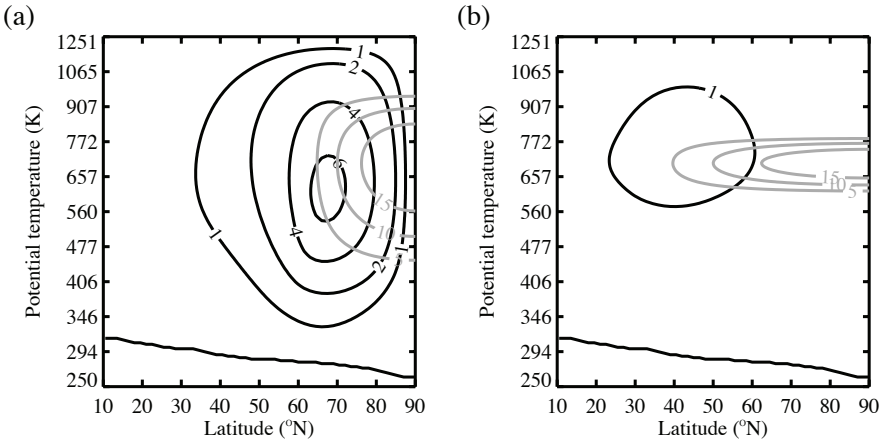

Figure 1.11: *PV anomaly (grey lines, in PVU) and accompanying inverted zonal wind (black lines, in m s^{-1}) for a PV anomaly between (a) 400 K - 1000 K and 60° N - 90° N, and (b) 600 K - 800 K and 30° N - 90° N, as a function of potential temperature (K) and latitude (° N). Contours as in Fig. 1.8.*

on the vorticity. This is tested by inverting a tall, narrow PV anomaly that stretches from 400 K to 1000 K in the vertical, and between 60° N and 90°N, and a flat, broad PV anomaly between 600 K and 800 K and 30°N and 90°N. Both PV anomalies have the same amplitude at their center (at 700 K at the pole). The resulting wind fields are presented in Fig. 1.11. The accompanying responses in the relative vorticity and isentropic density are shown in Fig. 1.12, where the response in σ' is shown as a percentage of the reference state σ_{ref}, and the response in ζ is shown as a percentage of the planetary vorticity f. For the tall anomaly, there is a clear response in ζ (Fig. 1.12a). There is also a clear response in σ (Fig. 1.12b), with the largest response in the lower part of the PV anomaly. For the flat, broad PV anomaly, there is indeed almost no response in ζ (Fig. 1.12c), while there is a clear response in σ (Fig. 1.12d). Although the maximum amplitude of the response in σ is smaller for the flat PV anomaly than for the tall PV anomaly, the response in σ at the center of the PV anomaly increases when the PV anomaly is flattened.

To further investigate the relation between the shape of the PV anomaly and its effect on ζ and σ, PV anomalies of different heights are inverted. The PV anomalies extend between 60°N and 90°N in the horizontal, and are centered at 700 K in the vertical, with heights ranging from 100 K to 700 K. Again the amplitude of the PV anomalies at their center is kept constant. The responses in ζ and σ at the pole at the center of the PV anomaly (700 K) are presented in Fig. 1.13. The absolute value of the response in σ is shown, to illustrate the relation between the amplitude of the response and the height of the PV anomaly. This figure shows that the response in ζ

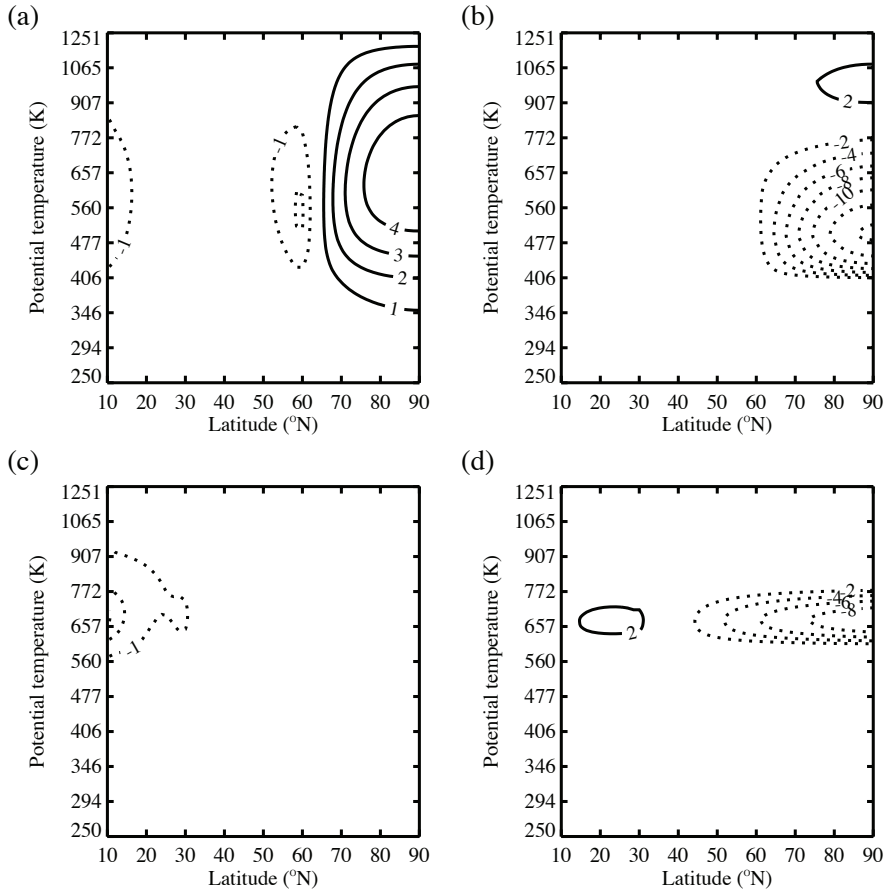

Figure 1.12: *The response in ζ (100%·ζ/f) for a PV anomaly between (a) 400 K - 1000 K and 60° N - 90° N, and (c) 600 K - 800 K and 30° N - 90° N, and the response in σ (100%·$(\sigma - \sigma_{\mathrm{ref}})/\sigma_{\mathrm{ref}}$) for a PV anomaly between (b) 400 K - 1000 K and 60° N - 90° N, and (d) 600 K - 800 K and 30° N - 90° N. Contours every 1% for (a) and (c) and contours every 2% for (b) and (d), with the zero contour omitted and negative values indicated by dashed lines.*

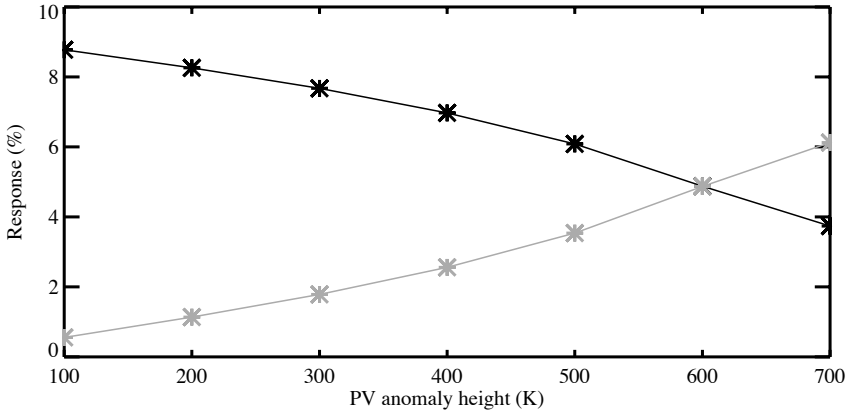

Figure 1.13: *The response in ζ (100%·ζ/f, grey) and in σ (100%·$abs(\sigma - \sigma_{\text{ref}})/\sigma_{\text{ref}}$, black) at 700 K at the pole, for a PV anomaly between 60° N - 90° N, centered at 700 K in the vertical, but with its height varying between 100 K and 700 K, as a function of the PV anomaly height.*

increases with increasing height of the PV anomaly, while the response in σ decreases. In line with *Hoskins et al.* (1985), Figure 1.13 thus shows that, at the center of the PV anomaly, the response in σ is larger for a flat PV anomaly, while the response in ζ is larger for a tall PV anomaly.

Piecewise PV inversion (*Davis*, 1992) is based on the idea that the PV anomaly field can be split into parts, that can each be inverted separately to investigate the effect of a certain PV anomaly on the wind field. This, however, only has a meaning if the sum of the inverted wind fields of the different parts is similar to the inverted wind field of the total PV anomaly field. To examine this aspect, a new polar PV anomaly is constructed, consisting of the PV anomalies shown in Fig. 1.8 (the PV anomaly between 600 K and 800 K is doubled in amplitude to increase its effect on the wind field). The PV anomaly and its accompanying wind field are shown in Fig. 1.14a. This inverted wind field is now compared to the sum of the wind fields that are obtained when the PV anomalies are inverted separately. The difference is given in Fig. 1.14b, showing that the sum of the inverted wind fields from the separate PV anomalies is practically identical to the inverted wind field from the sum of the PV anomalies. This indicates that, despite the nonlinearity of the inversion equation, piecewise PV inversion can be used to examine the influence of part of the PV anomaly on the wind field. Piecewise PV inversion is thus a suitable tool to examine the influence of the stratospheric PV anomaly, and changes therein, on the tropospheric winds.

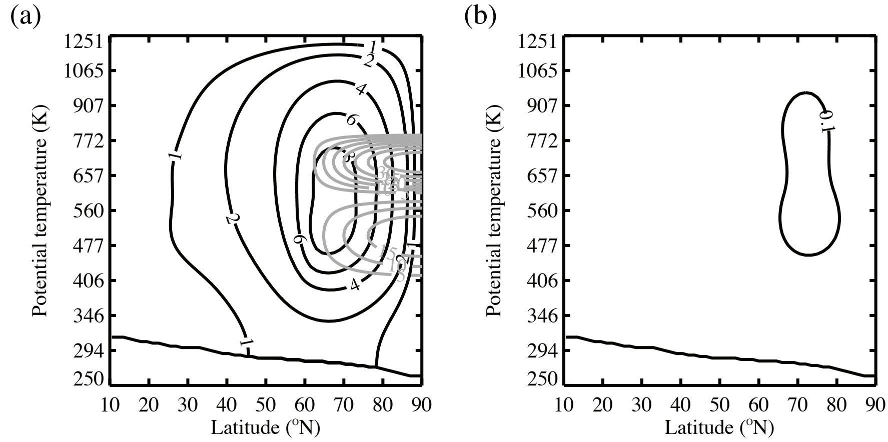

Figure 1.14: *(a) PV anomaly (grey lines, in PVU) and accompanying inverted zonal wind (black lines, in m s^{-1}) for a PV anomaly that is the sum of the PV anomaly between 400 K - 600 K, 60° N - 90° N and twice the PV anomaly between 600 K - 800 K, 60° N - 90° N. (b) The difference of the inverted wind field shown in panel (a) minus the sum of the inverted wind fields of the separate PV anomalies, as a function of potential temperature (K) and latitude (° N). Contours as in Fig. 1.8 for panel (a) and contours every 0.1 m s^{-1} with the zero line omitted in panel (b).*

1.3 This thesis

A way to represent the state of the stratosphere is by the isentropic PV distribution. The PV is a useful variable to represent the state of the atmosphere, since it presents a compact way to describe the dynamics of the atmosphere, it shows the influences of diabatic effects on the atmosphere, and through the invertibility principle the PV is directly linked to all other dynamical fields. Furthermore, local changes in the PV can have a nonlocal effect on the wind field, so that changes to the stratospheric PV distribution can be related to circulation changes in the troposphere.

The PV inversion examples shown in the previous section, indeed indicate that the stratospheric PV can affect the circulation in the troposphere. This can be in a climatological sense, where the monthly mean climatological PV anomaly in, for example, January might exert a certain influence on the climatological winds in the troposphere. Or it can be on shorter timescales, for example around the occurrence of an SSW, when large changes in the stratosphere occur, affecting the stratospheric PV anomaly, and thereby also changing the influence of the stratosphere on the troposphere. Furthermore, it is also possible that the PV anomaly in the stratosphere changes due to an increase in greenhouse gases or a change in stratospheric ozone concentrations. This means that the climatological influence of the stratosphere on the tropospheric winds could change due to climate change. The stratospheric PV anomaly field in the current

climate, its variations around the occurrence of an SSW, and its possible changes in the future are studied in this thesis.

To examine the current and future stratosphere-troposphere coupling, the following questions are addressed:

1. How does the stratosphere affect the tropospheric winds under different conditions of the Arctic Oscillation?
2. What are the seasonal cycle and interhemispheric differences in the climatological stratospheric potential vorticity distribution?
3. What determines the interannual variability of the winter stratosphere?
4. What was the influence of the 2009 major sudden stratospheric warming on the tropospheric winds?
5. To what extent does the stratosphere influence the tropospheric zonal wind response to CO_2 doubling?

The first question is addressed in chapter 2. It is based on the relation between the tropospheric AO index and the strength of the stratospheric polar vortex. Due to a large variability from year to year, it is difficult to find a clear trend in the stratospheric PV. A large part of the winter variability in the Northern Hemisphere is related to the Arctic Oscillation. The AO index also shows a large variability, but in general there seems to have been a positive trend from the 60's to the 90's. From the mid-90's on the AO has been in a more neutral phase. So whether this positive trend has to do with increases in greenhouse gases is not clear from the current timeseries. If this is indeed the case, January months with an average positive AO index might be more frequent in the future. Therefore it is interesting to look at the difference between January months with a positive AO index and January months with a negative AO index, and examine the stratospheric PV difference between these two cases for the NH. PV inversion is then used to relate this stratospheric PV difference to a wind difference, to examine the influence of changes in the stratospheric PV on the tropospheric wind.

Since a change in the stratospheric PV can affect the tropospheric winds, it is useful to examine what processes determine the PV distribution in the stratosphere and how the PV is affected by changes in ozone or greenhouse gases. To be able to understand future changes in the stratospheric PV, first the current PV distribution needs to be understood. Examination of the PV differences between the Northern and Southern Hemisphere, and its possible causes, allows us to study the processes that are important in forming the current PV distribution. This issue (question 2) is addressed in chapter 3.

An important difference between the NH and SH is the more frequent occurrence of SSWs in the NH, causing a larger interannual variability of the winter stratosphere

in the NH than in the SH. This raises the question whether the stratospheric interannual variability is mainly forced from below, or internally generated. Chapter 4 deals with this question (question 3), by examining the relation between the wave forcing of the stratosphere from below and the polar PV, for the period 1989 to 2008. Furthermore, it is studied to what extent the stratospheric polar PV around the major SSW that occurred in January 2009 can be estimated from the general wave-PV relation and the wave forcing in 2009.

An SSW is accompanied by large changes in the stratospheric PV, and PV inversion is used to examine if the tropospheric winds are affected by these stratospheric PV changes in chapter 5 (question 4). It is studied to what extent and on what timescales the troposphere is affected by the stratospheric changes that accompany the SSW in January 2009. If the SSW increases the persistence of the influence of the stratosphere on the troposphere, knowledge of the stratosphere might be useful for extended range weather forecasts.

Chapter 6 presents the effect of an increase in greenhouse gas concentrations on the stratospheric PV. Both hemispheres are discussed, to examine interhemispheric differences in the stratospheric response to an increase in greenhouse gas concentrations. PV inversion is used to examine to what extent the tropospheric zonal wind response to CO_2 doubling can be related to changes in the stratosphere (question 5).

Finally, a discussion and some of the remaining questions are presented in chapter 7.

2

Stratospheric impact on tropospheric winds deduced from potential vorticity inversion in relation to the Arctic Oscillation

The zonal mean state of the atmosphere in the Northern Hemisphere in winter is determined by the temperature at the Earth's surface and by two potential vorticity (PV) anomalies (defined as that part of the PV field that induces a wind field) centred over the North Pole: one in the upper troposphere/lower stratosphere (UTLS), extending to the subtropics and the other over the polar cap in the lower to middle stratosphere. Isentropic PV inversion demonstrates that the UTLS PV anomaly induces the main part of the zonal mean wind in the troposphere, including the subtropical jetstream, while the stratospheric PV anomaly induces the polar night stratospheric jet. The stratospheric PV anomaly has a greater amplitude and extends further downwards if the Arctic Oscillation (AO) index is positive. Also the UTLS PV anomaly has a slightly larger amplitude if the AO index is positive, but the meridional PV gradient in the subtropics that is associated with this anomaly is greatest when the AO index is negative, resulting in a stronger subtropical jet when the AO index is negative. PV inversion translates the UTLS PV anomaly in a wind anomaly and a static stability anomaly. The resulting differences in the vertical wind shear and in the Brunt-Väisälä frequency between the two AO phases show a larger baroclinicity in the extra-tropics when the AO index is positive. This explains why more extra-tropical cyclones are observed when the AO index is positive.

This chapter is based on:
Hinssen, Y., A. van Delden, T. Opsteegh, and W. de Geus, Stratospheric impact on tropospheric winds deduced from potential vorticity inversion in relation to the Arctic Oscillation, *Quarterly Journal of the Royal Meteorological Society*, *136*, 20-29, doi:10.1002/qj.542, 2010.
and
Hinssen, Y., A. van Delden, T. Opsteegh, and W. de Geus, Notes and Correspondence Correction to: 'Stratospheric impact on tropospheric winds deduced from potential vorticity inversion in relation to the Arctic Oscillation' by Yvonne Hinssen, Aarnout van Delden, Theo Opsteegh and Wouter de Geus, *Quarterly Journal of the Royal Meteorological Society*, In press, doi:10.1002/qj.716, 2010.

2.1 Introduction

Research over the past decade has shown that the stratosphere can have an important influence on surface climate (e.g., *Hartley et al.*, 1998; *Baldwin and Dunkerton*, 1999, 2001; *Black*, 2002; *Ambaum and Hoskins*, 2002). Many studies indicate a relation between the strength of the stratospheric polar vortex and the phase of the Arctic Oscillation (AO), a dominant pattern of natural climate variability at the Earth's surface in the mid- to high latitudes of the Northern Hemisphere in winter (*Thompson and Wallace*, 1998). A positive AO index is in general positively correlated with a stronger stratospheric polar vortex (e.g., *Hartmann et al.*, 2000; *Thompson and Wallace*, 1998, 2000).

In the present chapter, we adhere to the idea sketched by *Ambaum and Hoskins* (2002) that a positive North Atlantic Oscillation (NAO) index (an index strongly related to the AO index) is associated with a positive stratospheric potential vorticity (PV) anomaly over the pole (compared to the climatological average), because of more equatorward refraction of upward-propagating Rossby waves and therefore less mixing of PV over the pole by wave breaking. *Ambaum and Hoskins* (2002) use regression techniques and scale analysis based on PV dynamics to estimate the effect of a stratospheric PV anomaly on the tropopause, and subsequently on the surface pressure.

The present study is also related to the work of *Black* (2002), who examined the stratospheric forcing of the zonal mean surface winds associated with the AO for winter mean conditions. *Black* (2002) used quasi-geostrophic piecewise PV inversion to study the contribution of stratospheric PV anomalies on the tropospheric wind field. Here we use a PV inversion equation that is based on the nonlinear isentropic PV. Therefore, in contrast to *Black* (2002), we take variations of the static stability with latitude into account. This is an important aspect of the response of the atmosphere to a PV anomaly, especially, as we shall see, in the upper troposphere and lower stratosphere (UTLS).

Furthermore, whereas *Black* (2002) defines a PV anomaly as an anomaly with respect to the climate, we follow *Hoskins et al.* (1985) by defining a PV anomaly as that part of the PV field that induces a wind field according to the solution of the PV inversion equation. With this definition we are able to distinguish very clearly two separate PV-anomalies centred over the pole: one at the tropopause and the other in the polar night stratosphere above about 425 K. The former PV anomaly was not identified as such by *Black* (2002).

Following the ideas of *Davis* (1992) about piecewise PV inversion, we examine the effect of the two separate PV anomalies on the zonal mean zonal wind in the troposphere for episodes of positive and negative AO index in January. The month of January is chosen because the correlation between the stratospheric polar PV and

the AO index is largest in this month. Inversion of a PV anomaly results in a wind anomaly and a static stability anomaly, both of which affect baroclinic instability in the troposphere. We examine the differences in degree of baroclinic instability between the winter months with a strong positive average AO index and winter months with a strong negative average AO index. Furthermore, the influence of variations in the static stability on the Rossby scale height are presented, to estimate its effect on the downward influence of stratospheric PV anomalies on the wind field.

Section 2.2 gives an overview of the dataset that has been used. The differences in wind and PV between the two AO phases and the influence of variations in the static stability on the difference in PV are presented in section 2.3. The solutions of the PV inversion equation that provide an answer to the question of how stratospheric PV anomalies affect the tropospheric wind and baroclinic instability are discussed in section 2.4. Finally, conclusions are given in section 2.5.

2.2 Data

The European Centre for Medium-Range Weather Forecasts (ECMWF) ERA-40 reanalysis data at 23 pressure levels between 1000 hPa and 1 hPa, and with a horizontal resolution of 2.5° is used. The monthly mean January ERA-40 data of the zonal wind and the temperature for the 1958-2002 period are interpolated from isobaric to isentropic levels by the method described by *Edouard et al.* (1997). In order to make optimal use of the available ERA-40 data, a stretched grid in the vertical direction is employed. Zonal averaging and averaging over the whole 45-yr period gives a climatological dataset of zonal and January mean zonal wind, u, and pressure, p, at isentropic levels. The climatological isentropic potential vorticity, Z_θ, is then calculated from Eq. 1.1, using the zonal mean isentropic relative vorticity (ζ_θ, Eq. 1.2) and the zonal mean isentropic density (σ, Eq. 1.3). The domain of this dataset ranges from 90°N to 10°N in the horizontal, with a resolution of 2.5°, and from the Earth's surface to about 1600 K in the vertical, with a resolution varying from about 3.4 K near the surface to 20 K in the upper layers. We assume that the potential temperature (θ) of the Earth's surface coincides with the temperature of the 1000 hPa level. The lower boundary (also referred to as 'the surface') is defined as the lowest level of the grid that is above the Earth's surface. The potential temperature of the lower boundary thus varies with latitude, from 250 K at 90°N to about 300 K at 10°N. By putting the southern boundary well north of the equator, we avoid problems associated with the inversion of negative values of the potential vorticity that are found near the equator.

To study the relation between the potential vorticity and the zonal wind, we apply PV inversion (see section 1.2), which states that, together with a balance condition and suitable boundary conditions, the PV determines all other dynamical fields.

The boundary condition at the pole is simply that the zonal wind equals zero,

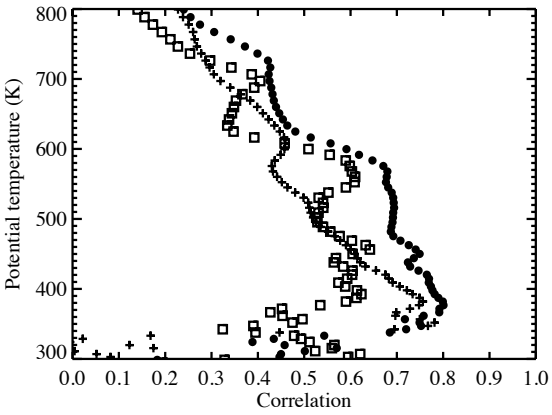

Figure 2.1: *Correlation between the AO index and the polar cap PV as a function of potential temperature (K) for years with an AO index larger than 0.5 times or smaller than -0.5 times the standard deviation of all the AO index values. Monthly mean values for December (squares), January (solid dots) and February (plusses).*

because the vortex is assumed to be axi-symmetric and centred at the pole. At the outer boundary at 10°N we prescribe the wind according to the circulation theorem (*Hoskins et al.*, 1985, p 897). At the upper boundary we impose the average wind of the specific months we are considering. At the lower boundary, thermal wind balance is imposed (Eq. 1.12)

2.3 The Arctic Oscillation and potential vorticity

In this section the relation between PV and the AO index is studied. For this study the monthly AO index from the National Centers for Environmental Prediction/National Center for Atmospheric Research (NCEP/NCAR) reanalysis is used (*Thompson and Wallace*, 2000). This index is defined as the leading empirical orthogonal function (EOF) of sea-level pressure poleward of 20°N. It is based on the period 1958-1997, which is close to the period we examine (1958-2002). A particular January month is defined as having a positive (negative) AO index if its average AO index is larger than (smaller than) plus (minus) 0.5 times the standard deviation of all the AO index values (this will be referred to as the "AO criterion"). With the AO criterion, the following 15 years with a positive AO index for January have been determined: 1962, 1964, 1973, 1975, 1981, 1983, 1984, 1988, 1989, 1990, 1991, 1992, 1993, 2000 and 2002, and the following 11 years with a negative AO index have been identified: 1959, 1960, 1963, 1966, 1969, 1970, 1977, 1979, 1980, 1985 and 1998.

The January mean PV is determined for all years (1958-2002) from the January

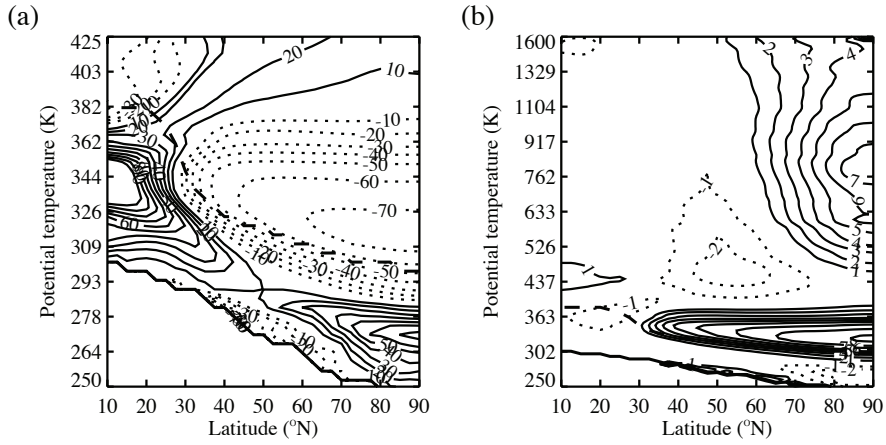

Figure 2.2: *(a) The deviation from the reference state of the isentropic density, as a percentage of the reference isentropic density, $\sigma'/\sigma_{\text{ref}} \cdot 100\%$ and (b) the deviation from the reference state of the scaled PV, Z'_θ, (in PVU). The fields are plotted as a function of potential temperature (K) and latitude (°N) (note the different scales on the vertical axes). The contour interval is 10% for (a) and 1 PVU for (b), with the zero lines omitted and negative values are indicated by thin dashed lines. The thick line near the lower boundary of the domain indicates the surface and the thick dashed line the tropopause (which is defined as the 2 PVU-isopleth).*

and zonal mean u and p fields. The same is done for the months December (1957-2001) and for February (1958-2002). The correlation between the AO index and the polar cap PV (area-weighted average PV north of 70°N) for the winter months is shown in Fig. 2.1 for the years that satisfy the AO criterion. There is a clear positive correlation between the AO index and the polar stratospheric PV. The correlation is largest in January, where it is larger than 0.6 in the lower stratosphere, between about 350 K and 600 K. This relation between the AO index and stratospheric PV does not present information about cause and effect, but it indicates that changes in the stratospheric PV are related to changes in the AO index. Based on this relation we expect a different stratospheric PV distribution for January months with a positive AO index than for January months with a negative AO index. PV inversion will be used to examine the influence of the stratospheric PV on the tropospheric winds, to see whether the stratospheric PV is associated with the winds in a similar way as the AO index. The results presented in the rest of this chapter are for January.

The zonal mean PV and the isentropic density are split into a reference state ($Z_{\theta,\text{ref}}$) and an anomaly (Z'_θ) as described in section 1.2.2. The reference isentropic density σ_{ref} is the area-weighted average of σ over the domain in question. In our case this is the area poleward of 10°N. Therefore, σ_{ref} depends only on the height (θ). The PV anomaly represents that part of the PV field that induces a wind field, according to the PV inversion equation (Eq. 1.6).

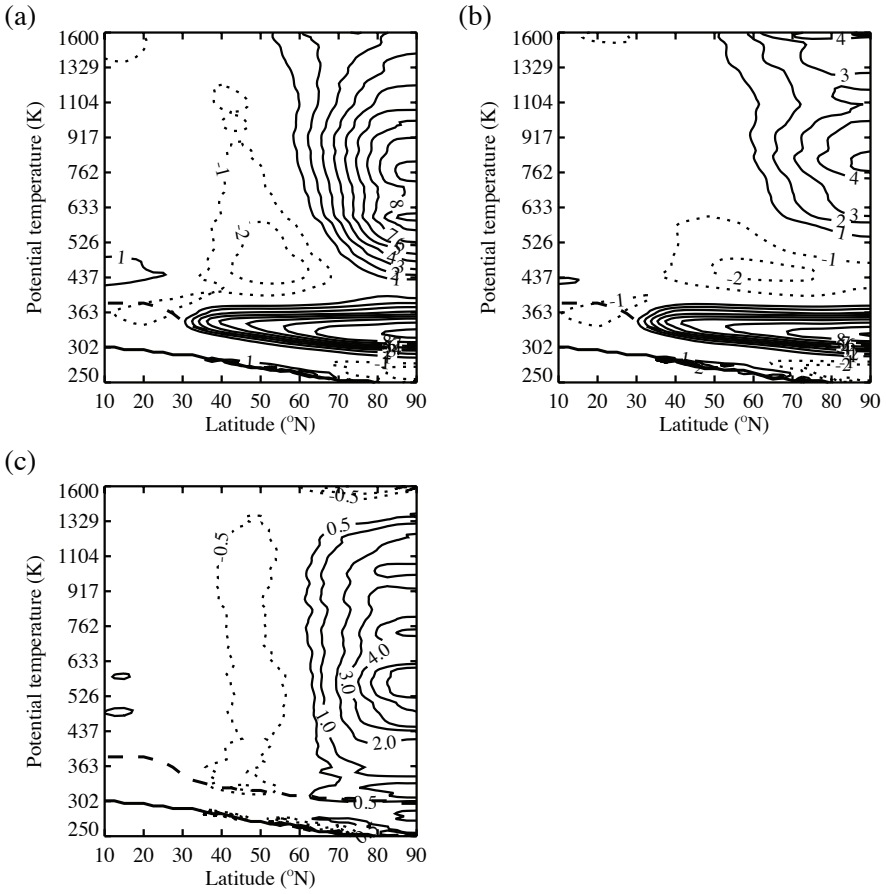

Figure 2.3: *Scaled Z'_θ (in PVU) for (a) positive AO case, (b) negative AO case and (c) positive - negative AO case. Contours as in Fig. 2.2b, for (c) also the ± 0.5 PVU contour is added.*

Figure 2.2a shows that $\sigma'/\sigma_{\text{ref}}$ is quite large (up to $\pm$ 70%) in the troposphere and in the polar lower stratosphere. Values are only shown up to 425 K, because σ' decreases to values of less than 20% of σ_{ref} in most of the domain above 425 K. The large latitudinal variations in the static stability in the UTLS region have important implications for the influence of stratospheric PV anomalies on the troposphere, since the depth at which the influence of a PV anomaly is felt is proportional to σ. An overestimation of σ will lead to an overestimation of the influence of the stratospheric PV anomaly on the tropospheric winds.

Figure 2.2b shows the January climatological Z'_θ-field in PVU (1 PVU = 10^{-6} K m^2 kg^{-1} s^{-1}), where for plotting purposes, the PV is multiplied by a scaling factor

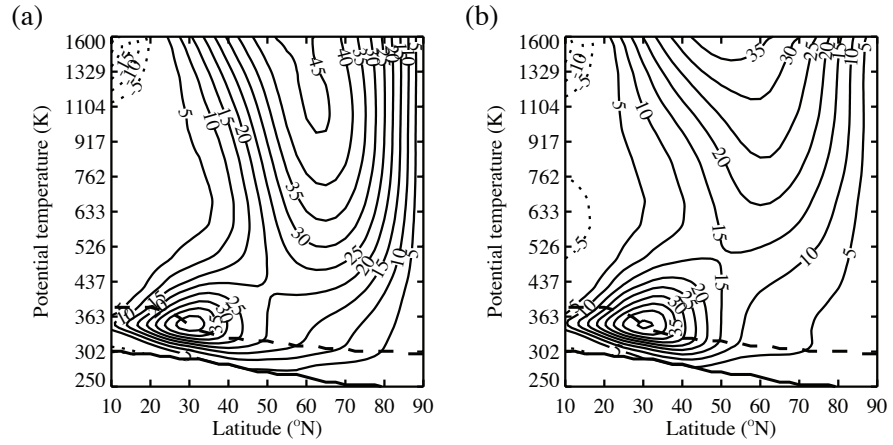

Figure 2.4: *January mean, zonal mean zonal wind (in m s^{-1}), derived from the ERA-40 dataset, for the (a) positive AO case and (b) negative AO case. Contours every 5 m s^{-1}, zero line omitted and negative values indicated by thin dashed lines.*

$(\theta/\theta_0)^{-9/2}$ (*Lait*, 1994), with $\theta_0 = 380$ K. We see two distinct positive PV anomalies: one broad, flat anomaly near the tropopause, below 425 K, that extends from the pole to the subtropics, and one more narrow, tall anomaly in the polar stratosphere, above 425 K, that only extends from the pole to about 60°N. We will refer to the former anomaly as the "UTLS PV anomaly". The latter anomaly will be referred to as the "stratospheric polar cap PV anomaly".

The average distributions of the January PV anomaly for the positive AO case, the negative AO case and the difference between the positive and negative AO case are plotted in Figs. 2.3a, 2.3b and 2.3c, respectively. The positive and negative AO case values are determined from the corresponding mean u and p fields, where the mean is taken over the January months that obey the AO criterion. Clearly, the stratospheric polar cap PV anomaly is larger in amplitude and extends further downward when the AO is in the positive phase. The amplitude of the UTLS PV anomaly is slightly stronger between 40°N and 50°N in the negative AO phase. This leads to a larger meridional PV gradient in the subtropics if the AO index is negative, resulting in a stronger subtropical jet. Nevertheless, the UTLS PV anomaly has a slightly larger amplitude over the pole if the AO index is positive. The zonal mean zonal wind averaged over the specific January months that satisfy the AO criterion is shown for the positive and negative AO cases in Fig. 2.4a and Fig. 2.4b, respectively. The observed subtropical jet is indeed stronger for the negative AO case. However, the polar night stratospheric jet is much stronger in the positive AO phase.

It is interesting to examine which part of the difference in PV as shown in Fig. 2.3c

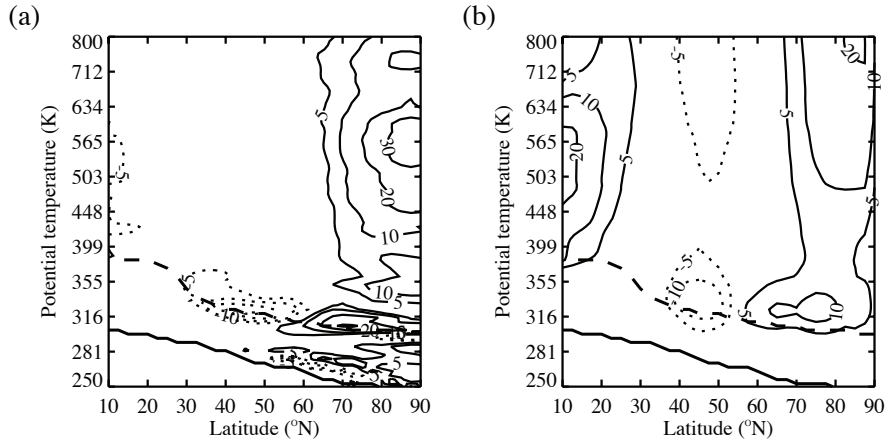

Figure 2.5: *Difference in scaled Z'_θ between the positive and negative AO case as a percentage of the climatological reference scaled PV for (a) calculation of the PV with ζ held at its climatological value and (b) with σ held at its climatological value. Contours at $\pm$ 5%, 10% and then every 10%.*

is related to variations in the relative vorticity, and which part to variations in the static stability. To study this, the PV is calculated twice for both the positive and negative AO cases, firstly the climatological relative vorticity is used, to study the influence of variations in σ, and secondly the climatological static stability is used, to study the influence of variations in ζ. The contributions to the PV anomaly difference are shown in Fig. 2.5a and 2.5b for the static stability and relative vorticity, respectively. The contributions are given as a percentage of the climatological reference PV field to make comparison of different isentropic levels easier. Between 600 K and 800 K, variations in static stability and in relative vorticity both contribute to the PV anomaly difference, by about equal amounts, while below 600 K the static stability contribution dominates. In the UTLS region the influence of static stability variations on the PV anomaly difference is about + 20% of the climatological reference PV from mid- to high latitudes and - 20% in the subtropics, compared to influences of the same sign of about 5 to 10% for the relative vorticity contributions. This indicates that the variations in the static stability to a large degree determine the difference in the UTLS PV anomaly between positive and negative AO cases. *Black* (2002) does not take these static stability variations into account, and therefore considers only the part that is related to variations in the relative vorticity (Fig. 2.5b). We consider the total PV difference, and PV inversion will result in a static stability anomaly as well as a wind anomaly. In section 2.4 we will examine how variations in the static stability affect the Rossby scale height.

2.4 Effect of stratospheric PV on tropospheric winds

Equation 1.6 is solved, by successive relaxation, for the climatological PV as derived from the zonal mean and time mean (1958-2002) January u and p ERA-40 fields. The resulting "inverted wind field" (Fig. 2.6a) is compared to the ERA-40 wind field and the difference is shown in Fig. 2.6b. The differences between the ERA-40 wind and the inverted wind are reasonably small in most of the domain. Differences up to 5 m s^{-1} occur near the surface in the subtropics, indicating that thermal wind balance might not be valid in these regions.

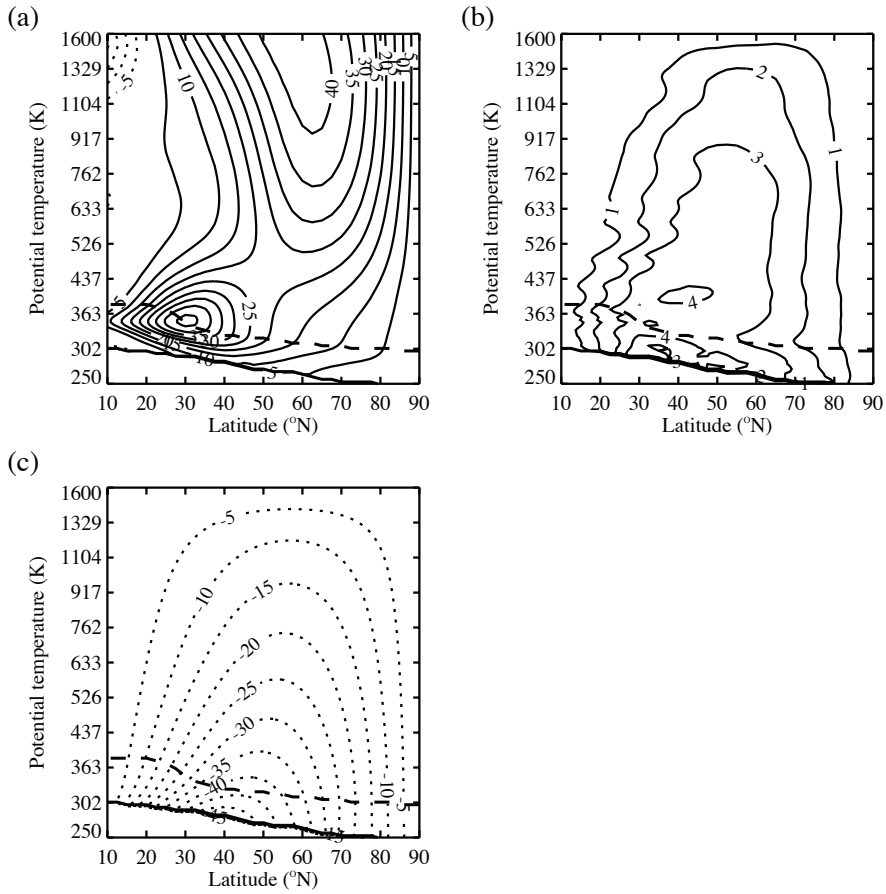

Figure 2.6: *(a) Wind (m s^{-1}) obtained from inverting the ERA-40 zonal mean PV field for January. (b) Inverted minus ERA-40 wind (m s^{-1}) for January. (c) Wind (m s^{-1}) obtained from inverting the ERA-40 zonal mean reference PV field for January and imposing thermal wind balance at the lower boundary. The contour interval is 5 m s^{-1} for (a) and (c) and 1 m s^{-1} for (b), zero lines are omitted and negative values are indicated by thin dashed lines.*

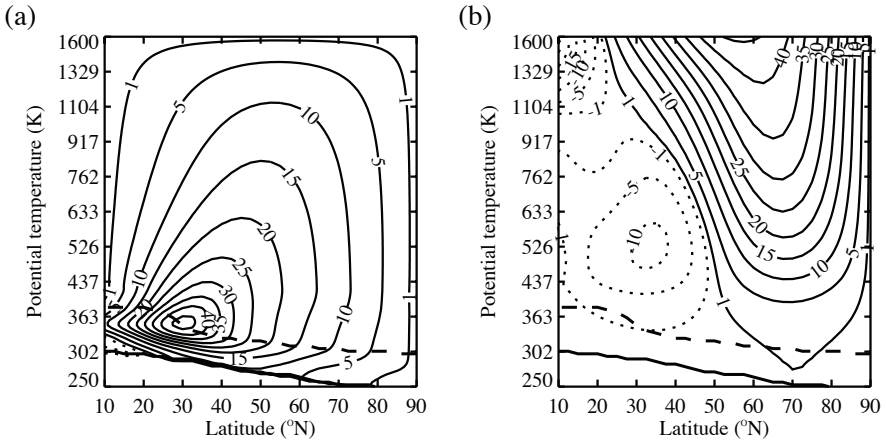

Figure 2.7: *Inverted wind (m s^{-1}) for the positive AO case, obtained from inverting the PV field with a nonzero part of the PV anomaly (a) between the surface and 425 K (UTLS PV anomaly) and (b) between 425 K and 1600 K (stratospheric polar cap PV anomaly). Contours as in Fig. 2.4, and 1 m s^{-1} contour added.*

Figure 2.6c shows the wind field that is obtained from inverting the reference PV, with zero wind as boundary conditions at the pole, at 10°N and at the top of the domain, but imposing thermal wind (Eq. 1.12) at the lower boundary. Since the reference PV does not induce a wind field, the resulting wind is the influence of the lower boundary condition on the wind field. This shows that, to obtain a realistic wind field, it is very important to take the variation with latitude of the temperature at the lower boundary into account.

The PV anomaly fields shown in Fig. 2.3 are now split into two parts: the UTLS PV anomaly which extends from the surface to 425 K and the stratospheric polar cap PV anomaly which extends from 425 K to 1600 K (425 K $\sim$ 17 km, 1600 K $\sim$ 40 km). Both PV anomalies are inverted separately (with the reference PV as a background state), for both the positive and negative AO cases. The results are shown in Fig. 2.7 and 2.8 for the positive and negative AO cases, respectively. The boundary condition at 10°N is zero wind outside the area of the PV anomaly (which is the same as determined with the circulation theorem when the reference PV and static stability are used). At the upper boundary we again impose the average ERA-40 wind of the specific months which we are considering for the stratospheric polar cap PV anomaly. The wind at the upper boundary is set to zero for the UTLS PV anomaly. At the lower boundary a realistic thermal wind (according to Eq. 1.12) is imposed for the UTLS PV anomaly, while zero thermal wind at the surface is imposed for the stratospheric polar cap PV anomaly. The surface temperature distribution is thus taken together with the PV anomaly that borders the surface. Figures 2.7a and

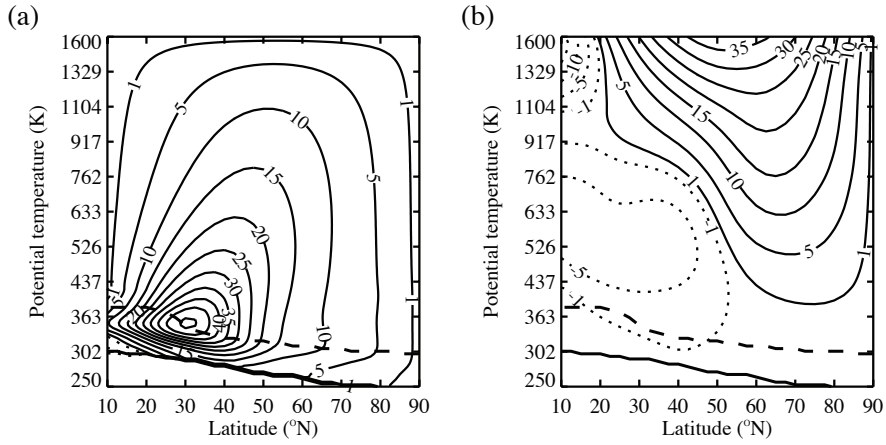

Figure 2.8: *Same as Fig. 2.7, but for the negative AO case.*

2.8a show that the subtropical jet can be attributed to the UTLS PV anomaly. This PV anomaly also affects the vertical wind shear in the midlatitude troposphere and affects the stratospheric winds up to the middle stratosphere from the subtropics to the high latitudes. Figures 2.7b and 2.8b show that the stratospheric polar cap PV anomaly is needed to explain the high wind speeds in the polar vortex, and that it mainly affects the midlatitude winds in the stratosphere itself. For the positive AO case (Fig. 2.7b) there is also some influence on the winds in the extratropical troposphere, in agreement with *Black* (2002) and *Ambaum and Hoskins* (2002). For the negative AO case (Fig. 2.8b), the wind speeds in the lower stratosphere are reduced compared to the positive AO case or the climatology.

The sum of the inverted winds from the separate PV anomalies is practically the same as the inverted wind from the sum of the PV anomalies, despite the nonlinearity of the inversion. This indicates that piecewise PV inversion can indeed be applied to the separate PV anomalies, using the appropriate boundary conditions. Whether the lower boundary condition can be seen as a separate part of the solution can be tested by inverting both climatological PV anomalies twice, once with thermal wind as lower boundary condition, and once with zero thermal wind as lower boundary condition. Subtracting the wind field that is obtained from inversion of the reference PV with thermal wind as lower boundary condition (Fig. 2.6c) from the wind field that is obtained by inverting the stratospheric PV anomaly with thermal wind as lower boundary condition, is indeed practically identical to the wind field that results from inversion of the stratospheric PV anomaly with zero thermal wind as lower boundary condition. This indicates that the stratospheric PV anomaly can be seen separately from the temperature at the lower boundary, and that piecewise PV inversion can be applied to

examine the influence of the stratospheric PV on the wind field. For the UTLS PV anomaly, the sum of the wind field that is obtained from inversion of the reference PV with thermal wind as lower boundary condition and the wind field that is obtained by inverting the UTLS PV anomaly with zero thermal wind as lower boundary condition, can be compared to the wind field from inversion of the UTLS PV anomaly with thermal wind as lower boundary condition. However, now large differences are found between the sum and the direct inversion, indicating that the UTLS PV anomaly is inextricably connected to the lower boundary temperature structure in the inversion. It is therefore not possible to examine the UTLS PV anomaly separately from the thermal wind at the lower boundary. Similarly, it is found that applying piecewise PV inversion on the tropospheric and stratospheric part of the UTLS PV anomaly separately is not possible, indicating that also the stratospheric part of this PV anomaly is strongly linked to tropospheric processes.

Figure 2.9 presents the difference in inverted wind between the positive and negative AO cases with a PV anomaly over the whole domain (Fig. 2.9a) and a PV anomaly above 425 K (Fig. 2.9b). The ERA-40 wind difference between positive and negative AO cases is very similar to the inverted difference given in Fig. 2.9a (with differences smaller than 1 m s^{-1} over most of the domain). Figure 2.9b shows that the stratospheric polar cap PV anomaly difference is related to a tropospheric wind difference of about 0.5 to 1 m s^{-1} from the mid- to high latitudes. Only a limited part of the difference between positive and negative AO cases in upper tropospheric vertical wind shear at midlatitudes can thus be attributed to the difference in stratospheric PV.

To examine the influence of the lower boundary condition on the inverted wind difference between positive and negative AO cases, the inversions that led to Fig. 2.9a have been repeated with the climatological lower boundary condition. The climatological surface temperature is thus used for the inversion of both AO cases, instead of the surface temperatures that correspond to the positive and negative AO cases. Figure 2.9c shows the difference as compared to using realistic boundary conditions. The difference in surface temperature between positive and negative AO cases thus decreases the inverted wind difference by the amount displayed in Fig. 2.9c. This means that use of the climatological surface boundary condition would clearly overestimate the wind difference. So in order to explain fully the observed wind differences between the positive and negative AO cases by means of PV inversion, the difference in surface temperature between the two AO cases needs to be taken into account. This is understandable, since the UTLS PV anomaly and the lower boundary temperature distribution are strongly coupled in the inversion.

The vertical wind shear in the troposphere at midlatitudes is much larger for the positive AO case than for the negative AO case (Fig. 2.4). The vertical wind shear is important for the baroclinic instability and cyclogenesis. As a measure of baroclinicity

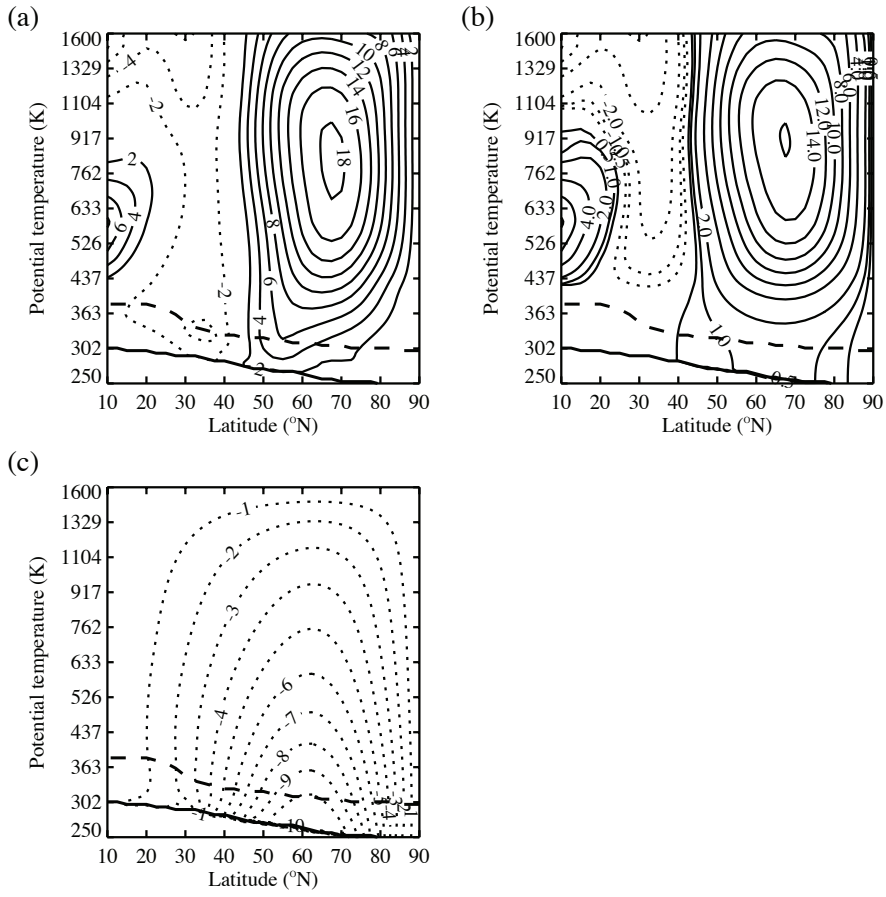

Figure 2.9: *Difference in inverted wind (m s^{-1}) (positive - negative AO case), obtained from inverting the PV field with a nonzero part of the PV anomaly in (a) the total domain, and (b) between 425 K and 1600 K (stratospheric polar cap PV anomaly). (c) Influence of the variations in surface temperature (positive - negative AO case) on the inverted wind difference, compared to using the climatological surface temperature distribution for both the positive and the negative AO case (see text for further explanation). Contours every 2 m s^{-1} for (a) and (b), with $\pm$ 0.5 and $\pm$ 1 m s^{-1} contours added for (b), and contours every 1 m s^{-1} for (c), zero lines are omitted and negative values are indicated by thin dashed lines.*

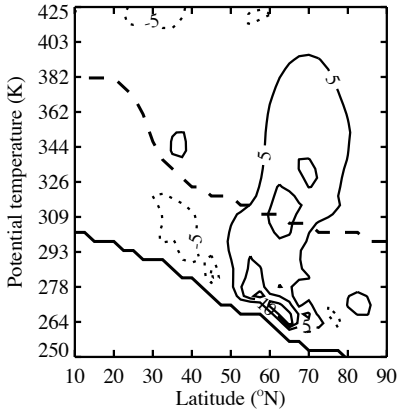

Figure 2.10: *January mean measure of the baroclinicity or Eady growth rate (in s^{-1}) for the positive AO case minus the negative AO case, derived from the wind field and static stability resulting from the inversion of the UTLS PV anomaly. Contours in units of 10^{-7} s^{-1} with a contour interval of $5{\cdot}10^{-7}$ s^{-1} (zero lines omitted).*

b we use the Eady growth rate (*Hoskins and Valdes*, 1990):

$$b = \frac{0.31 f \left| \frac{\partial u}{\partial z} \right|}{N} \tag{2.1}$$

with N the Brunt-Väisälä frequency, which is proportional to the square root of the static stability (and the static stability is proportional to the inverse of σ).

Since the stratospheric polar cap PV anomaly hardly influences the tropospheric winds, we only examine the baroclinicity that is related to the UTLS PV anomaly. Figure 2.10 demonstrates that the baroclinic growth rate between 50°N and 70°N is greater for the positive AO cases than for the negative AO cases throughout the full depth of the troposphere. It is indeed observed that more and deeper cyclones are formed during January months with a positive AO index than during January months with a negative AO index (e.g., *Sickmöller et al.*, 2000). The stronger equator-to-pole heat transport associated with the more numerous or stronger cyclones might explain an important part of the higher midlatitude temperatures during winter months with a positive AO index compared to winter months with a negative AO index. Our results agree with those of *Wittman et al.* (2007), who found that shear in the lower stratosphere affects baroclinic development, and that a higher shear is associated with a higher than normal tropospheric Northern Annular Mode (NAM) index (the NAM index is similar to the AO index).

Figure 2.5 showed that part of the PV anomaly field is related to differences in the static stability between positive and negative AO cases. The change of the wind shear

and the static stability during the PV inversion are coupled, therefore it is not possible to examine the separate influences on the baroclinicity. It is, however, possible to study the influence of variations in the static stability on the Rossby scale height, which is a measure of the depth at which the influence of a PV anomaly is felt. The Rossby scale height is proportional to the inverse of the Brunt-Väisälä frequency, and is calculated for both AO cases with only variations in N taken into account and other factors held at their climatological value. In the mid- to high latitude tropopause region the difference in Rossby scale height (positive AO - negative AO) is about -5% of the climatological Rossby scale height, or of the order of -500 m. This means that neglecting variations in the static stability would underestimate the influence of the stratospheric part of the UTLS PV anomaly on the tropospheric winds for the negative AO case compared to the positive AO case, and thus overestimate the difference between the cases. This explains the results of *Black* (2002), who does not take variations in static stability into account and indeed finds a somewhat larger influence of the stratospheric PV on the tropospheric winds than we find in the present study.

2.5 Conclusion

In this chapter the connection between the average AO index in January and the January average zonal mean potential vorticity distribution in the Northern Hemisphere is studied. Using nonlinear PV inversion, we determine the large-scale zonal mean adjustment to amplitude variations in the monthly average zonal mean potential vorticity that are associated with the Arctic Oscillation. By defining the PV anomaly as that part of the PV that induces a wind, we identify two separate positive PV anomalies in the Northern Hemisphere (centred over the north pole), i.e. a relatively broad and shallow PV anomaly in the upper troposphere and lower stratosphere and a relatively tall PV anomaly higher in the stratosphere (above 425 K). The amplitude of the latter PV anomaly is much larger during January months with a positive AO index than during January months with a negative AO index. According to the solution of the PV inversion equation, the influence on the wind of the latter PV anomaly is largest in the stratosphere, but can also explain a part of the difference in mid- to high latitude tropospheric wind between January months with a positive AO index and January months with a negative AO index. These results are in agreement with those of *Black* (2002) and also with the ideas presented by *Ambaum and Hoskins* (2002).

We find that by far the largest part of the monthly variability in the tropospheric zonal mean zonal wind that accompanies the variations in the monthly mean AO index is induced by the variability in the amplitude and form of the UTLS PV anomaly. In the lower stratosphere and upper troposphere the static stability deviates substantially from the latitude independent reference state. According to the solution of the PV inversion equation, the UTLS PV anomaly influences the vertical wind shear as well as

the static stability at midlatitudes, leading to a larger than average degree of baroclinic instability at midlatitudes when the AO index is positive. This is a possible explanation for the observed higher than average frequency of intense midlatitude cyclones during winter months with an average positive AO index.

We conclude that the zonal mean dynamical impact of the stratosphere on the troposphere can be described by large-scale adjustment to amplitude variations in the zonal mean stratospheric PV distribution. This conclusion seems to disagree with the conclusion of *Charlton et al.* (2005a), who state that "the dynamical impact of the stratosphere on the troposphere cannot be described by large-scale adjustment to the stratospheric PV distribution". The apparent inconsistency is routed in the fact that *Charlton et al.* (2005a) do not investigate the effect of amplitude variations in the zonal mean stratospheric PV distribution but only investigate the effect of zonal asymmetries in the stratospheric PV distribution.

The marked difference between the positive AO phase and the negative AO phase in the amplitude of the PV anomaly above 425 K is probably associated with meridional mixing or displacement of potential vorticity when Rossby waves, which propagate upwards from the troposphere, break in the stratosphere, especially during sudden stratospheric warming events, such as in January 1985. The question what determines the differences, between the positive AO phase and the negative AO phase, in the amplitude and form of the UTLS PV anomaly is open, but we hypothesize that the intensity of the hydrological cycle in the tropics and wave breaking near the tropopause (the formation of cut-off lows and blocking highs) in the latitude band between approximately 30°N and 70°N both play a role.

Acknowledgements

The ECMWF ERA-40 data used in this study have been provided by ECMWF. The AO related data set that is used has been provided by the Climate Explorer website (http://climexp.knmi.nl).

3

The seasonal cycle of the potential vorticity distribution in the stratosphere

- ⋆ -

A zonal mean climatology of the isentropic potential vorticity (PV) anomaly is presented for the Northern Hemisphere (NH) and the Southern Hemisphere (SH), based on ECMWF ERA-Interim reanalysis data for 1989-2008. The PV anomaly is defined as that part of the PV field that induces a wind field according to the invertibility principle. The advantages of this definition of the PV anomaly are that it can be intuitively translated to an average zonal wind, and that it illustrates better how very abrupt the transitions in potential vorticity are in spring and autumn. Two PV anomalies are distinguished: a stratospheric polar cap PV anomaly above 400 K and a flat but wide PV anomaly in the upper troposphere/lower stratospheric (UTLS) region between about 300 K and 360 K. The seasonal cycle in the UTLS PV anomaly is relatively small, and related to the tropical precipitation and the positions of the tropical and the extratropical tropopause. The annual cycle in the stratospheric polar cap PV anomaly is caused by radiative cooling in the polar night, which causes the stratospheric PV anomaly to increase in winter, while heating due to absorption of solar radiation by ozone reduces the PV in spring. In the SH, the break up of the polar vortex in spring starts in the upper stratosphere and extends downward in time, while the break up of the NH vortex seems to start in the lower stratosphere. Wave effects and ozone concentrations are discussed to explain these interhemispheric differences. The midlatitude PV anomaly exhibits an annual cycle in the lower stratosphere and a semi-annual cycle above. The midlatitude PV is strongly coupled to the polar PV, where wave events cause the polar (midlatitude) PV anomaly to be lower (higher) in the NH than in the SH.

This chapter is based on:
Hinssen, Y., A. van Delden, and T. Opsteegh, The seasonal cycle of the potential vorticity distribution in the stratosphere, *Submitted to Quarterly Journal of the Royal Meteorological Society*, 2010.

3.1 Introduction

Over the last decades, many studies have indicated that the coupling between the troposphere and stratosphere is a two-way interaction. The troposphere forces the stratosphere from below, but changes in the stratosphere can also influence the state of the troposphere (see *Haynes*, 2005, for a short overview of research on stratosphere-troposphere coupling, and a more extensive overview of stratospheric dynamics in general). *Baldwin and Dunkerton* (1999, 2001) showed that Arctic Oscillation anomalies first appear in the stratosphere and propagate downward in time. This triggered an increased interest in the stratosphere, as information from the stratosphere might be used to improve and/or extend weather forecasts (*Thompson et al.*, 2002; *Baldwin et al.*, 2003; *Charlton et al.*, 2004; *Roff et al.*, 2010). The influence of the stratosphere on the troposphere was also shown in potential vorticity (PV) inversion studies, which showed that changes in the stratospheric PV influence the winds in the troposphere (e.g., *Hartley et al.*, 1998; *Black*, 2002). *Scaife et al.* (2005) show that changes in the stratosphere could account for a large part of the regional surface climate change over Europe and North America between 1965 and 1995. Changes in the stratospheric greenhouse gas concentrations might thus have a non-negligible effect on the tropospheric circulation.

The above mentioned studies (and many more) point out that the state of the stratosphere influences the troposphere, indicating that it is important to understand the physical processes in the stratosphere. The European Centre for Medium-Range Weather Forecasts (ECMWF) ERA-Interim reanalysis dataset is a useful tool to examine the stratosphere, since it combines the available stratospheric measurements into a global dataset. The recent ERA-Interim dataset, available from 1989 onwards, has an improved representation of the stratosphere compared to the previous ECMWF reanalysis (ERA-40). *Fueglistaler et al.* (2009) treat some aspects of the quality of the ERA-Interim data compared to the ERA-40 data, and show that the ERA-Interim data gives a better representation of the diabatic heating in the stratosphere. The ERA-Interim data therefore provides a solid basis for the computation of a stratospheric climatology over the last 20 years (1989-2008), which gives a representation of the current state of the stratosphere. Such a climatology can be used to analyse the processes that play a role in the stratosphere and determine its seasonal cycle. Furthermore, it can be used as a reference for future changes of the stratosphere.

A way to represent the state of the stratosphere is by the isentropic PV distribution. The PV is a useful variable to represent the state of the atmosphere, since it presents a compact way to describe the dynamics of the atmosphere, it shows the influences of diabatic effects on the atmosphere, and through the invertibility principle (*Kleinschmidt*, 1950; *Hoskins et al.*, 1985) the PV is directly linked to all other dynamical fields. Furthermore, local changes in the PV can have a nonlocal effect on the wind

field, so that changes to the stratospheric PV distribution can be related to circulation changes in the troposphere.

Here we present a climatology (1989-2008) of the zonal mean stratospheric PV distribution for both hemispheres using the recent ERA-Interim reanalysis dataset. We define a PV anomaly as that part of the PV field that induces a wind field according to the solution of the PV inversion equation (see section 1.2.2). With this definition we are able to distinguish very clearly two separate PV anomalies centred over the pole: one at the tropopause and the other in the polar night stratosphere above about 400 K. We have computed the seasonal cycle of both anomalies. Distortions of the polar vortex, which are the result of for example sudden stratospheric warmings (SSWs), and also the break up of the vortex in spring are clearly visible in the polar cap PV anomaly. Comparison of the midlatitude PV anomaly with the polar cap PV anomaly provides information on the displacement and/or mixing of PV off the pole.

The importance of the difference in planetary wave activity between the Northern Hemisphere (NH) and Southern Hemisphere (SH) in explaining interhemispheric differences in the vortices and the impact of these differences on the amount of ozone depletion is noted, for example, by *Schoeberl and Hartmann* (1991). We use the 100 hPa eddy heat flux as a measure of the amount of wave forcing from the troposphere to the stratosphere and ERA-Interim ozone mass mixing ratio data in an attempt to explain the differences in stratospheric PV between the two hemispheres.

To understand the formation of the PV anomaly at the tropopause, the relation between the strength of the Hadley circulation, as measured by the ERA-Interim tropical precipitation, and the PV anomaly near the tropopause is investigated.

The climatological PV distribution in the NH has been described before by *Baldwin and Dunkerton* (1998) and *Brunet et al.* (1995). They respectively examine the PV on the 600 K and on the 315 K isentropic surface. The present work is also related to that of *Waugh and Randel* (1999) and *Harvey et al.* (2002), who present a climatology of the Arctic and Antarctic polar vortices using a vortex oriented framework. *Waugh and Randel* (1999) use elliptical diagnostics to define the area, centre, elongation and orientation of the vortices, while *Harvey et al.* (2002) show the mean geographical distribution of polar vortex and anticyclone frequency. The zonal mean climatology presented here complements the previous studies. The main driver of the seasonal cycle in the stratosphere is the incoming solar radiation, while the outgoing longwave radiation is to a large part determined by the concentration of greenhouse gases. To a first order, the forcing of the stratospheric seasonal cycle is thus zonally symmetric, while wave processes cause deviations from the zonal mean state. By using a PV anomaly framework instead of a vortex oriented framework we present a different view of the stratosphere. We do not study the exact form and position of the polar vortices, but show that the seasonal cycle, including vortex formation and break up, are very well visible in the PV anomaly and that influences of waves and ozone

concentrations can be detected as well. In addition, we present a climatology for the midlatitudes as well as for the polar area and for a wide range of stratospheric levels, ranging from the tropopause up to 1250 K. To our knowledge such a climatology of the PV anomaly has not been published before. We use the 1989-2008 ERA-Interim data, which is the most accurate and complete climatology of the stratosphere presently available.

Section 3.2 presents the data used to construct the climatology of the PV anomaly and our definition of a PV anomaly. The resulting monthly mean climatological PV anomalies are shown in section 3.3, together with the seasonal cycles of the polar cap PV and the midlatitude PV. Additionally, the NH and SH heat flux and ozone distributions are compared to find an indication for the interhemispheric differences in PV anomaly. Finally, a summary of our findings and some concluding remarks are given in section 3.4.

3.2 Data

The ECMWF ERA-Interim reanalysis data at 37 pressure levels between 1000 hPa and 1 hPa is used for the analysis. The daily data (from the analysis of the atmospheric model at 12.00 UTC) of the zonal wind, meridional wind, temperature and the ozone mass mixing ratio for the 1989-2008 period are interpolated from isobaric to isentropic levels by the method described by *Edouard et al.* (1997). Daily surface values of the total precipitation (from the forecast of the atmospheric model at 00:00 UTC, step 24, to get an idea of the daily precipitation) are also used for the years 1989-2008. In order to make optimal use of the available data, a stretched grid in the vertical direction is employed. The isentropic potential vorticity, Z_θ, is then calculated from Eq. 1.1, using the isentropic density (σ, Eq. 1.3) and the isentropic relative vorticity given by:

$$\zeta_\theta = -\frac{1}{a}\frac{\partial u}{\partial \phi} + \frac{u \tan \phi}{a} + \frac{1}{a cos\phi}\frac{\partial v}{\partial \lambda} \tag{3.1}$$

Here u is the zonal wind, v is the meridional wind, a is the radius of the Earth, ϕ is the latitude, λ is the longitude. The PV is calculated as a function of latitude, longitude and potential temperature (θ) to allow examination of the two dimensional structure of the vortex at isentropic levels (as shown in Fig. 1.3, for example). Zonal averaging and averaging over the whole 20-yr period gives a dataset of zonal mean PV, zonal wind, pressure (p) and ozone mass mixing ratio at isentropic levels. The domain ranges from 90°N to 90°S in the horizontal, with a resolution of 1.5°, and from the Earth's surface to about 1250 K in the vertical [1], with a resolution varying from about 1.7 K near the

[1] In chapter 2 the upper boundary of the domain is 1600 K, which was found to be a suitable upper boundary of the domain for the January monthly mean ERA-40 data. However, the daily ERA-Interim data occasionally attains pressure values below 1 hPa at 1600 K. Therefore, 1250 K was found to be a more

surface to 10 K in the upper layers. The lower boundary of the domain is determined by the available data, and for each latitude this is defined as the first isentropic level for which data is available along the full latitude circle, meaning that the pressure is below 1000 hPa at all longitudes along this latitude circle. We will refer to this lower boundary as the 'surface', but it should be noted that this does not correspond to the actual surface of the Earth, but is located in the lower troposphere. This surface-isentropic level varies with latitude, during NH winter from around 260 K at 90°N to about 310 K near the equator.

The zonal mean PV and the isentropic density are split into a reference state ($Z_{\theta,\mathrm{ref}}$) and an anomaly (Z'_θ) as described in section 1.2.2. The reference isentropic density σ_{ref} is the area-weighted average of σ over the domain in question. In our case we choose the area poleward of 10° north (south), for the NH (SH). Therefore, σ_{ref} only depends on the height (θ) and the hemisphere. The PV anomaly, Z'_θ, represents that part of the PV field that induces a wind field, according to the PV inversion equation, while the reference PV is defined in such a way that it does not induce a wind field. The seasonal cycle of the stratospheric PV distribution can be studied by examining the seasonal cycle in the PV anomaly, since the seasonal cycle in the reference PV is negligible.

For each year a daily polar cap PV anomaly is determined as the area-weighted average of the zonal mean PV anomaly poleward of 70°. This is done for the NH and SH separately. Similarly, a daily midlatitude PV anomaly is determined as the area-weighted average of the daily zonal mean PV anomaly between 35° and 55°.

The daily polar cap ozone mass mixing ratio is also determined for each year, as the area-weighted average zonal mean ozone mass mixing ratio between 70° and 90° for both hemispheres.

The daily heat flux, $[v^\star T^\star]$, is calculated from the meridional wind and temperature at pressure levels for every year (a star represents a deviation from the zonal mean quantity and the brackets indicate zonal averaging). The area-weighted average heat flux at 100 hPa is then determined between 40° and 80° for both hemispheres. This value is used as a measure of the wave forcing of the stratosphere by the troposphere.

The daily tropical precipitation is determined for each year, as the area-weighted average of the zonal mean precipitation between 20°N and 20°S. Since the tropical precipitation is strongly linked to the upward branch of the Hadley circulation, it is used as a measure of the strength of the Hadley circulation.

Daily climatologies of the polar cap PV anomaly, midlatitude PV anomaly, polar cap ozone mass mixing ratio and the 40°-80° 100 hPa heat flux are obtained by averaging over the 20 year period.

suitable upper boundary of the domain for the present study.

3.3 Seasonal cycle of the stratospheric potential vorticity

3.3.1 The monthly mean PV anomaly

The zonal and monthly mean PV anomaly in PVU (1 PVU = 10^{-6} K m^2 kg^{-1} s^{-1}) is shown in Fig. 3.1 and Fig. 3.2 for the NH and SH, respectively. Throughout the remainder of this chapter, we multiply the SH PV anomaly values by minus one. Therefore, with an increase in PV anomaly we indicate increases in the NH PV anomaly or in minus the SH PV anomaly. The position of the tropopause, defined as the 2 PVU line in the total PV field, is indicated in the figures. For each hemisphere two distinct PV anomalies are visible. One is a broad, flat PV anomaly in the upper troposphere/lower stratosphere (UTLS) region, between about 300 K and 360 K and extending from the pole to the subtropics. This PV anomaly is present throughout the whole year. The other is a tall PV anomaly in the polar stratosphere above about 400 K, which extends from the pole to about 50°. This PV anomaly is much more variable throughout the year. We will refer to the former anomaly as the "UTLS PV anomaly", while the latter anomaly will be referred to as the "stratospheric polar cap PV anomaly".

The positive stratospheric polar cap PV anomaly forms in autumn in the upper stratosphere, extends to the lower stratosphere in winter and disappears again in spring (early spring in the NH, late spring in the SH), after which a PV anomaly with a much smaller amplitude and of the opposite sign forms in summer. The seasonal cycle of the polar cap PV anomaly is strongly driven by radiative effects. The increase in PV in autumn is related to cooling due to emission of longwave radiation by greenhouse gases during the polar night. The emission of longwave radiation is proportional to temperature, and the temperature in the stratosphere in general increases with height (with possibly a slight decrease with height in the lower stratosphere). The upper levels therefore emit more radiation than they receive, which leads to cooling of the upper layers. The increase in cooling with increasing potential temperature due to the increasing importance of cooling to space and the increase in temperature with height is also mentioned by *Rosenfield et al.* (1994). Once the upper layers have cooled, the lower levels will receive less radiation from above, and the cooling extends downwards. The downward extension of the net radiative cooling over the pole during winter is illustrated in *Kiehl and Solomon* (1986) (their figure 8), *Gille and Lyjak* (1986) (their figure 11) and *Mlynczak et al.* (1999) (their plate 2). The cooling continues throughout winter, although the magnitude of the cooling decreases as the temperature decreases (*Rosenfield et al.*, 1994). The decrease of the PV anomaly in spring is related to heating of the stratosphere due to absorption of solar radiation by ozone, once the polar regions are sunlit.

The summer and autumn months are very similar for both hemispheres. In winter, however, the NH vortex is regularly disturbed by upward propagating planetary

waves from the troposphere, and wave breaking events by which the polar vortex is irreversibly deformed (*McIntyre and Palmer*, 1983, 1984) reduce the strength of the NH vortex compared to the SH vortex. These wave breaking events cause filaments of high PV being pulled from the polar vortex and transported to the low and midlatitudes, thereby increasing the midlatitude PV in late winter and spring (this is seen in latitude-longitude plots of the PV anomaly at isentropic levels, indications of these PV filaments can be seen in Fig. 1.4). In spring, a final wave event moves the remains of the vortex off the pole and because of the increased heating due to the absorption by ozone, the vortex does not recover. Figure 3.1 shows that in May the remains of the NH vortex are still present around 45° in the middle stratosphere, slowly dissipating (likely due to mixing with the surroundings). The SH vortex is less disturbed by waves in midwinter, but wave effects become important in spring (noted also by e.g., *Randel*, 1988; *Thompson et al.*, 2005), starting in the upper stratosphere. Again filaments of high PV are torn off the vortex, but now mainly increasing the low latitude PV (around 20°, October in Fig. 3.2), leaving a band of low PV in the midlatitudes. This transport of PV to the low latitudes is related to the presence of a quasi-stationary anticyclone in the SH spring as illustrated by *Lahoz et al.* (1996) and *Charlton et al.* (2005b). The Aleutian High plays a similar role in the NH winter and spring (e.g., *McIntyre and Palmer*, 1983, 1984; *Baldwin and Holton*, 1988; *Harvey and Hitchman*, 1996). However, the NH anticyclone weakens and moves somewhat closer to the pole from winter to spring (found by inspection of the PV anomaly as a function of latitude and longitude at isentropic levels, and consistent with the results of the anticyclone frequency shown by *Harvey et al.*, 2002). This results in transport of PV to the low latitudes in winter, but to the midlatitudes in spring, consistent with Fig. 3.1. In the SH there is hardly any transport of PV to the low latitudes during winter, while the quasi-stationary anticyclone in spring transports PV from the vortex to the low latitudes. This is consistent with the results of *Harvey et al.* (2002), which show that the high latitude anticyclone frequency is largest in the SH during spring. The SH anticyclone remains quite strong until the final break up of the vortex, therefore PV is transported to low latitudes throughout spring, with only a slight shift to the midlatitudes in early summer (December in Fig. 3.2).

The NH climatological PV anomaly is an average over years with SSWs and years without SSWs. After a midwinter SSW event the vortex recovers in the upper stratosphere, but not always in the lower stratosphere. This is related to the more effective emission of longwave radiation to space by the upper levels than by the lower levels after a warming, similar to the formation process of the vortex in autumn. The cooling (and thus the recovery) therefore starts in the upper levels. Consequently, the break up of the climatological vortex seems to start in the lower stratosphere (April in Fig. 3.1). This is the visible effect of the SSWs on the NH climatology.

The structure of the break up of the SH vortex starting in the upper stratosphere

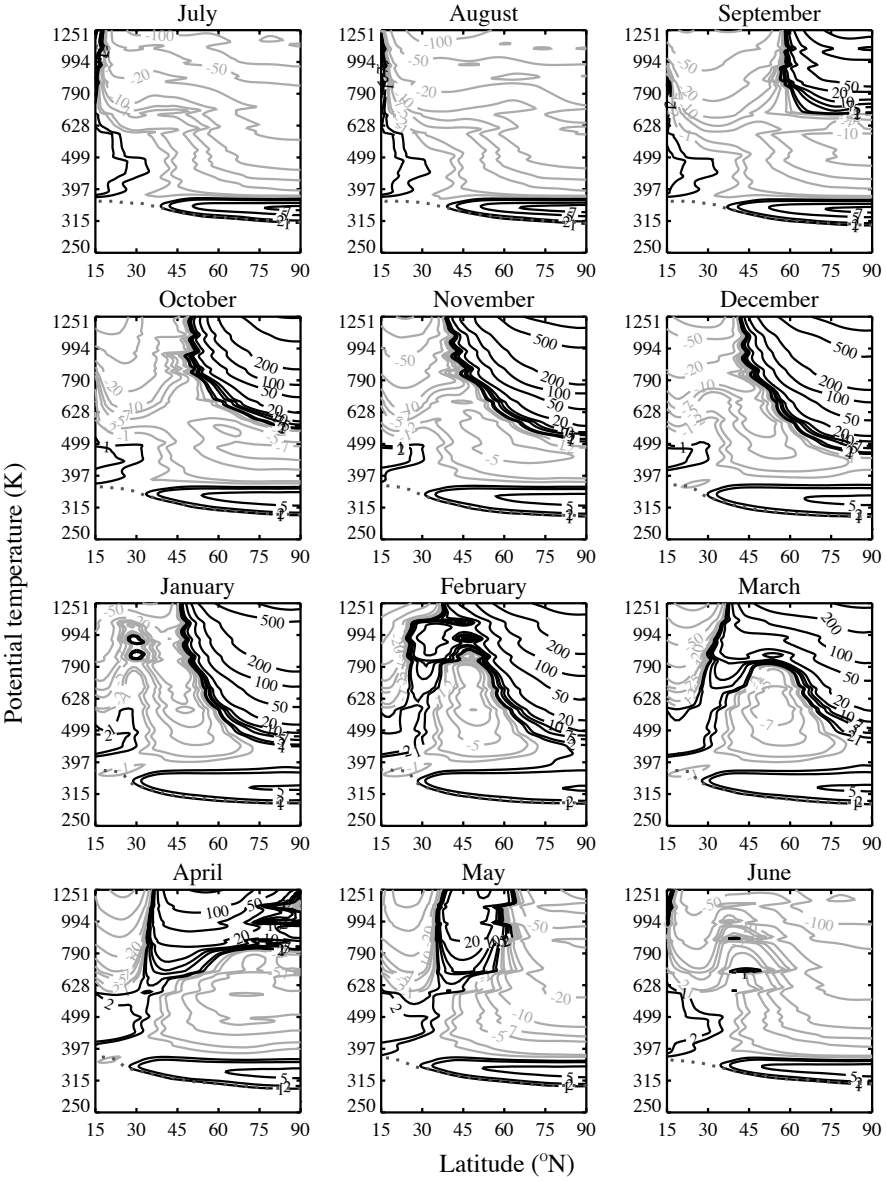

Figure 3.1: *Monthly mean zonal mean PV anomaly derived from the ERA-Interim climatology (1989-2008) as a function of latitude and potential temperature (K), for the Northern Hemisphere. Contours at ± 1, 2, 5, 7, 10, 20, 50, 100, 200, 500, 1000, 2000, 3000 PVU and negative values represented by grey lines. The monthly mean dynamical tropopause (2 PVU line in total PV field) is indicated by the dark grey dotted line.*

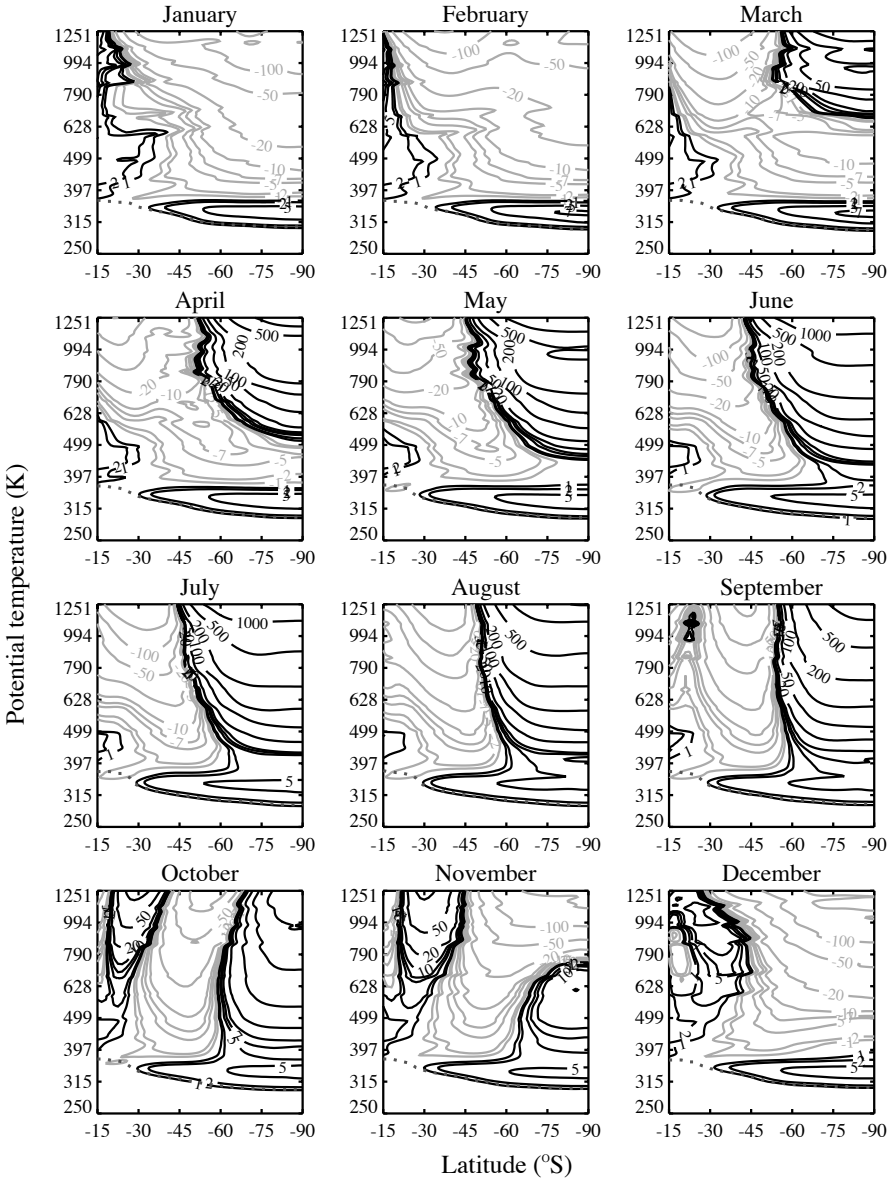

Figure 3.2: *Same as Fig. 3.1, but for minus the Southern Hemisphere values.*

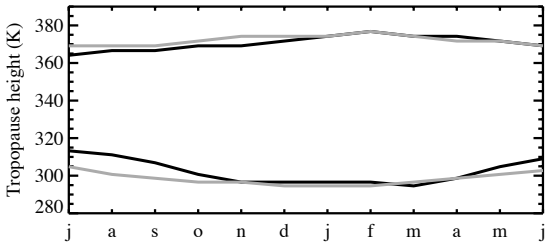

Figure 3.3: *Monthly mean tropopause height (in K) above the pole (lower lines) and above 15° (upper lines) for the NH (black lines) and the SH (grey lines). Months noted on the horizontal axis are for the NH, and the SH values are shifted by 6 months compared to this axis, so that winter is halfway the horizontal axis for both the NH and SH.*

and descending to the lower stratosphere in the following weeks, has been noted as a characteristic of the SH stratosphere in various other studies, among which those of *Hartmann* (1976) and *Mechoso et al.* (1988). The SH vortex does not break up until mid spring, when the absorption of solar radiation by ozone is a main driver of changes in the polar stratosphere. The incoming solar radiation will first be absorbed by the ozone in the higher levels of the stratosphere and extends its influence downward over time (*Shine*, 1987). Ozone depletion in the lower stratosphere will delay the break up of the vortex in the lower stratosphere even further, as will be illustrated in the next subsection. The break up of the SH vortex is thus for a substantial part driven by radiation, while the break up of the NH vortex is largely influenced by the wave activity during winter.

The seasonal cycle of the UTLS PV anomaly seems to be strongly related to the tropopause (see Figs. 3.1 and 3.2). The height of the tropical and polar tropopauses determine the upper and lower vertical boundaries of the UTLS PV anomaly, respectively. Figure 3.3 shows the height of the monthly mean tropopause (in terms of potential temperature) at the pole and at 15° for both hemispheres. As the pole warms in summer, the polar tropopause moves up. The vertical extent of the UTLS PV anomaly is then decreased compared to winter since the tropical tropopause has a smaller and opposite seasonal cycle. This effect is also visible in the SH, but the amplitude of the seasonal cycle in the SH is weaker than in the NH.

The horizontal extent of the UTLS PV anomaly is affected by the position of the Hadley circulation, and the related convection, release of latent heat and precipitation in the tropics. The Hadley circulation has its ascending branch over the summer hemisphere, thereby limiting the horizontal extent of the UTLS PV anomaly in this season.

To investigate the relation between the Hadley circulation and the UTLS PV anoma-

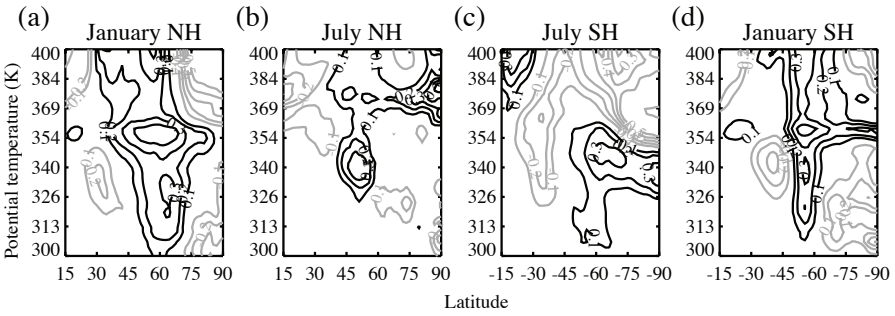

Figure 3.4: *Difference in monthly mean PV anomaly (in PVU) for the average of the five years with the highest monthly precipitation in the tropics (20° N-20° S) minus the average of the five years with the lowest monthly precipitation in the tropics, for (a) January (winter) in the NH, (b) July (summer) in the NH, (c) July (winter) in the SH and (d) January (summer) in the SH, as a function of latitude and potential temperature (K). Contours at ± 0.1, 0.2, 0.3, 0.4, 0.5 and then every 0.5 PVU.*

ly, we use the tropical precipitation (area-weighted average between 20°N and 20°S) as a measure of the strength of the Hadley circulation. We select the 5 years with the highest tropical precipitation in January (monthly total) (1990, 2007, 2006, 1991, 1998) and the 5 years with the lowest tropical precipitation in January (2000, 2004, 1996, 1992, 1993). The same is done for the month of July (highest precipitation years: 1991, 1992, 1989, 1994, 1993, lowest precipitation years: 2000, 2001, 2006, 1996, 2002). The difference between the total January precipitation averaged over the high precipitation years and the total January precipitation averaged over the low precipitation years is about 10 % of the total climatological January precipitation. For July this difference is about 7 % of the climatological value. The monthly and 5 year mean PV anomaly is calculated for the high and low tropical precipitation cases, for January and July. The difference in monthly mean PV anomaly for the high minus the low precipitation cases is shown in Fig. 3.4 for the UTLS region. This figure indicates that an increase in tropical precipitation is in general accompanied by an increase of the UTLS PV anomaly around 340 K at a latitude of about 60° in winter and 50° in summer, and a slight decrease of the PV anomaly equatorward of this. These changes in PV lead to an increase in the horizontal PV gradient in the subtropics, related to a stronger subtropical jet. A change in the PV gradient can also affect the position of the jet. However, the horizontal resolution of the data used here (1.5°) is too coarse to study small shifts in latitude. To study the influence of changes in tropical precipitation on the position of the jet and seasonal differences in more detail, model experiments are needed.

Since the seasonal cycle in the UTLS PV anomaly is much weaker than that in the stratospheric polar cap PV anomaly, the focus of this chapter will be on the polar cap

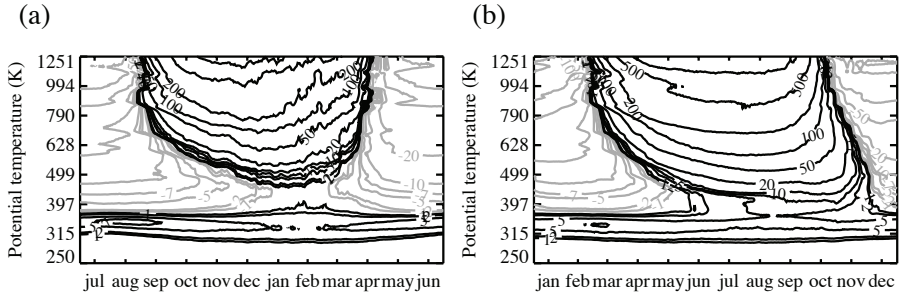

Figure 3.5: *Daily ERA-Interim climatological polar cap PV anomaly (area-weighted average between 70° and 90°, in PVU) for (a) the NH and (b) minus the SH, as a function of time (days) and potential temperature (K). Contours as in Fig. 3.1. The tickmarks accompanying the name of a month corresponds to the middle of the month. Note that for both hemispheres the horizontal axis starts in summer.*

PV anomaly.

3.3.2 Seasonal cycle of the polar cap PV anomaly

The seasonal cycle of the daily polar cap PV anomaly, defined as the area-weighted averaged PV anomaly between 70° and 90°, as a function of potential temperature and time is shown in Figs. 3.5a and 3.5b for the NH and SH, respectively. The build-up of the polar vortex in autumn is clearly visible in the PV anomaly, as the PV anomaly changes sign from negative to positive during this period. The formation of the vortex starts in early autumn in the upper parts of the stratosphere and descends to the lower stratosphere in the following months. The transition from negative PV anomaly values in summer to positive PV anomaly values in winter occurs in a short time span and the PV anomaly then continues to increase at all stratospheric levels. However, in the NH, the maximum PV anomaly in the upper stratosphere is reached in early winter, while the SH the maximum is not reached until late winter. The day in the winter on which the maximum polar cap PV anomaly is reached increases with decreasing altitude, to late winter for the NH 400 K level, while the SH maximum at 400 K is not attained until mid-spring. The maximum polar cap PV anomaly is reached later in the year in the SH than in the NH at all levels.

Another striking difference between the NH and SH that is clearly visible in the PV anomaly, is the transition from positive to negative PV anomaly values in spring (Fig. 3.5), which we refer to as the break up of the polar vortex. This is not a formal definition of the timing of the break up of the vortex, since the vortex can be displaced from the pole before eventually breaking up completely, but we use the term ‘break up of the vortex’ here to note that the PV over the pole decreases (independent from which process causes this decrease) and does not recover before the next autumn season. In the NH this transition in early spring is quite abrupt, and for most stratospheric

levels at approximately the same time. This is especially true for the separate years, and somewhat less for the climatology. As explained in the previous section, the apparent start of the break up in the lower stratosphere in the climatology is due to the contribution of years with SSWs, when the vortex does not recover in the lower stratosphere. In the SH, on the other hand, the transition starts in the upper stratosphere in early spring, descending to the lower stratosphere in about 1.5 months (the same structure is seen in separate years). The different structure of the break up of the Arctic and Antarctic vortices is also present if a larger polar cap area is considered. *Harvey et al.* (2002) note similar behaviour in the seasonal cycle of the vortex area. The differences between the NH and SH are presumably related to interhemispheric differences in wave forcing and ozone concentrations.

Figure 3.6 shows the seasonal cycle of the climatological daily polar cap PV anomaly at specific isentropic levels, while the polar cap PV anomaly for the separate years is also presented. Figure 3.6a and b show the polar cap PV anomaly at a level in the UTLS PV anomaly (340 K). Both the amplitude of the PV anomaly and the variability are of similar magnitude for the NH and SH at this level. The seasonal cycle is likely explained by heating of the stratosphere in summer, which increases the vertical temperature gradient in the UTLS region, leading to a larger static stability and thus a maximum in the polar cap PV anomaly (Fig. 3.6a and b). Planetary wave breaking might also contribute to the seasonal cycle by decreasing the polar cap PV in winter. The secondary maximum in the 340 K polar cap PV anomaly as seen in Fig. 3.6b in spring is related to the winter maximum in the stratospheric PV anomaly above, extending further downward in the SH than in the NH.

At 600 K, the amplitude of the winter SH PV anomaly (Fig. 3.6d) is about twice as large as the amplitude of the NH PV anomaly (Fig. 3.6c), while the variability is much larger in the NH. The large variability in the 600 K PV anomaly in the NH winter is mainly caused by the occurrence of sudden stratospheric warmings that substantially disturb the vortex. The only known SSW in the SH occurred in September 2002. The line with a sharp drop in the PV anomaly in September in Fig. 3.6d therefore is an example of the influence of an SSW on the polar cap PV anomaly. The variability in the PV anomaly in summer is small for both the NH and SH, as wave propagation to the stratosphere is prohibited by the easterly flow during this season (*Charney and Drazin*, 1961).

The topography and land-sea configuration are more favourable for wave excitation in the NH than in the SH, causing more wave propagation to the stratosphere in the NH. This leads to more and larger variations in the PV anomaly in the NH, a weaker climatological PV anomaly and an earlier break up of the polar vortex in spring. Following the studies by, for example, *Waugh et al.* (1999), *Polvani and Waugh* (2004), *Haklander et al.* (2007) and *Charlton et al.* (2007), we use the heat flux $[v^\star T^\star]$ at 100 hPa as a measure of the wave forcing from the troposphere to the stratosphere.

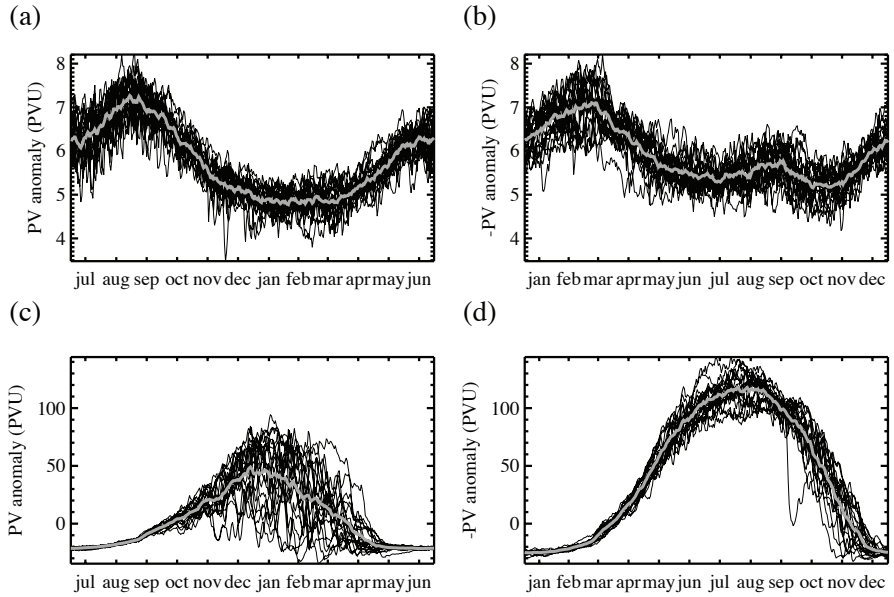

Figure 3.6: *Daily polar cap PV anomaly (PVU, -PV anomaly for the SH) for the climatology (thick grey line) and the separate years (thin black lines) as a function of time (days) on the potential temperature levels (a) 340 K NH, (b) 340 K SH, (c) 600 K NH, (d) 600 K SH.*

Since most planetary wave activity crosses the 100 hPa level between 40° and 80° degrees (see for example figure 2 in *Charlton et al.*, 2007), we show the area-weighted average of the 100 hPa heat flux between 40° and 80° in Fig. 3.7. This figure shows that the wave forcing of the winter stratosphere is much larger in the NH than in the SH. Furthermore, wave forcing influences the NH stratosphere throughout the whole winter, already weakening the vortex long before the break up, while the SH vortex can gain strength until late winter (as seen in Fig. 3.5). Most wave breaking events take place at the edge of the vortex, first affecting the midlatitudes in winter and causing the retreat of the vortex boundary to higher latitudes. Due to the weak wave forcing during winter in the SH, the SH polar area will not be affected until early spring, when the wave forcing increases, and the absorption of solar radiation by ozone also plays an important role in decreasing the vortex area.

The relation between the polar cap PV anomaly and the 100 hPa heat flux is further examined by comparing the five years with the strongest flux to the five years with the weakest flux. The 100 hPa heat flux (area-weighted average between 40° and 80°) is therefore averaged over the winter season (December - February) for the NH and over the spring season (September - November) for the SH (minus the SH values are used), since these are the seasons with the largest climatological flux and also the largest

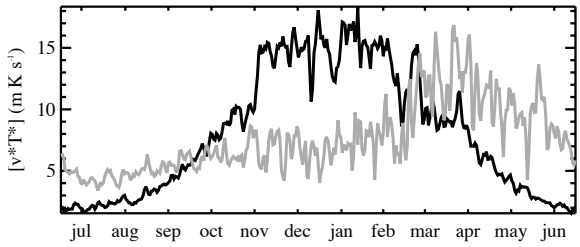

Figure 3.7: *Daily ERA-Interim climatological heat flux $[v^{\star}T^{\star}]$ at 100 hPa (area-weighted average between 40° and 80°, in m K s^{-1}) for the NH (black) and minus SH (grey) as a function of time (days). Months noted on the horizontal axis are for the NH, and the SH values are shifted by 6 months compared to this axis.*

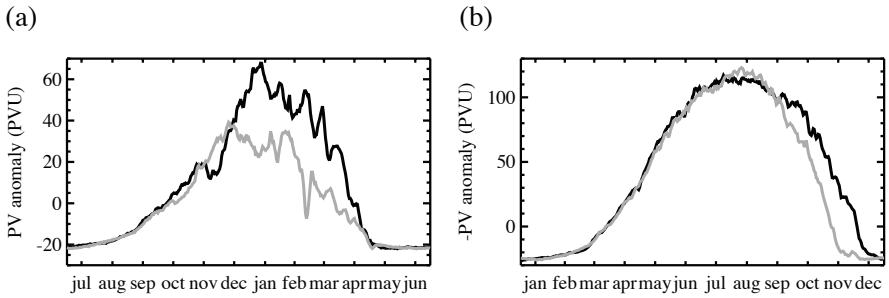

Figure 3.8: *Daily 600 K polar cap PV anomaly (PVU) (a) for the NH, averaged over the five years with the highest winter average 100 hPa heat flux (grey) and averaged over the five years with the lowest winter average 100 hPa heat flux (black) and (b) for minus the SH, averaged over the five years with the highest spring average 100 hPa heat flux (grey) and averaged over the five years with the lowest spring average 100 hPa heat flux (black).*

interannual variability in the flux. For both hemispheres the averaged polar cap PV anomaly is determined for the five years with the highest winter heat flux in the NH (2006/07, 1998/99, 2003/04, 2007/08 and 1997/98) or highest spring heat flux in the SH (2000, 1991, 1994, 2002 and 2005) and for the five years with the lowest NH winter flux (1999/2000, 1992/93,1989/90, 1996/97 and 1994/95) or SH spring flux (1990, 1996, 1998, 2006, 1999). The results are presented in Fig. 3.8 for the 600 K level, clearly showing that for both hemispheres the polar cap PV anomaly is lower for the high flux years than for the low flux years. Figure 3.8 confirms that a larger winter heat flux decreases the polar cap PV anomaly, thus giving a possible explanation for the differences in polar cap PV between the NH and the SH (compare Fig. 3.6c and Fig. 3.6d). The figure further illustrates that interannual variations in the 100 hPa heat flux might indeed lead to the large interannual variations in the polar cap PV anomaly

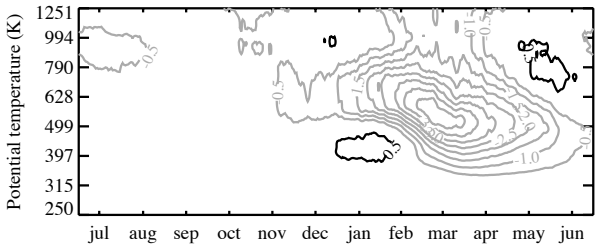

Figure 3.9: *Daily ERA-Interim climatological polar cap ozone mass mixing ratio (mg kg^{-1}) for the SH minus the NH as a function of time (days) and potential temperature (K). Months noted on the horizontal axis are for the NH, and the SH values are shifted by 6 months compared to this axis. Contours every 0.5 mg kg^{-1}, zero line omitted and negative values represented by grey lines.*

in the NH as seen in Fig. 3.6c. In the SH, a stronger spring heat flux decreases the persistence of the vortex over the pole in spring.

As noted previously, the break up of the climatological vortex seems to start in the lower stratosphere in the NH, as a consequence of the occurrence of SSWs. This is confirmed by the heat flux analysis, since SSWs are in general associated with a high heat flux, and it is indeed found that the timing of the transition from positive to negative polar cap PV anomaly values in spring is practically constant with height for the low flux years, while for the high flux years the transition is earlier in the lower stratosphere (not shown). A more detailed examination of the relation between the (interannual variability of the) polar cap PV and the 100 hPa heat flux is deferred to the next chapter.

A stronger, less distorted vortex is more likely to be associated with substantial ozone depletion in the lower stratosphere in spring (e.g., *Solomon*, 1999, and references therein). Less transport of ozone from the lower latitudes and higher levels of the stratosphere to the polar lower stratosphere in the SH compared to the NH also contributes to a difference in ozone between the two hemispheres. Figure 3.9 shows the difference in ozone mass mixing ratio between the SH and NH polar areas, demonstrating that the SH ozone concentration in the lower polar stratosphere in spring is indeed lower than that in the NH. A lower ozone concentration in spring delays the breakdown of the vortex, since heating due to absorption of sunlight by ozone is an important process for the break up of the vortex. Comparing Fig. 3.9 to Fig. 3.5 indicates that the SH-NH differences in spring ozone could explain the different structure of the break up of the vortices in the lower stratosphere.

To study the relation between the polar cap PV anomaly and the ozone concentration, we define a measure of the amount of spring ozone as the average over the three spring months (March - May for the NH and September - November for the SH) of the

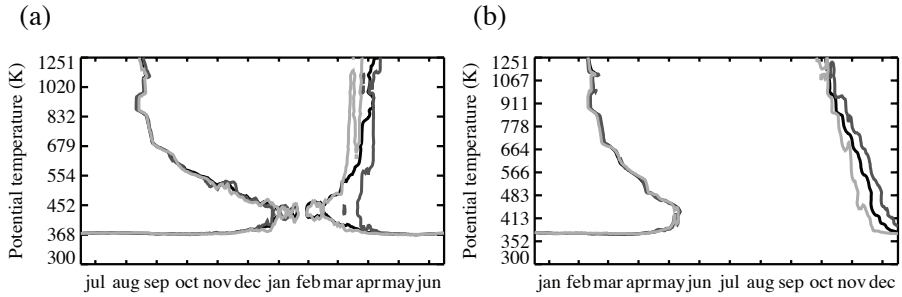

Figure 3.10: *Zero PVU contour of the daily polar cap PV anomaly for the climatology (black), the average of the five years with the highest spring ozone concentrations at 600 K (light grey) and the average of the five years with the lowest spring ozone concentration at 600 K (dark grey) for (a) the NH and (b) the SH, as a function of time (days) and potential temperature (K).*

ozone mass mixing ratio at 600 K (referred to as "springO_3"). For both hemispheres the averaged polar cap PV anomaly is determined for the five years with the highest springO_3 (2004/05, 1990/91, 1995/96, 1997/98 and 2002/03 for the NH and 2002, 2003, 2004, 1997 and 1991 for the SH) and for the five years with the lowest springO_3 (1989/90, 1994/95, 2001/02, 1996/97 and 1999/2000 for the NH and 1995, 2006, 1998, 2001 and 2007 for the SH). Comparison of the low-O_3 case and the high-O_3 case (Fig. 3.10) shows that for both hemispheres the main differences are seen in the lower stratosphere in spring, where a lower spring O_3 concentration is clearly related to a later break up of the vortex. These results are consistent with previous studies that showed a relation between ozone depletion, a cooling of the lower stratosphere and increased persistence of the vortices (e.g., *Randel and Wu*, 1999; *Waugh et al.*, 1999; *Zhou et al.*, 2000). A later transition from positive polar cap PV anomaly values in winter to negative polar cap PV anomaly values in summer in the lower stratosphere for the low-O_3 years indicates an increased persistence of the vortex over the pole in both hemispheres. This implies that recovery of the SH ozone hole will likely lead to an earlier break up of the SH vortex in the future, although it is not possible to completely uncouple the effect of ozone on the PV from the effect of waves on the PV, since wave effects influence the ozone concentration as well.

3.3.3 Seasonal cycle of the midlatitude PV anomaly

Baldwin and Dunkerton (1998) examined the seasonal cycle of the NH PV at the 600 K level. They found a clear annual cycle at the high latitudes, consistent with our study of the polar cap PV anomaly. However, they found a semi-annual cycle in the PV in the midlatitudes. Here we examine whether or not the semi-annual cycle in the midlatitude PV is visible in both hemispheres and throughout the whole depth of the stratosphere. *Baldwin and Dunkerton* show that the semi-annual cycle is important

between about 35°N and 55°N (their figure 3). We therefore define a daily midlatitude PV anomaly as the area-weighted average PV anomaly between 35° and 55° north or south.

Examination of the seasonal cycle of the midlatitude PV anomaly (Fig. 3.11) indicates that above 600 K (800 K) the NH (SH) midlatitude PV anomaly shows a semi-annual cycle with maxima in late autumn and in spring and minima in summer and in winter (maxima in the SH are shifted by about one month compared to the NH). This semi-annual cycle is also found by *Baldwin and Dunkerton* (1998) at 600 K for the NH, and is related to the influence of planetary waves. They state that midlatitude PV values during midwinter are decreased due to the formation of the surf zone. The autumn maximum is related to the formation of the polar vortex extending to the midlatitudes in the upper levels (see Fig. 3.1 and 3.2). In early winter planetary waves start to break at the edge of the vortex, forming the surf zone and causing a retreat of the vortex boundary to higher latitudes, leading to a winter minimum in the midlatitude PV anomaly. In the SH the low wave activity in winter prevents to a large extent mixing between the mid- and high latitudes. In the NH, the waves continue to affect the polar area, and displacement of the vortex and mixing of high PV filaments shed off the vortex are a source of PV for the midlatitudes. This explains the less clear winter minimum in the midlatitude PV anomaly in the NH (Fig. 3.11a) compared to the SH (Fig. 3.11b). The spring maximum in the PV anomaly is related to the mixing of high PV from the interior of the polar vortex to the midlatitudes as the vortex breaks up. The midlatitude PV anomaly values start to increase in late winter and spring after the polar cap PV anomaly values have started to decrease (compare Fig. 3.11 to Fig. 3.5). The presence of a late winter minimum and spring maximum in the midlatitude PV anomaly in the SH indicates that planetary wave breaking also plays a role in the SH stratosphere (which is in agreement with the presence of a heat flux at 100 hPa). Wave events erode the SH vortex in spring, but the main vortex remains situated over the pole (seen for example in the high PV anomaly values in the lower polar stratosphere in November in Fig. 3.2). The vortex vanishes due to a combination of radiative effects and transport of filaments of high PV off the vortex to the lower latitudes, where wave events in the SH spring transport polar PV to lower latitudes as compared to the NH (compare November in Fig. 3.2 with May in Fig. 3.1).

In the lower stratosphere the negative values dominate the midlatitude PV anomaly, since the high PV anomaly values associated with the polar vortex remain north of about 50° in the lower stratosphere (see Figs. 3.1 and 3.2). This is again related to the cooling starting in the upper stratosphere and extending downward in time. By the time wave breaking starts to play a role in early winter, the upper stratosphere at midlatitudes has already experienced substantial cooling (with associated increases in PV), but cooling of the midlatitude lower stratosphere is lagging. Formation of the surf zone by this wave breaking causes the edge of the vortex at the upper levels to

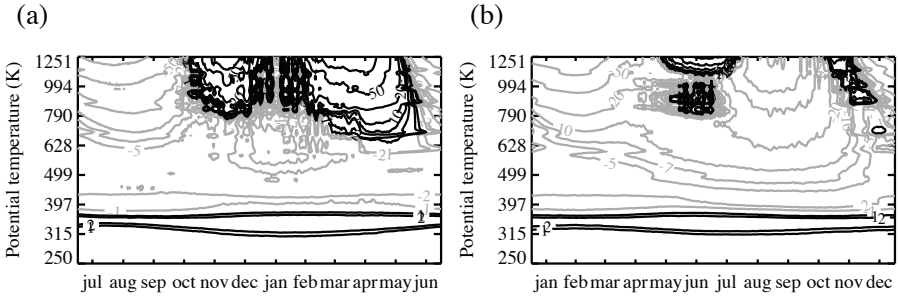

Figure 3.11: *Daily ERA-Interim climatological midlatitude PV anomaly (area-weighted average between 35° and 55°, in PVU) for (a) the NH and (b) minus the SH as a function of time (days) and potential temperature (K). Contours as in Fig. 3.1.*

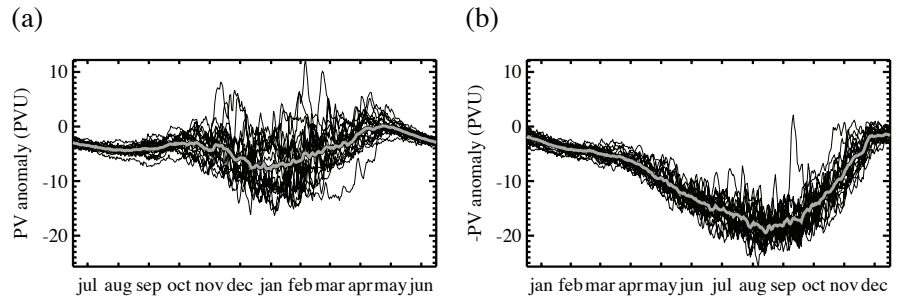

Figure 3.12: *Daily midlatitude PV anomaly (in PVU) for the climatology (thick grey line) and the separate years (thin black lines) as a function of time (days) at the 600 K potential temperature level for (a) the NH and (b) minus the SH.*

retreat to higher latitudes, and prevents the increase of the midlatitude PV in the lower stratosphere. Due to the absence of the autumn maximum, the seasonal cycle in the lower stratosphere is dominated by an annual cycle with a PV anomaly minimum in winter.

Figure 3.12 presents the midlatitude PV anomaly at the 600 K level for the NH and the SH. Besides the climatological PV anomaly also the values for the separate years are shown, to indicate the interannual variability. As for the polar cap PV anomaly, the winter variability is larger in the NH than in the SH. This is expected, since the midlatitude and the polar cap PV anomaly are strongly connected. Strong wave events will displace and mix high PV off the pole to lower latitudes, thereby decreasing the polar cap PV and increasing the midlatitude PV.

The analysis of the relation between the PV anomaly and the heat flux at 100 hPa as presented in the previous subsection is now extended to the midlatitude PV. For both hemispheres the averaged midlatitude PV anomaly is determined for the five

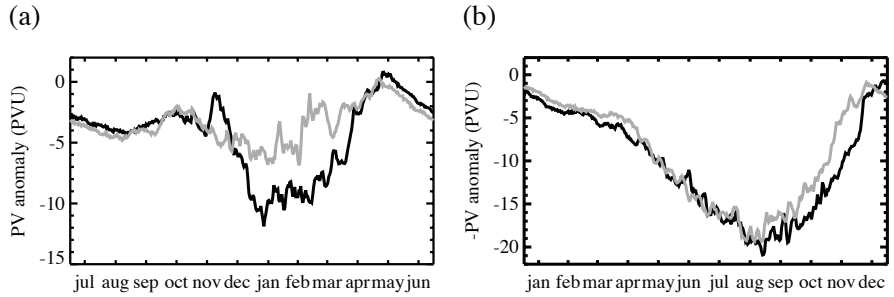

Figure 3.13: *Same as Fig. 3.8, but for the daily 600 K midlatitude PV anomaly (PVU).*

years with the highest and the five years with the lowest flux in the NH winter and the SH spring. The results, presented in Fig. 3.13 for the 600 K level, clearly show that the midlatitude PV is higher for the high flux years. Figure 3.13a shows that the NH winter minimum in the midlatitude PV anomaly is deeper for the low flux years. This supports the finding that the deeper winter minimum in midlatitude PV in the SH compared to the NH (as seen in Fig. 3.11 and 3.12) is related to the lower climatological winter heat flux in the SH compared to the NH (Fig. 3.7). Figure 3.13b further strengthens the finding that the spring maximum in the midlatitude PV anomaly is also related to wave effects. Furthermore, it confirms that waves also play a role in the break up of the vortex in the SH, since the midlatitude PV starts to increase earlier in spring for the high flux years than for the low flux years, accompanying an earlier decrease of the polar cap PV anomaly.

The connection between the polar cap PV and the midlatitude PV is further illustrated by the following examples, showing the PV anomaly at the 600 K level for the 1996/97 NH winter (3.14a and c), and the 2002 SH winter (Fig. 3.14b and d).

The NH winter of 1996/97 had an exceptionally strong polar vortex from midwinter to spring and a late break up of this vortex (*Coy et al.*, 1997). Figure 3.14a clearly shows a polar cap PV anomaly that is stronger than the climatological PV anomaly from January to April. However, in early winter a wave event lowered the polar cap PV. Comparison with the midlatitude PV anomaly (Fig. 3.14c) shows that the midlatitude PV was raised at the same time, indicating that high PV is transported off the pole by this wave event (examination of the PV anomaly as a function of latitude and longitude at an isentropic level shows a displacement of the vortex off the pole and wave breaking events tearing filaments of high PV off the vortex edge and mixing with midlatitude PV). During late winter, when the polar cap PV anomaly is exceptionally strong, the midlatitude PV anomaly is much lower than the climatological PV anomaly. This indicates that during this period the vortex edge was strong and preventing mixing of PV off the pole, so that there was no source of PV for the

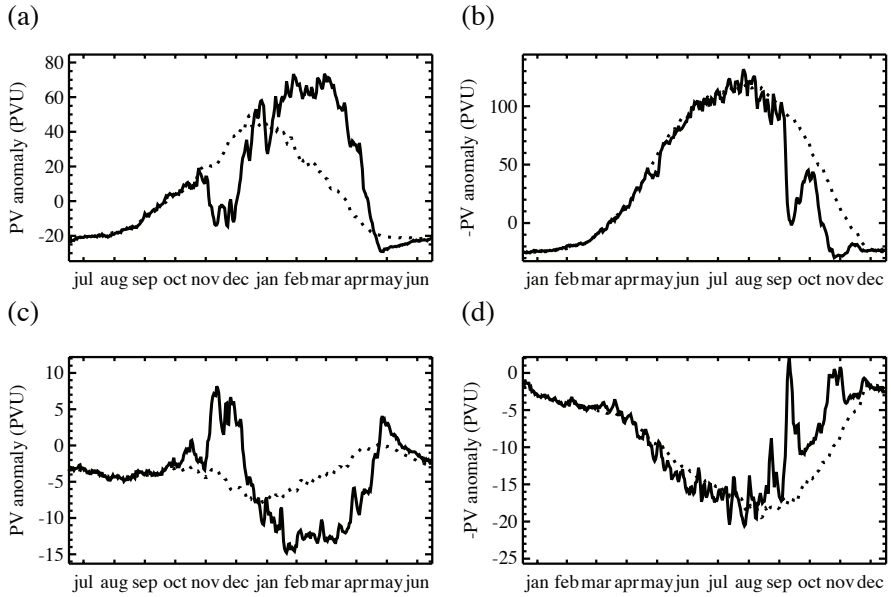

Figure 3.14: *Daily PV anomaly (in PVU) at the 600 K level for the climatology (dotted) and (a) the NH polar cap PV anomaly for 1996/1997 (solid), (b) the SH polar cap PV anomaly for 2002 (solid), (c) the NH midlatitude PV anomaly for 1996/1997 (solid), and (d) the SH midlatitude PV anomaly for 2002 (solid), as a function of time (days).*

midlatitudes.

The year 2002 was exceptional for the SH, since the only known sudden stratospheric warming in the SH occurred during September 2002 (*Charlton et al.*, 2005b, and other articles in the same special issue of the journal). During the first part of the winter the polar cap PV anomaly (Fig. 3.14b) and midlatitude PV anomaly (Fig. 3.14d) follow the climatological values closely. In September, however, the polar cap PV anomaly shows a sharp drop, while there is a peak visible in the midlatitude PV anomaly. During this SSW event the vortex split and one part was transported to the midlatitudes where it mixed with the background PV anomaly. These results are consistent with those of *Charlton et al.* (2004), who note that the signature of a sudden stratospheric warming in the lower stratospheric PV distribution is a reduction in PV over the polar cap, and an increase in PV in the midlatitudes.

3.4 Conclusions

We presented a zonal mean climatology of the PV anomaly for the Northern and Southern Hemispheres, derived from the daily 1989-2008 ERA-Interim data. The

PV anomaly is defined as that part of the PV field that induces a wind field according to the invertibility principle. Two clear PV anomalies can be distinguished in the PV anomaly field: a tall stratospheric polar cap PV anomaly above about 400 K and a flat but wide PV anomaly in the upper troposphere/lower stratospheric region between about 300 K and 360 K. The two PV anomalies have a different seasonal cycle. The stratospheric polar cap PV anomaly has a maximum positive value in winter, disappears in spring and is negative in summer, to start forming again in the upper stratosphere in autumn. The UTLS PV anomaly, on the other hand, is positive during the whole year, with relatively small variations in horizontal and vertical extent. The sign changes in the stratospheric PV anomaly are a clear advantage of the PV anomaly framework compared to the total PV field in examining the formation and break up of the polar vortex.

The seasonal cycle of the stratospheric polar cap PV anomaly is strongly related to radiative effects. The PV anomaly forms in autumn and winter due to radiative cooling in the polar night, and vanishes in spring due to absorption of solar radiation by ozone. The formation of the vortex in autumn is similar for the NH and SH, but interhemispheric differences in wave effects and ozone concentrations cause a difference in the break up of the vortex in spring. Waves affect the NH stratosphere throughout winter, weakening the vortex compared to the less disturbed SH vortex. The PV anomaly maximum is reached earlier in winter in the upper stratosphere than in the lower stratosphere, indicating that wave breaking events occur first in the upper stratosphere, extending their region of influence downward in time. Since the SH experiences less wave forcing in winter, the SH polar cap PV anomaly is not affected by waves until spring, when absorption of solar radiation by ozone already plays a role as well. The stronger and colder SH vortex allows for (more) ozone depletion in spring. Lower ozone concentrations in the polar area for the SH compared to the NH result in a delayed break up of the SH vortex, especially in the lower stratosphere. The break up of the SH vortex is thus driven by a combination of radiation and wave effects in spring, while wave effects already cause a substantial weakening of the NH vortex in winter before radiation effects start heating the stratosphere in spring. In summer, the easterly stratospheric flow prohibits wave propagation from the troposphere to the stratosphere in both the NH and SH, leading to small interhemispheric differences during this season.

The seasonal cycle in the UTLS PV anomaly is relatively small, and likely related to the Hadley circulation and wave breaking in the tropopause region. The horizontal boundary of the UTLS PV anomaly is coupled to the position of the subtropical jet, while the upper and lower boundaries are determined by the position of the tropical and polar tropopauses, respectively. We find indications that a stronger Hadley circulation, measured by a higher tropical precipitation, leads to an increase in the horizontal PV gradient in the subtropics, which is accompanied by a stronger subtropical jet.

However, the differences in PV between high and low precipitation years are small, and it is difficult to separate the influence of different processes in the data, which makes it difficult to draw conclusions about the relation between tropical precipitation and the UTLS PV anomaly from the present analysis. Therefore, model studies are needed to examine how the UTLS region is affected by separate forcings, to be able to test the validity of the indications presented here.

Comparison of the midlatitude and polar cap PV anomaly indicates that wave effects displace, transport and eventually mix stratospheric PV off the pole to lower latitudes. We find a semi-annual cycle in the climatological midlatitude PV anomaly in both hemispheres in the mid- to high stratosphere, with maxima in autumn and spring. This semi-annual cycle is due to a combination of radiative effects and wave effects. The radiative effects cause the formation of the polar vortex and the maximum PV anomaly values in autumn. Wave breaking at the edge of the vortex then forms the surf zone, which causes the vortex boundary to retreat to higher latitudes, and results in a midlatitude PV minimum in winter. Transport and mixing during the break up of the polar vortex, on the other hand, cause the PV anomaly maximum in spring. The winter minimum is more clear in the SH, since the SH midwinter polar vortex is nearly undisturbed, while distortion of the NH polar vortex by waves presents a source of midlatitude PV. Wave breaking events therefore cause the polar cap PV anomaly to be lower in the NH than in the SH, while they cause the midlatitude PV anomaly to be higher in the NH than in the SH.

Some implications of the effect of climate change on the stratosphere can be derived from the results presented here. Our results suggest that recovery of the ozone hole will decrease the SH lower stratospheric polar PV anomaly in spring, and lead to an earlier vortex break up. Cooling of the stratosphere due to increases in greenhouse gas concentrations will increase the polar stratospheric PV anomaly in winter, leading to a stronger polar vortex. This might lead to more resistance against wave forcing from below and less major warming events in the NH when the forcing from the troposphere remains unchanged. Changes in the Hadley circulation or in the height of the tropopause are likely to affect the UTLS PV anomaly, possibly changing the influence of the lower stratosphere on the tropospheric circulation. Further research is needed to extend these qualitative descriptions and to quantify their effects on the PV. The climatology presented here can then be used as a reference for future studies dealing with the influence of climate change on the state of the stratosphere.

Acknowledgements

The ECMWF ERA-Interim data used in this study have been provided by ECMWF. We are thankful for useful discussions at the University of Reading and at the Royal Meteorological Society's 2009 Conference.

4

Relation between the 100 hPa heat flux and stratospheric potential vorticity

It is shown that a quantitative relation exists between the stratospheric polar cap potential vorticity (PV) and the 100 hPa eddy heat flux. A difference in potential vorticity between years is found to be linearly related to the flux difference integrated over time, taking into account a decrease in relaxation timescale with height in the atmosphere. This relation (the PV-flux relation) is then applied to the 100 hPa flux difference between 2008/2009 and the climatology (1989-2008), to obtain a prediction of the polar cap PV difference between the 2008/2009 winter and the climatology. A prediction of the 2008/2009 polar cap PV is obtained by adding this PV difference to the climatological PV. The observed polar cap PV for 2008/2009 shows a large and abrupt change in the PV in midwinter, related to the occurrence of a major sudden stratospheric warming in January 2009, and this is also captured by the PV predicted from the 100 hPa flux and the PV-flux relation. The results of the mean PV-flux relation shows that, on average, about 50% of the interannual variablity in the state of the Northern Hemisphere stratosphere is determined by the variations in the 100 hPa heat flux. This explained variance can be as large as 80% for more severe events, as demonstrated for the 2009 major warming.

This chapter is based on:
Hinssen, Y. B. L. and M. H. P. Ambaum, Relation between the 100 hPa heat flux and stratospheric potential vorticity, *Journal of the Atmospheric Sciences*, In press, doi:10.1175/2010JAS3569.1, 2010.

4.1 Introduction

Major sudden stratospheric warmings (SSWs) are phenomena during which the polar stratosphere is substantially warmed and the stratospheric winds reverse direction from westerlies to easterlies. These stratospheric changes can affect the tropospheric circulation directly through hydrostatic and geostrophic adjustment, or indirectly due to changes in the reflection and propagation of planetary waves.

Since the work of *Charney and Drazin* (1961) and *Holton and Mass* (1976), SSWs are believed to be primarily forced from below by wave activity entering the stratosphere from the troposphere (see also *Andrews et al.*, 1987). For example, *Charlton and Polvani* (2007) show that the 100 hPa heat flux (which is a measure of the upward propagating wave forcing to the stratosphere) is increased in the weeks before the occurrence of a sudden stratospheric warming. Here we examine to what extent the wave forcing of the stratosphere drives the large scale stratospheric variability in general, and the stratospheric variations accompanying the 2009 sudden stratospheric warming in particular.

First, we examine the relation between the stratospheric polar cap potential vorticity (PV) and the 100 hPa heat flux. The importance of such a relationship was highlighted in, for example, *Ambaum and Hoskins* (2002), who showed that stratospheric PV anomalies are important for the troposphere. They found a positive feedback loop between stratospheric PV anomalies and tropospheric circulation, mediated by upper tropospheric Eliassen-Palm fluxes.

The relation between poleward heat flux and stratospheric PV (the PV-flux relation) is based on the idea that a wave forcing can erode the stratospheric PV structure. The values of the Northern Hemisphere PV are for example much lower than those of the Southern Hemisphere PV, and it is generally known that wave propagation to the stratosphere plays a larger role in the Northern Hemisphere since the topography and land-sea configuration are more favorable for wave excitation in the Northern Hemisphere than in the Southern Hemisphere.

In the present study we will examine this PV-flux relation on a daily basis, using the European Centre for Medium-Range Weather Forecasts (ECMWF) ERA-Interim reanalysis data from 1989 to 2008. Although it is often assumed that the 100 hPa heat flux is the driving force behind stratospheric variability, to our knowledge a PV-flux relation of the form presented here, directly relating a flux difference to a PV difference on a daily basis, has not been published before.

Secondly, we use this mean PV-flux relation to predict the daily 2008/2009 polar cap PV anomaly from the 2008/2009 100 hPa heat flux anomaly. Comparison of the predicted PV with the actual ERA-Interim PV for the 2008/2009 winter then indicates to what extent the stratospheric PV can be predicted from the 100 hPa heat flux. The differences will also indicate the importance of other factors, such as those internal to

the stratosphere.

The present work is related to that of *Newman et al.* (2001) and *Austin et al.* (2003), who present a relation between the winter heat flux and the spring polar temperatures, based on monthly timescales. In the present study this idea is applied to daily differences in PV and heat flux between different years in the Northern Hemisphere.

The physical basis of the PV-flux relation is described in section 4.2. Section 4.3 presents an overview of the data. The procedure to find the mean PV-flux relation is given in section 4.4. Section 4.5 presents the results of the 2009 sudden stratospheric warming case study and sensitivity studies are described in section 4.6. Finally, section 4.7 presents a discussion and some conclusions.

4.2 Physical basis

The PV-flux relation we use is derived from the zonal mean quasigeostrophic potential vorticity equation (e.g., *James*, 1995). It reads

$$[q]_t + [v^\star q^\star]_y = [S], \tag{4.1}$$

where subscripts denote partial derivatives, square brackets denote zonal means, and the superscripts * denote deviations from the zonal mean. In the above equation, q is the quasigeostrophic potential vorticity (or pseudo-potential vorticity, see *Hoskins et al.*, 1985), v is the meridional wind, and S is some diabatic source term on the quasigeostrophic potential vorticity. We use cartesian coordinates for simplicity of notation.

If we integrate this equation poleward of some given latitude y_0 (the polar cap in spherical coordinates) to find the average $\langle q \rangle$ over the polar cap northward of this latitude, then we get

$$\langle q \rangle_t = \langle S \rangle + L\,[v^\star\, q^\star](y_0), \tag{4.2}$$

with L the longitudinal extent of the domain at latitude y_0. In Eq. 4.2 we now replace the average source term by a Newtonian relaxation and we rewrite the poleward PV flux as the divergence of the Eliassen–Palm flux, $\boldsymbol{F}$,

$$\langle q \rangle_t = \frac{\langle q \rangle_R - \langle q \rangle}{\tau} + \frac{L}{\rho_R} \nabla \cdot \boldsymbol{F}(y_0). \tag{4.3}$$

Here $\langle q \rangle_R$ is the radiative equilibrium value of the polar cap mean PV, τ is the radiative timescale at the given level, and ρ_R is the reference density profile which is required in the quasigeostrophic framework.

We now make the assumption that the spatial structure of the Eliassen–Palm flux

divergence does not vary, so that

$$\nabla \cdot \boldsymbol{F} = \phi(y,z)\,\chi(t), \tag{4.4}$$

where ϕ is the spatial structure function and χ its temporal modulation. This is a strong assumption, which can only be justified in hindsight by the success of our model (or lack thereof). However, some a priori justification is found in the fact that the linear paradigm of Rossby wave propagation on a background flow is defined for a fixed background, where the mean zonal state defines the refractive index for the waves. Our assumption further implies that the propagation of the Rossby waves (where the local group velocity is assumed to be parallel to $\boldsymbol{F}$) is immediate, which is in contradiction with observations (e.g., *Harnik*, 2002). Nonetheless, the time scale of propagation is short enough for this assumption to be reasonably satisfied.

We can now express the time modulation $\chi(t)$ in terms of the mean poleward heat flux at the lower boundary of the domain. To this end, we integrate $\nabla \cdot \boldsymbol{F}$ over the whole stratosphere, with as lower boundary the 100 hPa level, for simplicity. Using Gauss' theorem, this integral can be expressed as a boundary integral for the Eliassen–Palm fluxes perpendicular to the boundaries. We assume that the meridional boundaries do not contribute to this integral (there are weak heat fluxes at the equatorward edge of the domain and there are, by definition, no meridional fluxes through the pole). We also assume that the notional top of the domain (this could be space, in principle) does not support strong upward Eliassen–Palm fluxes. We then find that the only contribution to the integral comes from the vertical Eliassen–Palm fluxes at the lower boundary. The integral is therefore proportional to the meridional average value of the 100 hPa poleward heat flux, that is,

$$\int_{\text{strat}} \nabla \cdot \boldsymbol{F}\,\mathrm{d}y\,\mathrm{d}z = \chi \int_{\text{strat}} \phi\,\mathrm{d}y\,\mathrm{d}z = \\ - \int_{\text{lower bdy}} F^{(z)}\,\mathrm{d}y = f_0 W \rho_R \{[v^\star\, T^\star]\}_{100\text{hPa}}/T_R. \tag{4.5}$$

Here the two integrals are over the whole stratosphere in the meridional plane and its lower boundary, respectively. Further, $\{[v^\star T^\star]\}_{100\text{hPa}}$ is the meridional mean of the 100 hPa poleward heat flux, W the meridional extent of the lower boundary, f_0 a suitable reference value for the Coriolis parameter, and T_R a suitable reference temperature at 100 hPa. This result allows us to write χ as a function of the mean poleward heat fluxes at the lower boundary only,

$$\chi(t) = \frac{f_0 W \rho_R}{T_R \int_{\text{strat}} \phi\,\mathrm{d}y\,\mathrm{d}z} \{[v^\star\, T^\star]\}_{100\text{hPa}}. \tag{4.6}$$

With this expression for χ, we can rewrite Eq. 4.3 as

$$\langle q \rangle_t = \frac{\langle q \rangle_R - \langle q \rangle}{\tau} - A(z)\{[v^\star\, T^\star]\}_{100\text{hPa}}, \tag{4.7}$$

with the vertical structure function A given by

$$A(z) = \frac{f_0 W L}{T_R} \frac{\phi(y_0, z)}{\int_{\text{strat}} \phi \, \mathrm{d}y \, \mathrm{d}z}. \tag{4.8}$$

Equation 4.7 describes some well-known properties of the polar cap PV: it relaxes radiatively to some radiative equilibrium value and any poleward heat flux (upward Eliassen–Palm flux) at the lower boundary tends to decelerate the mean stratospheric wind and decrease the PV value at the poles.

Equation 4.7 contains only the polar cap PV and 100 hPa poleward flux. It can be straightforwardly solved as

$$\langle q \rangle(t) = \langle q \rangle(0) e^{-t/\tau} + \int_0^t \frac{\langle q \rangle_R (t - t')}{\tau} e^{-t'/\tau} dt' - A \int_0^t F(t - t') e^{-t'/\tau} dt', \tag{4.9}$$

where for brevity we write

$$F = \{[v^\star\, T^\star]\}_{100\text{hPa}}. \tag{4.10}$$

The first term in Eq. 4.9 is the transient effect of the initial condition, the second term is the radiative contribution to the polar cap PV, and the last term represents the effect of waves on the polar cap PV.

After the initial transients have died away, the first two terms on the right hand side are the same every year as long as we investigate the same hemisphere. Furthermore, we start our integrations in the summer, so there are only small differences between the initial conditions anyway. Comparing two different years Y_1 and Y_2 on the same hemisphere therefore leaves us with an equation relating the PV difference between the years to the flux difference between the years:

$$\Delta_{Y_1 Y_2} \langle q \rangle(t) = -A \int_0^t \Delta_{Y_1 Y_2} F(t - t') e^{-t'/\tau} dt' \tag{4.11}$$

The relaxation timescale τ is related to the radiative timescales in the stratosphere and is height dependent, with an increasing timescale with decreasing height (e.g., *Dickinson*, 1973). Therefore, the integrated flux difference is a function of height, even though the flux difference itself is not. In the next sections the Northern Hemisphere potential vorticity difference and time integrated flux difference are determined from the ERA-Interim data for different year combinations for the years 1989 to 2008 and A is empirically determined. In what follows, the perturbation Ertel PV anomaly

(defined in section 1.2.2) will be used to determine the relevant value for q.

4.3 Data

The ECMWF ERA-Interim reanalysis data at 37 pressure levels between 1000 hPa and 1 hPa, and a horizontal resolution of 1.5° is used. This is the most recently produced reanalysis dataset, with an improved representation of the stratosphere compared to the previous ERA-40 reanalysis (*Fueglistaler et al.*, 2009). The daily ERA-Interim data (from 12.00 UTC) of the zonal and meridional wind and the temperature for the January 1989 to June 2009 period are interpolated from isobaric to isentropic levels by the method described by *Edouard et al.* (1997). In order to make optimal use of the available ERA-Interim data, a stretched grid in the vertical direction is employed.

The isentropic potential vorticity, Z_θ, is then calculated from Eq. 1.1, using the isentropic density (σ, Eq. 1.3) and the isentropic relative vorticity given by:

$$\zeta_\theta = -\frac{1}{a}\frac{\partial u}{\partial \phi} + \frac{u \tan \phi}{a} + \frac{1}{a \cos \phi}\frac{\partial v}{\partial \lambda} \tag{4.12}$$

Here u is the zonal wind, v is the meridional wind, a is the radius of the Earth, ϕ is the latitude, λ is the longitude. The PV is calculated as a function of latitude, longitude and potential temperature (θ) to allow examination of the two dimensional structure of the vortex at isentropic levels (as shown in Fig. 1.4, for example). Zonal averaging gives a dataset of zonal mean PV, zonal wind and pressure (p) at isentropic levels. The domain of this dataset ranges from 90°N to 90°S in the horizontal, with a resolution of 1.5°, and from the Earth's surface to about 1250 K in the vertical, with a resolution varying from about 1.7 K near the surface to 10 K in the upper layers. The lower boundary of the domain is determined by the available data, and for each latitude this is defined as the first isentropic level for which data is available along the full latitude circle, meaning that the pressure is below 1000 hPa at all longitudes along this latitude circle. We will refer to this lower boundary as the 'surface', but it should be noted that this does not correspond to the actual surface of the Earth, but is located in the lower troposphere. This surface-isentropic level varies with latitude, during Northern Hemisphere winter from around 260 K at 90°N to about 310 K near the equator.

The zonal mean PV and the isentropic density are split into a reference state ($Z_{\theta,\mathrm{ref}}$) and an anomaly (Z'_θ) as described in section 1.2.2. The reference isentropic density σ_{ref} is the area-weighted average of σ over the domain in question. In other words, the reference isentropic density is the area-weighted average of σ over the domain in question. In our case we focus on the Northern Hemisphere and choose the area poleward of 10°N. Therefore, σ_{ref} depends only on the height (θ). The PV anomaly, Z'_θ, represents that part of the PV field that induces a wind field, according to the PV

inversion equation (see 1.2).

The polar cap PV anomaly is defined as the area-weighted average of the PV anomaly poleward of 70°N. We consider a year running from July to June the next year. With the year 2008/2009 we thus mean the period July 2008 to June 2009.

The meridional wind and temperature fields at pressure levels are used to determine the zonal mean heat flux, $[v^\star T^\star]$, with the brackets denoting a zonal mean and the stars a deviation from zonal mean. The 100 hPa heat flux is often used as a measure of the wave forcing from the troposphere to the stratosphere (e.g., *Waugh et al.*, 1999; *Polvani and Waugh*, 2004; *Charlton et al.*, 2007). Since most planetary wave activity crosses the 100 hPa level between 40° and 80° degrees (see for example Fig. 2 in *Charlton et al.*, 2007), we use the area-weighted average of the 100 hPa heat flux between 40°N and 80°N as a measure of wave forcing from the troposphere to the stratosphere. This quantity is determined for each day of each year. A more detailed discussion of the heat flux can be found in *Newman and Nash* (2000).

4.4 The climatological PV-flux relation

First a mean relaxation timescale τ is determined as a function of potential temperature. There are 171 different year combinations, the first being 1989/1990 - 1990/1991 and the last 2006/2007 - 2007/2008 (we only examine different year combinations, so if 1989/1990 - 1990/1991 is examined, 1990/1991 - 1989/1990 is not, as it provides no new information). For each year combination the polar cap PV anomaly difference and flux difference are determined. The flux difference is then integrated from day zero (the first of July) to day t to determine the integral on the right hand side of Eq. 4.11 as a function of t (day of the year) and τ for each year combination. The covariance between the integrated flux difference and minus the polar cap PV anomaly difference is determined for the time period December to March (DJFM) as a function of τ and θ (minus the PV values are only used to obtain a positive correlation, and eventually positive values for A in Eq. 4.11). The variance of the polar cap PV anomaly difference as a function of θ and the variance of the integrated flux difference as a function of τ are determined for the same period. The months December to March are chosen because the influence of waves on the stratosphere is largest in the winter season, since waves can only propagate to the stratosphere when the winds are westerly (*Charney and Drazin*, 1961). The mean covariance and variances over all year combinations are then calculated, and these are used to determine a mean DJFM correlation coefficient as a function of τ and θ.

The mean τ as a function of height is then found by determining for which τ the correlation coefficient is 95 % of its maximum value at each level. We do not use the actual maximum value, since in the lower stratosphere the correlation coefficient is found to increase with increasing τ to values of τ exceeding 200 days, while a

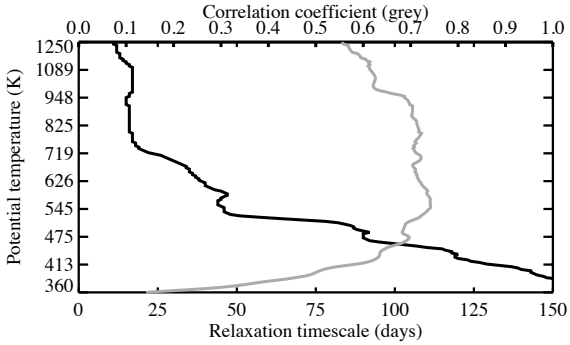

Figure 4.1: *Mean relaxation timescale τ (in days, bottom axis, black line) and mean correlation coefficient between DJFM integrated flux difference and minus DJFM polar cap PV anomaly difference (top axis, grey line) for this τ, both as a function of potential temperature (K). Note the logarithmic scaling of the potential temperature axis in this and following figures.*

correlation of 95 % is obtained at much lower values of τ. The resulting τ and accompanying correlation are given in Fig. 4.1. The value of τ increases from about 10 days in the upper levels, to about one month near 700 K and three months around 500 K.

Figure 4.1 also shows that for the lower to middle stratosphere the mean correlation coefficient is about 0.7. This indicates that Eq. 4.11 may indeed provide a reasonable predictive model for the polar cap PV. These values of the correlation coefficient indicate that about 50% of the variance in the polar cap PV can be predicted from the preceding 100 hPa heat flux.

Examples of the integrated flux difference and minus the polar cap PV anomaly difference as a function of time at the 600 K level are given in Fig. 4.2 for the year combinations 1994/1995 - 1996/1997, 1998/1999 - 2000/2001 and 2003/2004 - 2004/2005. Here the optimal value of τ from Fig. 4.1 was used. Figure 4.2 shows that there is a strong relation between the flux difference and PV anomaly difference in general, although not all variations in PV anomaly are accompanied by a flux variation, consistent with the correlation values of Fig. 4.1.

To determine a general PV-flux relation based on all year combinations, all DJFM flux differences and minus polar cap PV anomaly differences are determined. The -PV anomaly differences versus flux differences are shown for the 600 K level in Fig. 4.3a, and a linear fit is plotted through the data. This can be done for each isentropic level, and the slope (A in Eq. 4.11) as a function of θ is given in Fig. 4.3b. The assumption behind Eq. 4.11 is that a flux difference of zero is accompanied by a zero PV anomaly difference and it is indeed found that the best linear fit through the data nearly crosses through the (0,0) point (see Fig. 4.3a for the 600 K level).

We have determined a mean PV-flux relation based on ERA-Interim data for the

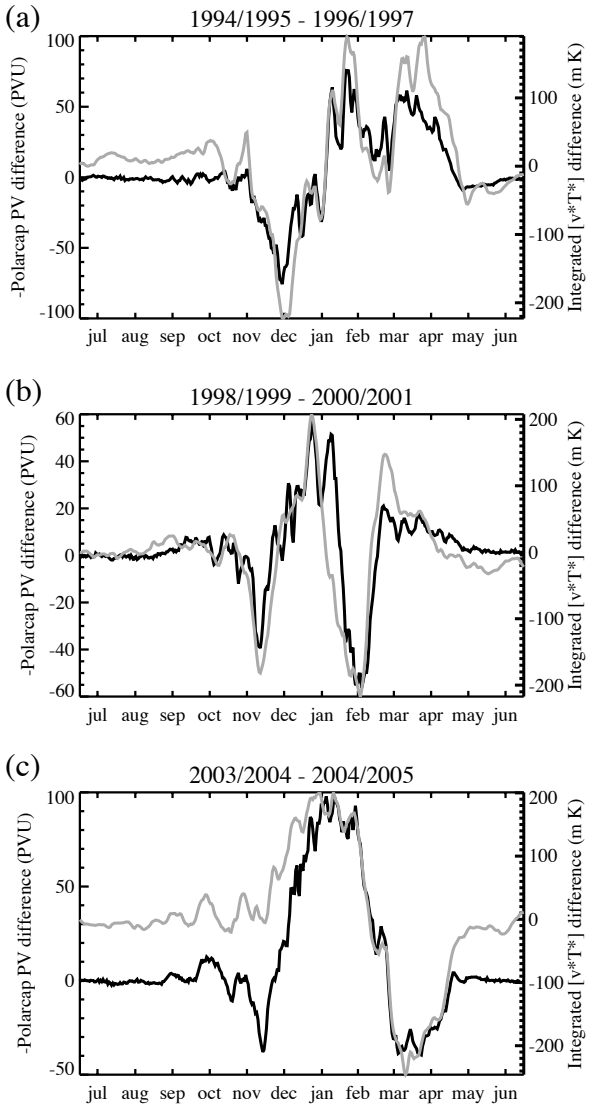

Figure 4.2: *Daily minus polar cap PV anomaly difference (in PVU, 1 PVU = 10^{-6} K m^2 kg^{-1} s^{-1}, left axis, black line) and daily integrated flux difference (in m K, right axis, grey line), both at the 600 K isentrope, as a function of time for the year combinations (a) 1994/1995 - 1996/1997, (b) 1998/1999 - 2000/2001 and (c) 2003/2004 - 2004/2005. The tickmarks indicate the middle of each month.*

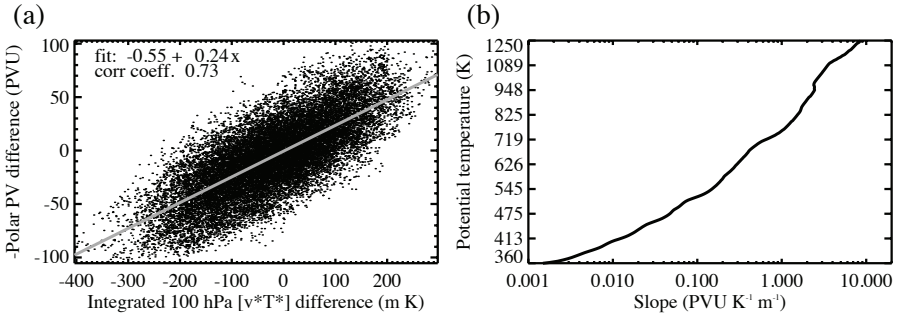

Figure 4.3: *(a) Minus polar cap PV anomaly differences (PVU) against integrated flux differences (m K) at 600 K for the months December to March, for all year combinations (points), and a linear fit through the data (line). (b) Slope (PVU K^{-1} m^{-1}) of the linear fit as a function of potential temperature, note the logarithmic scaling on both axes.*

period July 1989 to June 2008. The general form of the PV-flux relation is given by Eq. 4.11. The values of τ and A (both as a function of θ) have been determined from the 1989-2008 data, and can now be applied to any 100 hPa flux difference to obtain a PV anomaly difference. The PV-flux relation at the 600 K level as visualized in Fig. 4.3a, shows that interannual variations in the polar cap PV anomaly are to a good approximation linearly related to the interannual variations in the integrated 100 hPa heat flux.

4.5 The PV-flux relation applied to the 2008/2009 winter

The mean PV-flux relation is now used to predict the polar cap PV anomaly from the 100 hPa heat flux for the 2008/2009 winter. This is an independent test case, since the 2008/2009 data is not used in the determination of the general PV-flux relation. Applying the PV-flux relation to the 2008/2009 flux therefore presents a test on how well the variation in the polar cap PV anomaly can be predicted from the variation in the 100 hPa heat flux. The polar cap PV anomaly for 2008/2009 is given in Fig. 4.4a, clearly showing the drop in stratospheric polar cap PV anomaly during the sudden stratospheric warming in late January (24 January 2009 according to *Labitzke and Kunze*, 2009). For comparison: the 1989-2008 climatological stratospheric polar cap PV anomaly (Fig. 4.4b) is positive throughout the whole winter season. Comparison of the climatological and 2008/2009 (not integrated) 100 hPa heat flux (Fig. 4.5) shows that during the second half of January 2009 the flux was about three times as large as the climatological flux, indicating that the wave forcing of the stratosphere was exceptionally large.

We apply the PV-flux relation to the 2008/2009 winter with respect to the clima-

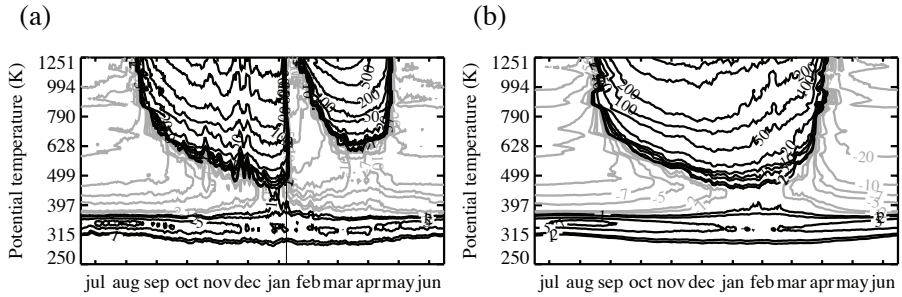

Figure 4.4: *Daily polar cap PV anomaly (PVU) for (a) July 2008 to June 2009 and (b) the 1989-2008 climatology, as a function of potential temperature (K) and time. Contours at ± 1, 2, 5, 7, 10, 20, 50, 100, 200, 500, 1000, 2000, 3000 PVU and negative values represented by grey lines. In (a) 24 January is indicated by a vertical line.*

tology, and thus use the difference in flux between 2008/2009 and the climatology. Eq. 4.11 is used to calculate the PV anomaly difference from the flux difference, using the mean τ and A determined in the previous section. The 2008/2009 polar cap PV anomaly is then predicted by adding this PV anomaly difference to the climatological polar cap PV anomaly. The result is shown in Fig. 4.6a. At first sight the predicted polar cap PV anomaly looks very similar to the ERA-Interim polar cap PV anomaly (Fig. 4.4a), with as most striking feature the sudden warming event, accompanied by a change in sign of the polar cap PV anomaly in the second half of January. Other similarities between the predicted and ERA-Interim PV anomaly are the increasing stratospheric PV anomaly values in autumn as the pole cools, the recovery of the positive polar cap PV anomaly values after the SSW, starting in the upper stratosphere and extending downward in time (due to the longer relaxation timescales in the lower stratosphere compared to the upper stratosphere), but not reaching the lower stratosphere before the final break up of the vortex in spring.

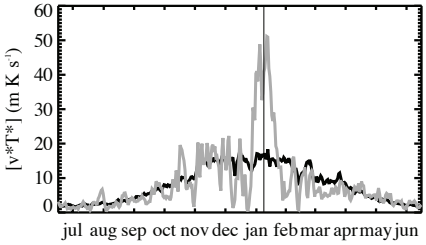

Figure 4.5: *Daily 100 hPa heat flux, $[v^\star T^\star]$ (in K m s^{-1}), as a function of time for the climatology (black) and 2008/2009 (grey). 24 January is indicated by a vertical line.*

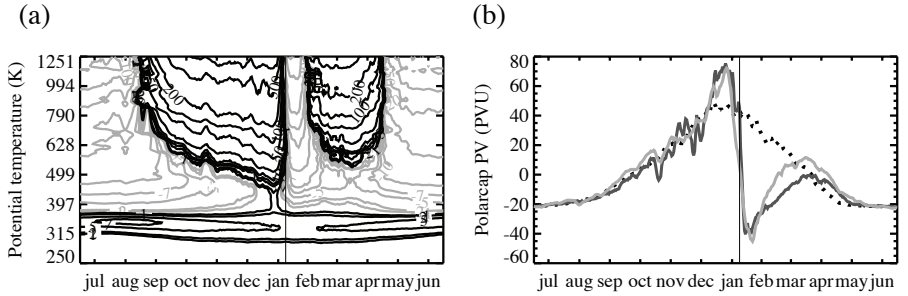

Figure 4.6: *(a) Predicted 2008/2009 daily polar cap PV anomaly (PVU) as a function of potential temperature (K) and time, contours as in Fig. 4.4 (b) Daily 2008/2009 polar cap PV anomaly (PVU) at the 600 K isentrope for the predicted (light grey), ERA-Interim (dark grey) and climatological (dotted) PV anomaly as a function of time. 24 January is indicated by a vertical line.*

The main differences between the predicted and ERA-Interim polar PV anomaly are a too small variability in early winter for the predicted PV anomaly, and some differences in the timing and amplitude of the recovery of the PV anomaly after the SSW. However, in general it can be concluded that the predicted polar cap PV anomaly captures the main features and large scale variability of the actual PV anomaly quite well.

This is supported by Fig. 4.6b, which shows a cross section at 600 K of the predicted polar cap PV anomaly for 2008/2009, the ERA-Interim polar cap PV anomaly for 2008/2009 and the climatological polar cap PV anomaly. The 600 K polar cap PV anomaly values show that the predicted PV anomaly captures the high values before the sudden warming event, the quick decrease during the SSW and the slow recovery afterwards. The clear resemblance between the predicted and ERA-Interim polar cap PV anomaly is also visible in Fig. 4.7, which shows the zero contour of the daily polar cap PV anomaly as a function of time and potential temperature for the climatology, ERA-Interim 2008/2009 case and the predicted 2008/2009 case, indicating the structure of the formation and break up of the polar vortex. This figure also shows that, although the recovery of the PV anomaly after the SSW is somewhat different for the predicted case compared to the ERA-Interim data, the break up of the vortex for the predicted case is later than for the climatology and the structure of the predicted PV anomaly is clearly closer to the observed structure than to the climatology.

The good agreement between the predicted and actual polar cap PV anomaly indicates that, for the 2009 case, the information for the sudden stratospheric warming was already present in the 100 hPa heat flux. A supporting result is obtained by *Kinnersley* (1998) in a model study. For the winter of 1987/1988 *Kinnersley* (1998) finds that the state of the extratropical stratosphere during this winter is hardly influenced by the phase of the QBO, while it strongly depended on the planetary wave forcing

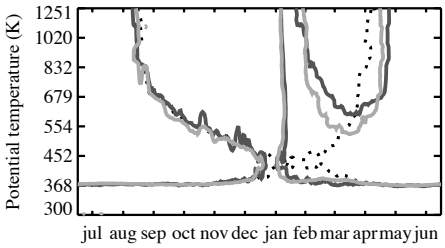

Figure 4.7: *Daily polar cap PV anomaly (PVU) for the 1989-2008 ERA-Interim climatology (dotted), for the 2008/2009 ERA-Interim data (dark grey) and for 2008/2009 predicted from the climatological polar cap PV anomaly and the 2008/2009 - climatology 100 hPa heat flux difference (light grey) as a function of potential temperature (K) and time. Only the zero contour is shown.*

from the lower stratosphere.

Figures 4.6 and 4.7 thus show that it is possible to predict the polar cap PV anomaly for 2008/2009 from just the 2008/2009 100 hPa heat flux, together with the climatological polar cap PV anomaly and flux, and the mean PV-flux relation.

4.6 Sensitivity studies

In this section the sensitivity of the results presented in section 4.5 to the choice of the relaxation timescale τ and to the slope of the PV-flux relation (A in Eq. 4.11) is studied.

4.6.1 Sensitivity of the predicted PV anomaly to the value of the slope

The results presented in the previous section are based on the general PV-flux relation as given by Eq. 4.11, with the slope A empirically determined in section 4.4. However, Fig. 4.3a shows quite some scatter of the data around the linear fit. Therefore we study the sensitivity of the results presented in the previous section to the value of the slope, by repeating the estimation of the 2008/2009 polar cap PV anomaly from the PV-flux relation, with a 50% increased or decreased slope. The values of τ are kept at the values obtained in section 4.4. The observed 2008/2009 polar cap PV anomaly is shown in Fig. 4.8, together with the predicted polar cap PV anomaly with the slope A as presented in Fig. 4.3b and with a slope of $0.5 * A$ and $1.5 * A$, with a larger drop in PV anomaly during the SSW for a larger slope. Figure 4.8a shows the results at the 600 K level, while Fig. 4.8b presents the zero contours of the observed and predicted polar cap PV anomaly as a function of potential temperature. Figure 4.8 indicates that the slope determines the value of the PV anomaly minimum during the SSW.

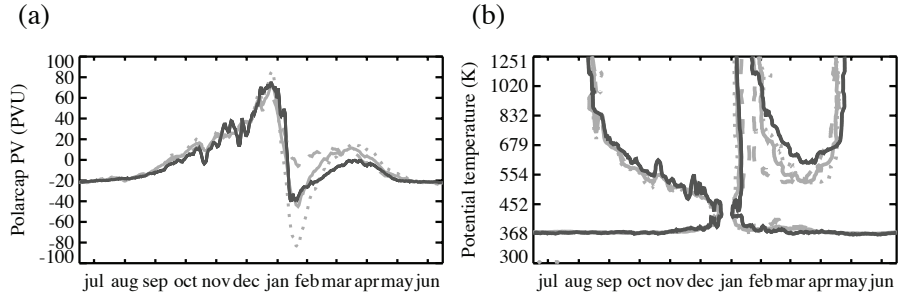

Figure 4.8: *(a) Daily 2008/2009 polar cap PV anomaly (PVU) at the 600 K isentrope for the ERA-Interim polar cap PV anomaly (dark grey) and for the predicted polar cap PV anomaly (light grey) with slopes A (solid), $0.5 * A$ (dashed) and $1.5 * A$ (dotted), as a function of time. (b) Daily polar cap PV anomaly (PVU) for the 2008/2009 ERA-Interim data (dark grey) and for 2008/2009 predicted from the climatological polar cap PV anomaly and the 2008/2009 - climatology 100 hPa heat flux difference with slopes A (light grey, solid), $0.5 * A$ (light grey, dashed) and $1.5 * A$ (light grey, dotted) as a function of potential temperature (K) and time. Only the zero contour is shown.*

4.6.2 Sensitivity of the predicted PV anomaly to the value of τ

The value of the relaxation timescale τ also plays an important role in the PV-flux relation. Therefore we also examine the sensitivity of the results presented in section 4.5 to variations in τ. The value of τ is increased or decreased by 50%, after which the procedure described in section 4.4 is repeated to obtain the accompanying slope values. The polar cap PV anomaly is then predicted again from Eq. 4.11 with the new values for τ and A. The observations and different predictions of the 2008/2009 polar cap PV anomaly are shown in Fig. 4.9a for the 600 K level, and in Fig. 4.9b for the zero contours as a function of potential temperature. Figure 4.9 illustrates that the value of τ determines the speed and strength of the recovery of the PV anomaly after the SSW, where the recovery is less strong and takes longer for a larger τ, as you would expect. The results for the 2008/2009 winter are, however, not very sensitive to variations in τ.

Another way to obtain an estimate for the relaxation timescale, is by approximating τ as a linear function of $\ln(\theta)$ (with θ in kelvin). Assuming $\tau = 5$ days at 1600 K (at a height of about 40 km) and $\tau = 90$ days at 300 K (comparable to the damping timescales mentioned in *Newman et al.*, 2001, to give good correlations between the heat flux and polar temperatures), τ is given by:

$$\tau = -50 \ln(\theta) + 375. \tag{4.13}$$

The value of τ as a function of potential temperature obtained from Eq. 4.13 is presented in Fig. 4.10, together with the correlation coefficient that accompanies this τ (found by inserting this τ into the correlation coefficient obtained in section 4.4). Note

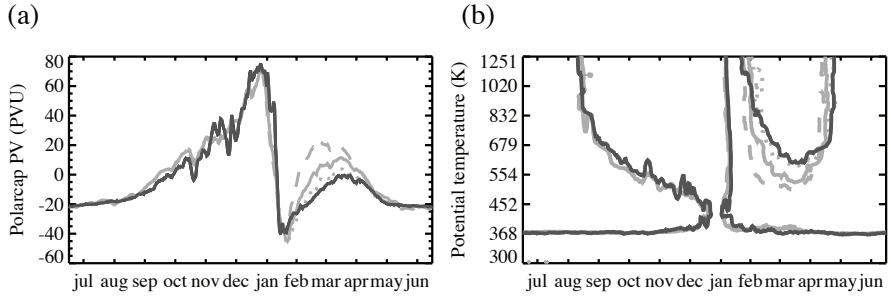

Figure 4.9: *(a) Daily 2008/2009 polar cap PV anomaly (PVU) at the 600 K isentrope for the ERA-Interim polar cap PV anomaly (dark grey) and for the predicted polar cap PV anomaly (light grey) with relaxation timescales τ (solid), $0.5 * \tau$ (dashed) and $1.5 * \tau$ (dotted), as a function of time. (b) Daily polar cap PV anomaly (PVU) for the 2008/2009 ERA-Interim data (dark grey) and for 2008/2009 predicted from the climatological polar cap PV anomaly and the 2008/2009 - climatology 100 hPa heat flux difference with timescales τ (light grey, solid), $0.5 * \tau$ (light grey, dashed) and $1.5 * \tau$ (light grey, dotted) as a function of potential temperature (K) and time. Only the zero contour is shown.*

that due to the logarithmic scaling of the vertical axis τ is a straight line in Fig. 4.10. The correlation coefficient for this τ is very similar to the correlation found for the mean τ in section 4.4 (Fig. 4.1). This τ is now used to obtain a general PV-flux relation, following the method described in section 4.4, after which the values for the slope and τ are applied to predict the PV anomaly difference between 2008/2009 and the climatology. The 2008/2009 polar cap PV anomaly is then determined by adding this PV anomaly difference to the climatological polar cap PV anomaly, and the results are shown in Fig. 4.11a for the 600 K level and in Fig. 4.11b for the structure

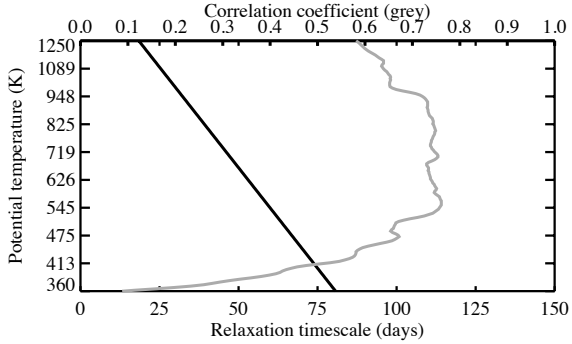

Figure 4.10: *Predicted relaxation timescale: $\tau = -50 \ln(\theta) + 375$ (in days, bottom axis, black line) and corresponding correlation coefficient between DJFM integrated flux difference and minus DJFM polar cap PV anomaly difference derived from the ERA-Interim data 1989-2008 (top axis, grey line), both as a function of potential temperature (K). Note the logarithmic scaling of the potential temperature axis.*

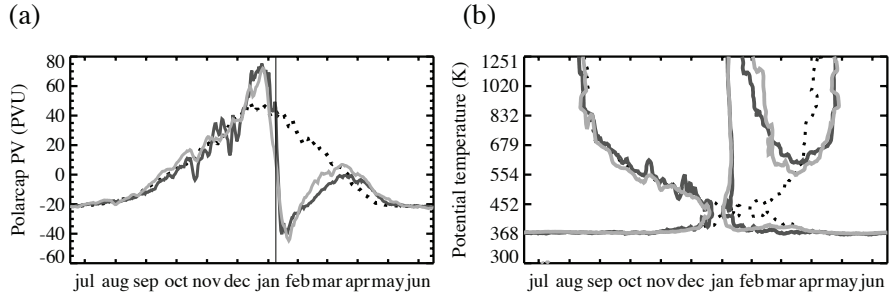

Figure 4.11: *(a) Daily 2008/2009 polar cap PV anomaly (PVU) at the 600 K isentrope for the climatological PV anomaly (dotted), ERA-Interim PV anomaly (dark grey) and predicted PV anomaly (with the relaxation timescale τ as in Eq. 4.13, light grey) as a function of time. (b) Daily polar cap PV anomaly (PVU) for the 1989-2008 ERA-Interim climatology (dotted), for the 2008/2009 ERA-Interim data (dark grey) and for 2008/2009 predicted from the climatological polar cap PV anomaly and the 2008/2009 - climatology 100 hPa heat flux difference, with τ as in Eq. 4.13 (light grey) as a function of potential temperature (K) and time. Only the zero contour is shown. In (a) 24 January is indicated by a vertical line.*

of the polar cap PV anomaly as a function of potential temperature. The results are very similar to those presented in Fig. 4.6b and Fig. 4.7 for the τ determined from the ERA-Interim data, again showing that the results for 2008/2009 are not very sensitive to the choice of τ.

4.7 Conclusions

We have shown that a quantitative, predictive relation exists between the stratospheric polar cap PV anomaly and the 100 hPa heat flux. A difference in PV anomaly is found to be linearly related to the integrated flux difference, with an integration over time of the flux difference times a factor $\exp(-t/\tau)$, to include the effect of decreasing relaxation timescales with height. This general PV-flux relation was then applied to the 100 hPa flux difference between 2008/2009 and the climatology (1989-2008), to obtain a prediction of the polar cap PV anomaly difference between the 2008/2009 winter and the climatology. A prediction of the 2008/2009 polar cap PV anomaly was obtained by adding this PV anomaly difference to the climatological PV anomaly. The ERA-Interim polar cap PV anomaly for 2008/2009 shows a large and abrupt change in the PV anomaly in midwinter, related to the occurrence of the sudden stratospheric warming, and this is also captured by the PV anomaly predicted from the 100 hPa flux and the PV-flux relation.

The results of the general PV-flux relation show that, on average, about 50% of the interannual variability in the state of the stratosphere that is observed in the Northern Hemisphere can be explained by the interannual variations in the 100 hPa heat flux. For the individual winter of 2008/2009, the fraction of the variability explained by the

100 hPa heat flux was even larger ($\sim$ 80%). This is consistent with the conclusion of *Christiansen* (2001), who found that the stratospheric variability is driven by the vertical component of the Eliassen-Palm flux (which is proportional to the heat flux used in the present study) based on covariance analyses.

Furthermore, we conclude that for the 2009 SSW the information for the SSW was already present in the 100 hPa heat flux, indicating that the state of the upper stratosphere prior to the SSW was of minor importance for the occurrence of the SSW. Previous studies have shown that before the occurrence of sudden warming events the stratosphere is often in a preconditioned state, with a poleward displaced polar jet (*Labitzke*, 1981; *Limpasuvan et al.*, 2004). This corresponds to a steeper PV gradient near the pole, allowing for stronger vertical wave propagation and stronger erosion of the polar vortex (*Polvani and Saravanan*, 2000; *Scott et al.*, 2004). Although a steep stratospheric PV gradient at a more poleward location than for the climatology was indeed present in early January 2009, this is only of secondary importance for our study, since we predicted the polar cap PV anomaly for the 2008/2009 winter from just the climatological PV (which is not preconditioned), the mean PV-flux relation and the 2008/2009 100 hPa heat flux. So the state of the upper stratosphere in 2008/2009 is not needed to obtain a reasonable prediction of the polar cap PV anomaly.

However, the state of the lower stratosphere before the SSW could be of importance in determining the amount of wave activity that can propagate into the stratosphere, thereby influencing the 100 hPa flux. In a model study, *Scott and Polvani* (2004) indeed find that SSW-like variability in the stratosphere may exist in the absence of tropospheric variability. *Bell* (2009, chapter 5) further shows that the increased wave driving of the stratosphere that is found for enhanced greenhouse gas concentrations can partly be attributed to increased tropospheric wave generation, but that changes in the radiative state of the stratosphere are also important. *Haklander et al.* (2007), on the other hand, show that the interannual variability of the 100 hPa heat flux is dominated by stationary waves (which are excited in the troposphere). Furthermore, transient wave excitation is abundant in the troposphere, so that it is realistic to assume that the 100 hPa heat flux is influenced by tropospheric waves. This is supported by the 2008/2009 heat flux at 850 hPa (not shown), which also shows a peak in January, a few days before the peak at 100 hPa. We therefore believe that at least part of the variability in the 100 hPa heat flux is related to wave forcing from the troposphere to the stratosphere, but can not exclude a dependence of the 100 hPa flux on the state of the lower stratosphere in the present study.

Smaller scale stratospheric variability, as seen in December 2008 in Fig. 4.4a, is only partly captured in the PV anomaly predicted from the 100 hPa flux, and might thus be due to stratospheric internal variability.

Sensitivity studies show that the results for the 2008/2009 predicted polar cap PV anomaly are not very sensitive to the values of the slope A of the general PV-flux

relation (Eq. 4.11) or to the values of the relaxation timescale τ. Changes of $\pm$ 50% in A or τ hardly affect the qualitative results. The value of A influences the value of the PV anomaly minimum during the SSW, where a higher A leads to a stronger decrease in PV anomaly during the SSW. The value of τ, on the other hand, influences the recovery of the PV anomaly after the SSW, with a faster and stronger recovery for a smaller τ.

The occurrence of an SSW and its effect on the stratosphere depend on the climatological state of the stratosphere, although the stratospheric climate itself is also partly set by the presence of SSWs. Nonetheless, our study implies that the occurrence or strength of SSWs might change due to climate change. If, for example, diabatic cooling of the stratosphere due to increased greenhouse gas concentrations increases the climatological PV, the same wave forcing will lead to a less severe disturbance of the polar vortex, and the criterion of a major SSW might not be met. Since the PV-flux relation as applied to 2008/2009 directly links the climatology and the wave forcing, the PV-flux relation framework might be a useful tool to examine the influence of climate change on the occurrence of SSWs. It should, however, be noted that changes in the PV-flux relation should then also be taken into account.

Similar to its application to climate change studies, the PV-flux relation can be used to evaluate the ability of models to simulate realistic sudden stratospheric warmings (see *Maycock et al.*, 2009, for a discussion about the inability of some seasonal forecasting models to simulate realistic SSWs). Three aspects of the model climate can be compared to, for example, the ERA-Interim climate. The first is the 100 hPa heat flux, representing the forcing of the stratosphere. The second is the polar cap PV anomaly distribution of the stratosphere, representing the state of the stratosphere. The third aspect is the PV-flux relation, representing the coupling between the troposphere and the stratosphere. The present PV-flux relation provides a useful framework in which to diagnose the performance of models with respect to stratospheric warmings.

Acknowledgements

The ECMWF ERA-Interim data used in this study have been provided by ECMWF.

5

Influence of the 2009 sudden stratospheric warming on the tropospheric winds

- ⋆ -

The influence of the zonal mean stratospheric potential vorticity (PV) on the zonal mean wind in the troposphere is investigated for the period November 2008 to March 2009, with special focus on the major sudden stratospheric warming (SSW) that occurred during January 2009. The 2009 SSW has a strong influence on the stratospheric PV over the pole, with a positive polar stratospheric PV anomaly before the SSW, and negative values of the polar PV anomaly afterwards. The stratospheric influence on the tropospheric winds, found by piecewise potential vorticity inversion, is westerly before the SSW (of the order of 1 m s^{-1}), while it is easterly afterwards (-2 to -4 m s^{-1}). This results in changes in the stratospheric influence on the tropospheric winds up to 5 m s^{-1} within a few weeks. These changes are found to be a substantial contribution to the wind difference observed in the ECMWF ERA-Interim data, indicating that the stratosphere influences the tropospheric conditions, leading to a weakening of the westerlies or even a switch to easterlies due to the occurrence of the January 2009 SSW. The PV changes accompanying the SSW in the lower stratosphere persist for several months, and in late winter a difference of the order of 5 m s^{-1} in stratospheric influence is found between a year with and a year without an SSW. Stratospheric information might therefore be valuable for extended range weather forecasts.

This chapter is based on:
Hinssen, Y., A. van Delden, and T. Opsteegh, Influence of sudden stratospheric warmings on tropospheric winds, *Submitted to Meteorologische Zeitschrift*, 2010.

5.1 Introduction

The winter of 2008/2009 was cold in Western Europe and parts of Northern America. The persistence of the coldness throughout winter was exceptional and might suggest a link to the stratosphere above. *Thompson et al.* (2002), for example, note that a weakening of the wintertime stratospheric polar vortex is often followed by cold conditions over North-East America, Northern Europe and Eastern Asia, that can persist for about two months. Related to this, it is noted in observational data (*Baldwin and Dunkerton*, 1999, 2001) as well as in model data (*Gerber and Polvani*, 2009) that the tropospheric annular mode (a measure of the pressure difference between the pole and the midlatitudes) remains in the negative phase for an extended period after a sudden stratospheric warming (SSW). The negative phase of the annular mode is in general associated with a more easterly flow in the midlatitudes, and thereby less advection of relatively warm air from the ocean across Western Europe.

In January 2009, a major SSW occurred in the Northern Hemisphere, splitting the polar vortex in two (*Manney et al.*, 2009; *Labitzke and Kunze*, 2009). Major SSWs are phenomena during which the polar stratosphere is substantially warmed and the stratospheric winds reverse direction from westerlies to easterlies (see, for example, *Matsuno*, 1971; *Gerber and Polvani*, 2009; *Gerber et al.*, 2009; *Limpasuvan et al.*, 2004; *Charlton and Polvani*, 2007; *Charlton et al.*, 2007; *Matthewman et al.*, 2009, for a more elaborate discussion on SSWs, based on conceptual models, general circulation models and observational studies). On 24 January 2009 the conditions of a major warming were fulfilled, as the zonal wind and the temperature gradient reversed direction at 60°N and 10 hPa (*Labitzke and Kunze*, 2009). The 2009 SSW presented the ideal stratospheric circumstances for a persistence of the negative phase of the annular mode, and thus persistent cold conditions in Western Europe. If the troposphere is affected by the occurrence of an SSW, (extended range) weather forecasts will benefit from improved understanding and representation of SSW events in models. The idea that information from the stratosphere can be useful to extend weather forecasts is put forward in, for example, *Thompson et al.* (2002) and *Baldwin et al.* (2003). In the present chapter we examine to what extent an SSW in the stratosphere influences the troposphere, by examining how the zonal mean winds in the troposphere are affected by the changes in the zonal mean state of the stratospheric potential vorticity (PV) that accompanied the SSW in January 2009.

Stratospheric changes can affect the tropospheric circulation directly through hydrostatic and geostrophic adjustment, or indirectly due to changes in the reflection and propagation of planetary waves. The term ‘direct’ is used to indicate that adjustment to a change in the stratosphere directly results in changes in the troposphere, but the cause of the change in the stratosphere might still be located in the troposphere. The term ‘indirect’, on the other hand, is used to indicate that beside the direct tropo-

spheric adjustment to the stratospheric changes, additionally the propagation of waves changes (*Perlwitz and Graf*, 2001; *Perlwitz and Harnik*, 2003, 2004; *Shaw et al.*, 2010).

The direct pathway is examined by means of piecewise potential vorticity inversion (*Davis*, 1992), which makes use of the relation between the PV and other dynamical fields, that is given by the invertibility principle (*Kleinschmidt*, 1950; *Hoskins et al.*, 1985). Previous PV inversion studies (e.g., *Hartley et al.*, 1998; *Black*, 2002; *Black and McDaniel*, 2004) showed that changes in the lower stratospheric PV influence the winds in the troposphere. An SSW is accompanied by a clear change in the stratospheric PV, and the effect of an SSW is therefore not necessarily restricted to the stratosphere. In the present study we use PV inversion to examine the effect of the zonal mean stratospheric PV on the zonal mean zonal wind in the troposphere on a daily basis from November 2008 to March 2009. The results of 2008/2009 are compared to those of a more undisturbed winter without an SSW (1996/1997) to highlight the influence of the SSW.

Our study is related to that of *Black and McDaniel* (2004) and *Gerber et al.* (2009). *Black and McDaniel* (2004) used quasigeostrophic PV inversion to show that PV anomalies in the stratosphere associated with northern annular mode events affect the tropospheric circulation, although tropospheric PV anomalies can overshadow the stratospheric effect. They show that a change in the stratospheric PV over a nine day period around a stratospheric event is related to a geostrophic wind change in both the stratosphere and the troposphere. Here we examine the PV anomalies associated with the 2009 SSW event using isentropic PV inversion. A whole winter season is considered, to examine the influence of the stratosphere on the troposphere before, during and after the SSW. Furthermore, we study a real SSW event, while *Gerber et al.* (2009) examine the coupling between the stratosphere and the troposphere around SSWs in an idealized atmospheric general circulation model.

In chapter 2 we used PV inversion to examine the influence of the stratospheric PV above 425 K on the tropospheric winds for January months with an averaged positive or negative Arctic Oscillation (AO) index, and found only a small influence of the stratosphere on the troposphere. However, here we use daily PV values, instead of monthly means. Furthermore, we examine the winter of 2008/2009 with a strong SSW, instead of an average over years with a similar AO index. We use 400 K as the lower boundary of the stratospheric PV anomaly rather than 425 K, since the daily PV anomaly distributions show that the stratospheric PV anomaly can reach down to 400 K, while the tropopause PV anomaly is located below this level.

Section 5.2 presents an overview of the data used. The results of inverting the stratospheric part of the PV distribution is shown in section 5.3. Finally, section 5.4 presents a summary and some conclusions.

5.2 Data

The European Centre for Medium-Range Weather Forecasts (ECMWF) ERA-Interim reanalysis data at 37 pressure levels between 1000 hPa and 1 hPa is used for the analysis. This is the most recently produced reanalysis dataset, with an improved representation of the stratosphere compared to the previous ERA-40 reanalysis (*Fueglistaler et al.*, 2009). The daily data (from 12.00 UTC) of the zonal wind and the temperature for November 2008 to March 2009 and for November 1996 to March 1997 are interpolated from isobaric to isentropic levels by the method described by *Edouard et al.* (1997) and the zonal wind (u) and pressure (p) at potential temperature (θ) levels are zonally averaged. In order to make optimal use of the available ERA-Interim data, a stretched grid in the vertical direction is employed.

The isentropic potential vorticity, Z_θ, is then calculated from Eq. 1.1, using the zonal mean isentropic relative vorticity (ζ_θ, Eq. 1.2) and the zonal mean isentropic density (σ, Eq. 1.3). This gives a dataset of zonal mean PV, zonal wind and pressure at isentropic levels. The domain of this dataset ranges from 10.5°N to 90°N in the horizontal, with a resolution of 1.5°, and from the lower troposphere to about 1250 K in the vertical, with a resolution varying from about 2 K in the troposphere to 10 K in the upper layers. 10°N is chosen as the equatorward boundary of the domain, since the PV changes sign near the equator, and the PV inversion equation is not solvable for negative PV values. The lower boundary of the domain is determined by the available data and for each latitude this is defined as the first isentropic level for which data is available along the full latitude circle, meaning that the pressure is below 1000 hPa at all longitudes along this latitude circle.[1] We will refer to this lower boundary as the 'surface', but it should be noted that this does not correspond to the actual surface of the Earth, but is located in the lower troposphere. This 'surface-isentropic level' varies with latitude and from day to day, from around 260 K at 90°N to about 310 K near the equator in winter.

To study the relation between the potential vorticity and the zonal wind, we apply PV inversion (see section 1.2), which states that, together with a balance condition and suitable boundary conditions, the PV determines all other dynamical fields.

The boundary condition at the pole is simply that the zonal wind equals zero, because the vortex is assumed to be axi-symmetric and centred at the pole. At the outer boundary at 10.5°N we prescribe the wind according to the circulation theorem (*Hoskins et al.*, 1985, p 897). At the upper boundary we impose the ERA-Interim wind. At the lower boundary thermal wind balance is imposed (Eq. 1.12).

On the basis of the PV inversion equation, the zonal mean PV and the isentropic

[1] If a gridpoint is at the lower boundary, but the gridpoints at the same isentropic level at the latitudes directly north and south of this gridpoint are below the lower boundary, this particular gridpoint is also put below the lower boundary for the inversion, to smooth the lower boundary and ease the calculation of horizontal gradients at this point.

density are split into a reference state ($Z_{\theta,\mathrm{ref}}$) and an anomaly (Z'_θ) as described in section 1.2.2. The reference isentropic density σ_{ref} is the area-weighted average of σ over the domain in question. In our case this is the area poleward of 10°N. Therefore, σ_{ref} depends only on the height (θ). The reference PV is associated with the solution $u = 0$ and $\sigma = \sigma_{\mathrm{ref}}$, indicating that the PV anomaly represents that part of the PV field that induces a wind field, according to the PV inversion equation. With this definition we are able to distinguish two separate PV anomalies centred over the pole: one at the tropopause and the other in the polar night stratosphere above about 400 K (see also chapter 3). In this study, we examine the influence of the stratospheric polar cap PV anomaly between 400 K and 1250 K on the tropospheric winds, since this PV anomaly is most affected by the SSW. The total PV is used for the inversion, but the PV anomaly will be discussed in relation to the resulting wind field, since variations in the PV anomaly are associated with variations in the wind field.

5.3 PV inversions

Equation 1.6 is solved by successive relaxation (see section 1.2.3). The wind field that is obtained from inversion of the daily PV in the full domain is reasonably close to the ERA-Interim wind field during November 2008 to March 2009. There are some differences between the inverted and ERA-Interim wind field, especially in the subtropics to midlatitudes near the lower boundary, where the inverted wind speed is on average a few m s^{-1} lower than the ERA-Interim wind speed. We, however, believe that the inversion of the stratospheric PV between 400 K and 1250 K will give a good indication of the balanced influence of the stratospheric PV on the tropospheric wind. In the stratospheric inversions, the reference PV is used as a background distribution in the whole domain, and zero thermal wind is applied as the lower boundary condition, while the other boundary conditions remain the same as described in the previous section. By applying zero thermal wind at the lower boundary, we assume that the influence of the stratospheric PV on the surface thermal wind is negligible. This is an assumption, but it is believed that the surface temperature distribution is mainly related to the tropopause PV anomaly, since this PV anomaly is located much closer to the lower boundary than the stratospheric polar cap PV anomaly.

The daily stratospheric inversions are discussed in section 5.3.1, where comparison between 2008/2009 and 1996/1997 shows that an influence of the January 2009 SSW is still present in late winter. Inversion results for 25 day averages before and after the SSW are discussed in section 5.3.2. Comparison with the ERA-Interim wind allows us to examine the importance of the stratosphere in explaining the observed wind difference that is associated with the SSW.

5.3.1 Daily influence of the stratosphere on the troposphere

Figure 5.1 presents the wind speed obtained from inverting the daily stratospheric PV anomaly as a function of time, at 304 K and 50°N, at 298 K and 60°N, and at 292 K and 70°N. These isentropic levels are located in the mid troposphere, approximately halfway between the average tropopause level (as measured by the 2 PVU isopleth, 1 PVU = 10^{-6} K m^2 kg^{-1} s^{-1}) and the average lower boundary of the domain for each latitude (averaged over all 151 days). The results are, however, not strongly dependent on the choice of the isentropic levels, and similar results are obtained for other isentropic levels in the troposphere.

Figure 5.1a clearly shows that the influence of the stratospheric PV on the tropospheric wind changes due to the 2009 SSW. The influence is easterly in early winter (-1 to -2 m s^{-1}), decreasing in magnitude and becoming westerly in January (1 to 2 m s^{-1}), until the occurrence of the SSW in mid January, after which the stratospheric influence becomes easterly (-3 to -4 m s^{-1}). The largest easterly influence is found in early to mid February, but the influence remains easterly up to March 31 2009 (which is the last day that is considered here).

The easterly stratospheric influence in the beginning of the winter is related to the formation of the polar vortex. Figure 5.2a presents the polar cap PV anomaly (defined as the area-weighted average PV anomaly between 70°N and 90°N) for July 2008 to June 2009, and shows that a negative PV anomaly is present in the lower stratosphere in early winter, as a remnant from the summer PV anomaly distribution. The PV anomaly in the lower stratosphere increases from negative values in November to positive values in mid January, after which it decreases again during the SSW. In

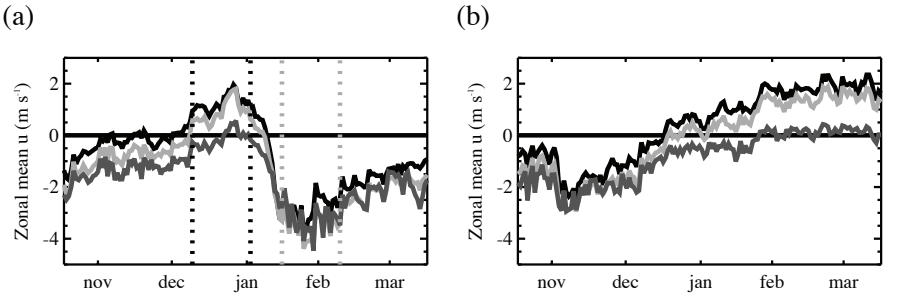

Figure 5.1: *Daily zonal mean zonal wind (m s^{-1}), obtained from inverting the stratospheric PV anomaly between 400 K and 1250 K, at 70° N and 292 K (black, upper line), at 60° N and 298 K (light grey, middle line) and at 50° N and 304 K (dark grey, lower line), as a function of time for (a) 1 November 2008 to 31 March 2009, and (b) 1 November 1996 to 31 March 1997. The tickmark accompanying the name of a month corresponds to the middle of the month. In (a), the vertical black dashed lines indicate the 25 day period 25 December 2008 to 18 January 2009 before the SSW, and the vertical grey dashed lines indicate the 25 day period 31 January to 24 February 2009 after the SSW.*

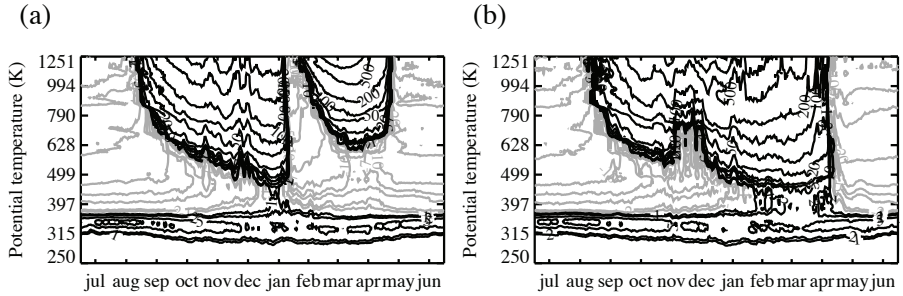

Figure 5.2: *Daily polar cap PV anomaly (PVU) for (a) July 2008 to June 2009 and (b) July 1996 to June 1997, as a function of potential temperature (K) and time. Contours at ± 1, 2, 5, 10, 20, 50, 100, 200, 500, 1000, 2000, 3000 PVU and negative values represented by grey lines.*

the beginning of February, the PV anomaly over the pole starts to recover in the upper stratosphere, but the PV anomaly in the lower stratosphere remains negative until the end of March (Fig. 5.2a). The influence of the stratosphere on the troposphere depends on the PV anomaly in the lower stratosphere, a result that is consistent with previous studies (*Black and McDaniel*, 2004; *Gerber et al.*, 2009). The lower stratospheric PV anomaly can either be a positive PV anomaly, as is the case in early January, or a negative PV anomaly, as is the case in November and February.

To illustrate the effect of the SSW, the results for the more undisturbed winter of 1996/1997 are shown in Fig. 5.1b, representing a winter without an SSW. In 1996/1997, the stratospheric influence is also easterly in early winter, similar to 2008/2009, but after it turns westerly in January, it remains westerly (1 to 2 m s^{-1}) at high latitudes, until spring. This is in agreement with the 1996/1997 polar cap PV anomaly (Fig. 5.2b), which increases in the lower stratosphere from midwinter to spring. Totally undisturbed winters are hardly ever found in the Northern Hemisphere, and a distortion of the vortex in 1996/1997 is seen in late November to mid December as a decrease in the lower stratospheric polar cap PV and an increase in the easterly influence of the stratosphere on the troposphere. The late winter vortex of 1996/1997 is, however, representative of an undisturbed vortex, indicating that the influence of the 2009 SSW is felt until long after the SSW (Fig. 5.1). The difference in stratospheric influence in March between the undisturbed winter of 1996/1997 and the disturbed winter of 2008/2009 is of the order of 5 m s^{-1} in the high latitude troposphere. The influence of the SSW is thus felt for a long time in the lower stratosphere, and also in the troposphere. This is consistent with the findings of *Baldwin and Dunkerton* (2001), who also find that the anomalies in the lower stratosphere can persist for more than two months, while the anomalies in the middle to upper stratosphere are less persistent.

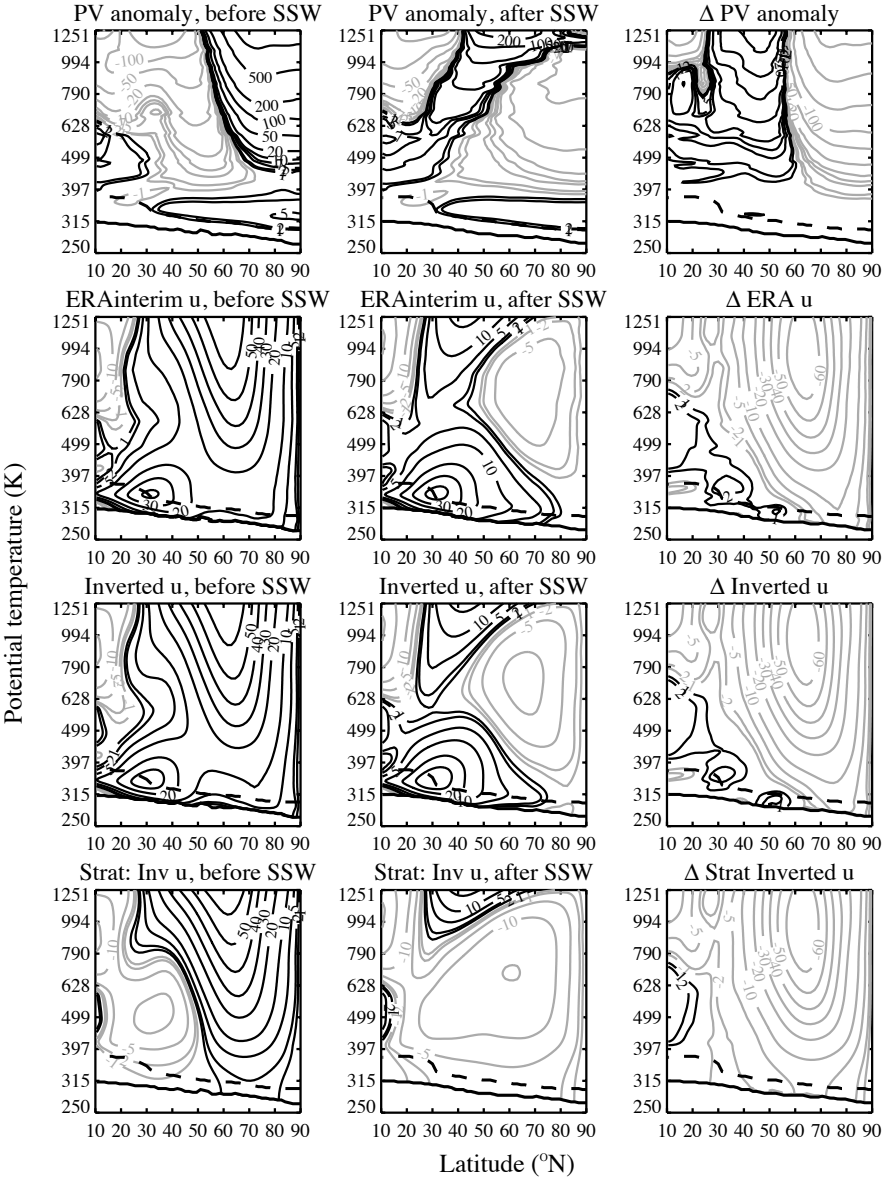
PV anomaly, before SSW
PV anomaly, after SSW
Δ PV anomaly
ERAinterim u, before SSW
ERAinterim u, after SSW
Δ ERA u
Inverted u, before SSW
Inverted u, after SSW
Δ Inverted u
Strat: Inv u, before SSW
Strat: Inv u, after SSW
Δ Strat Inverted u
Potential temperature (K)
Latitude (°N)
1251
994
790
628
499
397
315
250
10 20 30 40 50 60 70 80 90

5.3.2 Wind and PV changes due to the SSW

To examine the importance of the stratosphere in explaining the change in the zonal wind due to the SSW, two 25 day periods are considered: 25 December 2008 to 18 January 2009 before the SSW and 31 January to 24 February after the SSW (see Fig. 5.1). The zonal mean zonal wind and pressure are averaged over these periods, after which the PV is calculated for each period from Eqs. 1.1 to 1.3, and the PV anomaly is determined from Eqs. 1.8 to 1.10. The stratospheric PV anomaly above 400 K is then inverted for both periods.

Figure 5.3 presents the PV anomaly (first row), the ERA-Interim zonal mean zonal wind field (second row), the inverted zonal wind field from the inversion of the total PV (third row) and the inverted zonal wind from the inversion of the stratospheric PV above 400 K (fourth row), for the period before the SSW (left column), the period after the SSW (middle column), and for the difference between the period after minus the period before the SSW (right column). The stratospheric PV anomaly over the pole is strong and positive before the SSW, while it is negative after the SSW. This is clearly visible in the difference plot, which shows a strong decrease of the PV anomaly over the pole after the SSW compared to before. A strong decrease is also seen in the ERA-Interim wind field, showing strong westerly winds in the stratosphere before the SSW and weak easterlies afterwards. The wind difference shown in the right panel of the second row illustrates that the change in wind is not restricted to the stratosphere, but that also the high latitude troposphere experiences an easterly "forcing" of about 5 m s^{-1}. The wind speeds from inverting the total PV are somewhat lower than the ERA-Interim wind speeds, mainly in the subtropics to midlatitudes in the lower part of the domain, but the inverted wind change due to the SSW (Fig. 5.3 third row, right panel) is practically the same as the ERA-Interim wind change (Fig. 5.3 second row, right panel). The wind fields obtained from inverting the stratospheric PV (fourth row of Fig. 5.3) show that there is a weak westerly influence (1 to 2 m s^{-1}) of the stratosphere above 400 K on the troposphere before the SSW in the high latitudes, and a stronger easterly influence (-2 to -4 m s^{-1}) poleward of 20° after the SSW. The

Figure 5.3: *Daily zonal mean PV anomaly (in PVU, first row), ERA-Interim zonal mean zonal wind (in m s^{-1}, second row), zonal wind obtained from inverting the total PV (in m s^{-1}, third row) and zonal wind obtained from inverting the stratospheric PV between 400 K and 1250 K (in m s^{-1}, fourth row), averaged over a 25 day period before the SSW (25 December 2008 to 18 January 2009, left column), averaged over a 25 day period after the SSW (31 January to 24 February 2009, middle column), and the difference between the period after the SSW minus the period before the SSW (right column), as a function of potential temperature (K) and latitude (°N). The position of the tropopause is indicated by the thick dashed line, while the thick solid line near the bottom of each figure represents the lower boundary of the inversion domain. Contours for the PV anomaly as in Fig. 5.2, and contours for the wind field are every 10 m s^{-1} with the ± 1, 2 and 5 m s^{-1} contours added, with negative values represented by grey lines and zero contours omitted.*

difference (lower right panel of Fig. 5.3) is not restricted to the stratosphere, but attains values of the order of 5 m s^{-1} in the mid to high latitude troposphere.

Both the wind change related to the stratospheric PV change (Fig. 5.3 lower right panel) and the total observed and inverted wind change (Fig. 5.3 right column middle panels) show clear tropospheric changes in the wind, indicating that the stratosphere played an important role in the 2008/2009 winter. The maximum stratospheric influence on the troposphere is found between 60°N and 70°N, while the maximum wind difference seen in the ERA-Interim data and also in the inverted wind from the total PV is between 70°N and 80°N, similar to the results *Black and McDaniel* (2004) find for the negative stratospheric northern annular mode event during March 1989 (their figure 5). Internal tropospheric variability can mask part of the stratospheric signal (*Black and McDaniel*, 2004; *Gerber et al.*, 2009), so tropospheric processes can adjust the wind change that would result from the stratosphere alone. However, it is clear from Fig. 5.3 that the stratosphere imposes a strong easterly forcing on the tropospheric wind due to the SSW, and that without the stratospheric changes the tropospheric winds would have been substantially different.

5.4 Conclusions

We investigated the influence of the zonal mean stratospheric PV on the zonal mean wind in the troposphere for the period November 2008 to March 2009, with special focus on the SSW that occurred during January 2009. Piecewise potential vorticity inversion was used to invert the stratospheric PV between 400 K and 1250 K and study its influence on the tropospheric wind field.

The 2009 SSW had a strong influence on the stratospheric PV anomaly over the pole, with positive values before the SSW, and negative values after the SSW, especially in the lower to middle stratosphere. Accordingly, the influence of the stratospheric PV on the tropospheric winds was westerly before the SSW, while it was easterly afterwards. This resulted in changes up to 5 m s^{-1} within a few weeks, which are also visible in the difference between a 25 day average before the SSW and a 25 day average after the SSW. These changes were found to be a substantial contribution to the wind difference observed in the ERA-Interim data, indicating that the stratosphere influenced the tropospheric conditions, leading to a weakening of the westerlies or even a switch to easterlies after the occurrence of the January 2009 SSW.

These conclusions are consistent with the conclusions of *Black and McDaniel* (2004) and *Gerber et al.* (2009). The results of *Black and McDaniel* (2004) are based on quasi-geostrophic PV inversion. We used isentropic PV inversion, where σ is part of the solution. The similarity between our results and those of *Black and McDaniel* (2004) shows that σ in the troposphere is hardly affected by the stratospheric PV above 400 K, an assumption already made in advance in the quasi-geostrophic theory.

Our results thus confirm that the quasi-geostrophic theory is suitable to examine the influence of the stratospheric PV on the wind field in the troposphere.

Comparison of 2009 to an undisturbed winter (1996/1997) indicated that the effect of the SSW in the troposphere and lower stratosphere is felt for months after the occurrence of the SSW. In March 2009, an easterly influence of about 2 m s^{-1} was found, while a westerly influence of the same order of magnitude was found in absence of an SSW in March 1997.

An SSW, initially forced by waves from the troposphere, affects the stratospheric PV distribution for a long time. This presents a possibility for extended range weather forecasts.

Acknowledgements

The ECMWF ERA-Interim data used in this study have been provided by ECMWF.

6

The influence of the stratosphere on the tropospheric zonal wind response to CO_2 doubling

- ⋆ -

The influence of a CO_2 doubling on the stratospheric potential vorticity (PV) is examined in two climate models. Subsequently, the influence of changes in the stratosphere on the tropospheric zonal wind response is investigated, by inverting the stratospheric PV. Radiative effects dominate the stratospheric response to CO_2 doubling in the Southern Hemisphere. These lead to a stratospheric PV increase at the edge of the polar vortex, resulting in an increased westerly influence of the stratosphere on the tropospheric midlatitude winds in late winter. In the Northern Hemisphere, dynamical effects are also important. Both models show a reduced polar PV and an enhanced midlatitude PV in the Northern Hemisphere winter stratosphere. These PV changes are related to an enhanced wave forcing of the winter stratosphere, as measured by an increase in the 100 hPa eddy heat flux, and result in a reduced westerly influence of the stratosphere on the high latitude tropospheric winds. In one model, the high latitude PV decreases are, however, restricted to higher altitudes, and the tropospheric response due to the stratospheric changes is dominated by an increased westerly influence in the midlatitudes, related to the increase in midlatitude PV in the lower stratosphere. The tropospheric response in zonal wind due to the stratospheric PV changes is of the order of 0.5 to 1 m s^{-1}. The total tropospheric response has a somewhat different spatial structure, but is of similar magnitude. This indicates that the stratospheric influence is of importance in modifying the tropospheric zonal wind response to CO_2 doubling.

This chapter is based on:
Hinssen, Y. B. L., C. J. Bell, and P. C. Siegmund, The influence of the stratosphere on the tropospheric zonal wind response to CO_2 doubling, *Submitted to Atmospheric Chemistry and Physics*, 2010.
Published online in *Atmospheric Chemistry and Physics Discussions*, 10, 23895-23925, doi:10.5194/acpd-10-23895-2010.

6.1 Introduction

Numerous studies have examined model simulations of climate change due to increasing greenhouse gas concentrations. In general, a warming of the troposphere and a cooling of the stratosphere are observed in these simulations (e.g., *Gillett et al.*, 2003; *Sigmond et al.*, 2004; *Bell et al.*, 2010). The response in the zonal wind is, however, sensitive to the changes in the horizontal temperature gradient, which shows more variability among models. Cooling in the polar lower stratosphere and warming in the tropical upper troposphere enhances the horizontal temperature gradient near the midlatitude tropopause. Through the thermal wind relationship, this is related to increased westerly winds in the midlatitudes, in the tropopause region, but with a possible downward influence toward the surface. There are indeed model studies that predict an increase in the Arctic Oscillation (AO) index, which is a measure of the tropospheric flow at midlatitudes, for increasing greenhouse gas concentrations (*Shindell et al.*, 1999; *Gillett et al.*, 2002; *Moritz et al.*, 2002). However, *Baldwin et al.* (2007) note that most climate models with a well-represented stratosphere indicate that the meridional overturning circulation in the stratosphere, the Brewer-Dobson circulation, will accelerate under climate change. This would lead to adiabatic warming and higher temperatures in the Arctic lower stratosphere, resulting in weaker westerly winds in the Northern Hemisphere extratropics. Although the exact future response of the AO index is still uncertain, it is likely that stratospheric processes play a role in forming the tropospheric response to climate change.

Sigmond et al. (2004) performed simulations with a global climate model in which the carbon dioxide (CO_2) concentration was separately doubled in the stratosphere, the troposphere, and the entire atmosphere. They found that the CO_2 doubling in the entire atmosphere leads to an increase of the tropospheric midlatitude westerlies in the Northern Hemisphere winter, and that this increase in the troposphere is mainly due to the CO_2 doubling in the stratosphere. There are two ways by which stratospheric climate change due to increased CO_2 can have an effect on the troposphere, namely the effect of stratospheric CO_2 increase on the troposphere, and the effect of stratospheric climate changes, due to tropospheric CO_2 increase, on the troposphere. Only the former effect was investigated by *Sigmond et al.* (2004). However, they also find that a CO_2 doubling in the troposphere leads to an enhanced Brewer-Dobson circulation in the stratosphere and warming of the polar lower stratosphere in northern winter. It is not yet known how this troposphere-induced stratospheric change affects the troposphere. Or, more general, it is still a question what the effect is of stratospheric climate change, indirectly due to CO_2 increase in the troposphere and directly due to CO_2 increase in the stratosphere, on the troposphere. This question is considered in the present study. More specifically, we investigate the effect of stratospheric climate change due to CO_2 increase in the entire atmosphere on the tropospheric wind,

by applying piecewise potential vorticity (PV) inversion on the stratospheric PV in a reference climatology and the stratospheric PV in a doubled CO_2 climatology.

This work is based on simulations with the middle-atmosphere version of the ECHAM4 climate model as performed by *Sigmond et al.* (2004) and simulations with the Unified Model (UM), which is based on the Hadley Centre Atmosphere Model (HadAM3) coupled to a thermodynamic slab ocean model (*Gillett et al.*, 2003). These models will be referred to as the 'ECHAM model' and the 'UM model', respectively. For both models, results from a control run and a run with doubled carbon dioxide (CO_2) concentrations are used. The studies of *Sigmond et al.* (2004) and *Gillett et al.* (2003) describe the effect of CO_2 doubling in terms of temperature and wind changes. *Bell et al.* (2010) further show that the doubled CO_2 response in the UM model is robust, as a similar structure of the response, but with larger amplitude, is found under quadrupled CO_2 concentrations. Here we focus on changes in the stratospheric PV that are related to CO_2 doubling, and investigate to what extent these stratospheric changes influence the tropospheric zonal mean zonal wind response.

Piecewise PV inversion (*Davis*, 1992) is used on a monthly basis to examine to what extent the zonal mean influence of the stratosphere on the tropospheric winds changes due to an increase in greenhouse gases. PV inversion makes use of the relation between the PV and other dynamical fields, that is given by the invertibility principle (*Kleinschmidt*, 1950; *Hoskins et al.*, 1985). Previous PV inversion studies (e.g., *Hartley et al.*, 1998; *Black*, 2002; *Black and McDaniel*, 2004) showed that changes in the lower stratospheric PV influence the winds in the troposphere. A change in the stratospheric PV due to an increase in CO_2 might therefore affect the tropospheric wind.

Section 6.2 presents an overview of the data used. The influence of a CO_2 doubling on the stratospheric PV is presented in section 6.3, while the influence of the stratosphere on the tropospheric zonal wind response is studied in section 6.4. Finally, some conclusions are given in section 6.5.

6.2 Data

The climatological PV is determined from the monthly mean temperature and zonal mean wind at 30 pressure levels between 1000 hPa and 0.01 hPa for the UM model, where a 25-yr control run (pre-industrial CO_2 concentration of 289 ppmv) and a 25-yr doubled CO_2 run are considered (*Gillett et al.*, 2003). A zonal mean reconstruction of pre-industrial ozone concentrations was prescribed, and the CO_2 concentrations were kept constant within a run. The monthly mean data of the zonal wind and the temperature are interpolated from isobaric to isentropic levels with the method described by *Edouard et al.* (1997). Zonal averaging and averaging over the 25 years is performed at levels of equal potential temperature (θ) to obtain a climatological dataset

of the zonal mean zonal wind and pressure at isentropic levels. In order to make optimal use of the data, a stretched grid in the vertical direction is employed. The zonal mean isentropic potential vorticity, Z_θ, is then calculated from Eq. 1.1, using the zonal mean isentropic relative vorticity (ζ_θ, Eq. 1.2) and the zonal mean isentropic density (σ, Eq. 1.3). This gives a climatological dataset of zonal mean PV, zonal wind (u) and pressure (p) at isentropic levels. The domain of this dataset ranges from 90° to 10° north and south, with a horizontal resolution of 2.5°, and from the lower troposphere to about 1250 K in the vertical, with a resolution varying from about 2 K in the troposphere to 10 K in the upper layers. The tropical band is excluded to avoid problems associated with the inversion of negative values of the potential vorticity that are found near the equator. The lower boundary for each latitude is defined as the lowest isentropic level for which data is available along the full latitude circle (meaning that the pressure is below 1000 hPa at all longitudes along this latitude circle). We will refer to this lower boundary as the 'surface', but it should be noted that this does not correspond to the actual surface of the Earth, but is located in the lower or middle troposphere.

Similarly, the climatological PV is determined from the monthly mean temperature and zonal mean wind at 33 pressure levels between 1000 hPa and 0.01 hPa for the ECHAM model, where the last 20 years of both the control run (CO_2 concentration of 353 ppmv, note that this concentration is higher than in the UM model) and the doubled CO_2 run are considered (*Sigmond et al.*, 2004). As stated in *Sigmond et al.* (2004), the ozone distribution is prescribed. The horizontal resolution of the ECHAM model is about 2.8° (T42 horizontal resolution), and the data is interpolated to the same isentropic levels as the UM model data.

The European Centre for Medium-Range Weather Forecasts (ECMWF) ERA-Interim reanalysis data at 37 pressure levels between 1000 hPa and 1 hPa, and a horizontal resolution of 1.5° is used for comparison with the model results. The monthly mean data (at 12.00 UTC) of the zonal wind and the temperature for the period 1989 to 2008 are again interpolated from isobaric to isentropic levels. Zonal averaging and averaging over the 20 years is performed to obtain a climatological dataset of u and p at isentropic levels, after which the isentropic potential vorticity is calculated (Eq. 1.1).

To study the relation between the potential vorticity and the zonal wind, we apply PV inversion (see section 1.2), which states that, together with a balance condition and suitable boundary conditions, the PV determines all other dynamical fields.

The boundary condition at the pole is simply that $u = 0$, because the vortex is assumed to be axi-symmetric and centred at the pole. At the outer boundary, at 10°, we prescribe the wind according to the circulation theorem (*Hoskins et al.*, 1985, p 897). At the upper boundary we impose the ERA-Interim wind or the modeled wind. Since we only consider inversion of the stratospheric PV distribution, zero thermal wind is

imposed at the lower boundary:

$$\frac{\partial u}{\partial \theta} = 0 \tag{6.1}$$

The surface temperature distribution is strongly coupled to the PV in the lower part of the domain (below 400 K), so a realistic thermal wind (Eq. 1.12) should be imposed at the lower boundary to obtain a realistic subtropical jet from inversion of the tropospheric PV. Zero thermal wind is, however, believed to be a reasonable boundary condition for the inversion of the stratospheric part of the PV. PV inversion is performed on the monthly PV values between 400 K and 1250 K, by solving Eq. 1.6 by successive relaxation (see section 1.2.3 for the method of solution of the PV inversion equation).

On the basis of the PV inversion equation, the zonal mean PV and the isentropic density are split into a reference state ($Z_{\theta,\text{ref}}$) and an anomaly (Z'_θ) as described in section 1.2.2. The reference isentropic density σ_{ref} is the area-weighted average of σ over the domain in question. In our case this is the area poleward of 10°. Therefore, σ_{ref} depends only on θ. The reference PV is associated with the solution $u = 0$ and $\sigma = \sigma_{\text{ref}}$, indicating that the PV anomaly represents that part of the PV field that induces a wind field, according to the PV inversion equation. With this definition two separate PV anomalies centred over the pole are distinguished: one at the tropopause and the other in the polar night stratosphere at potential temperatures above about 400 K (see also chapter 3). In this study, we examine the influence of the stratospheric polar cap PV anomaly between 400 K and 1250 K on the tropospheric winds, since the PV anomaly in this altitude range is most affected by CO_2 doubling. The total PV is used for the inversion, but the PV anomaly will be discussed in relation to the resulting wind field, since only variations in the PV anomaly are associated with variations in the wind field.

The eddy heat flux is proportional to the vertical component of the Eliassen-Palm flux, which represents the vertical propagation of atmospheric waves. The heat flux in the lower stratosphere (100 hPa) is therefore often used as a measure of the wave forcing from the troposphere to the stratosphere (see also *Waugh et al.*, 1999; *Polvani and Waugh*, 2004; *Charlton et al.*, 2007). The monthly heat flux $[v^\star T^\star]$ (a star represents a deviation from the zonal mean quantity and the brackets indicate zonal averaging) is determined from the monthly mean meridional wind (v) and temperature (T) at pressure levels for every year, for the models as well as for the ERA-Interim data. In the next section, it is shown that the heat flux calculated from the monthly mean data gives a reasonable estimate of the seasonal cycle of the heat flux calculated from daily data. The area-weighted average heat flux at 100 hPa is determined between 40° and 80° for both hemispheres, since most wave activity enters the stratosphere in this latitude band. The climatological flux values are determined by averaging over all years (20 years for the ERA-Interim data and the ECHAM model, 25 years for the UM model).

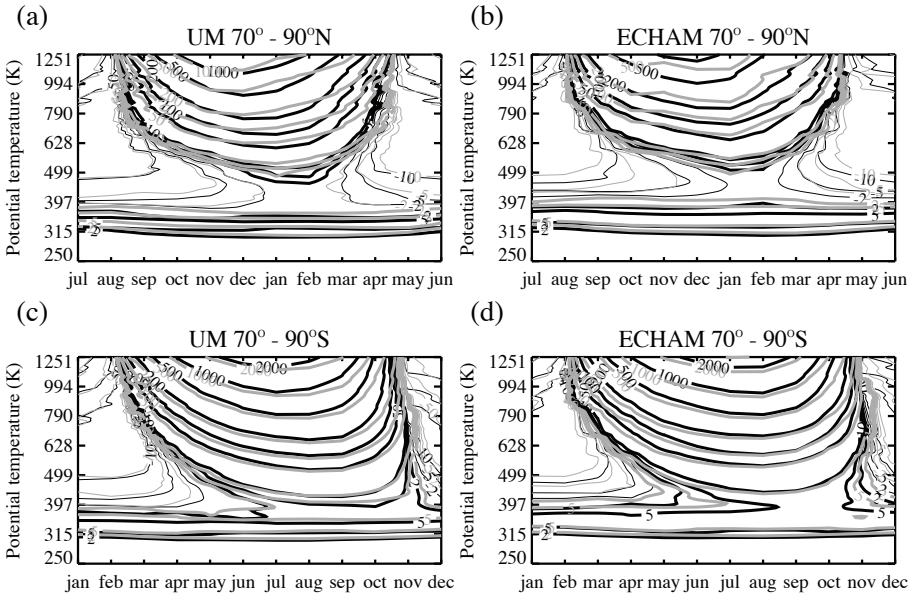

Figure 6.1: *Monthly climatological polar cap PV anomaly (area-weighted average between 70° and 90°, in PVU, 1 PVU = 10^{-6} K m^2 kg^{-1} s^{-1}) for the control run (black) and the doubled CO_2 run (grey), for (a) the NH in the UM model, (b) the NH in the ECHAM model, (c) minus the SH in the UM model and (d) minus the SH in the ECHAM model, as a function of time (months) and potential temperature (K). Contours at ± 2, 5, 10, 50, 100, 200, 500, 1000, 2000, 3000 PVU, positive values represented by thick lines and negative values represented by thin lines. Note that for both hemispheres the horizontal axis starts in summer.*

6.3 Stratospheric PV changes

Figure 6.1 presents the polar cap PV anomaly, defined as the area-weighted average isentropic PV anomaly between 70° and 90°, for the control runs (in black) and for the doubled CO_2 runs (in grey), for both hemispheres. The polar PV anomaly is studied since the zonal wind field is related to horizontal gradients in PV (first term on the right hand side of Eq. 1.6), so that changes in the polar PV can affect the midlatitude winds. Comparison of the ERA-Interim data to the model data (not shown) indicates that the model results are realistic, in amplitude as well as in seasonal cycle. Both models show a similar polar cap PV response to CO_2 doubling. The Northern Hemisphere (NH) polar stratospheric PV increases somewhat in autumn and spring due to CO_2 doubling, while it decreases in winter. An increase in Southern Hemisphere (SH) polar stratospheric PV is found from autumn through spring. These PV changes are consistent with the results of *Butchart et al.* (2000), who find enhanced cooling in the SH stratosphere in spring, and also in the NH upper stratosphere in late autumn and spring, while they find a warming in the NH lower stratosphere in winter.

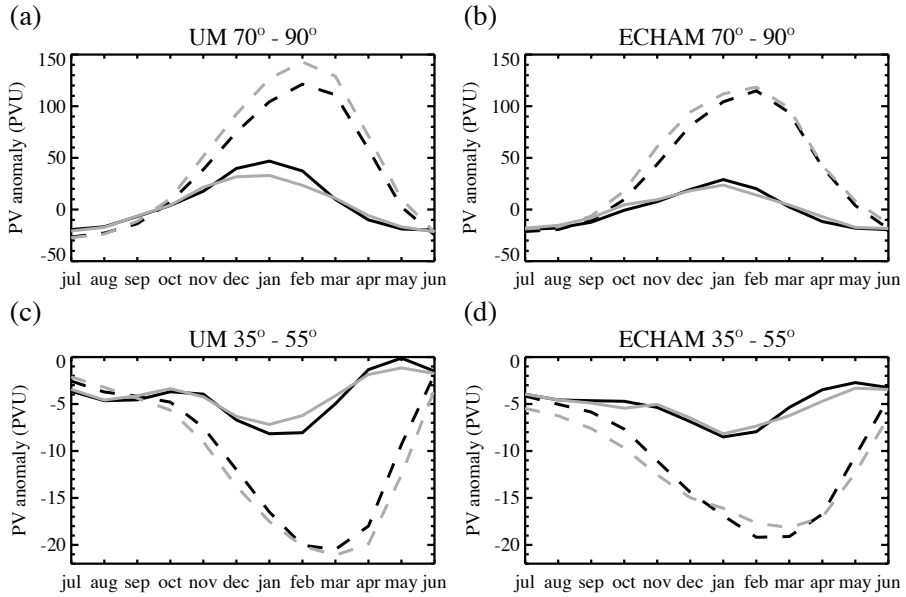

Figure 6.2: *Monthly climatological 600 K polar cap PV anomaly (PVU) for (a) the UM model and (b) the ECHAM model, and 600 K midlatitude PV anomaly (area-weighted average between 35° and 55°, in PVU) for (c) the UM model and (d) the ECHAM model, for the control run (black lines) and the doubled CO_2 run (grey lines) for the NH (solid) and minus the SH (dashed). Months noted on the horizontal axis are for the NH, and the SH values are shifted by 6 months compared to this axis.*

The stratospheric polar cap PV at 600 K is shown in Fig. 6.2a and 6.2b, for the UM model and ECHAM model, respectively. At 600 K the midwinter PV response is largest in the UM model. This is also true at higher levels in autumn and spring, while at higher levels the NH midwinter PV changes are somewhat larger in the ECHAM model than in the UM model (Fig. 6.1).

The midlatitude PV anomaly (area-weighted average PV anomaly between 35° and 55°) at 600 K is given in Figs. 6.2c (UM model) and 6.2d (ECHAM model). The NH polar cap PV anomaly decreases in winter due to CO_2 doubling, while the NH midlatitude PV anomaly increases (the amplitude of the seasonal cycle decreases in both cases), indicating increased wave breaking, mixing PV off the pole (*McIntyre and Palmer*, 1983, 1984). In the SH, the polar cap PV anomaly increases, and a slight decrease in the midlatitude PV is found throughout most of the year, with an increase in winter in the ECHAM model.

The stratospheric PV distribution is determined by radiative effects and wave effects. Since the ozone concentrations are kept fixed in the models, the PV differences between the control run and the doubled CO_2 run are not related to ozone variations. The change in CO_2 has a radiative effect. A higher stratospheric CO_2 concentration

will lead to an enhanced cooling to space (*Fels et al.*, 1980; *Butchart et al.*, 2000; *Shindell et al.*, 2001), and an accompanying increase in stratospheric PV. This is indeed seen in the SH (Figs. 6.1c and d and Figs. 6.2a and b), and in the NH autumn and spring, but not in the NH winter.

CO_2 doubling can also influence the wave forcing. *Eichelberger and Hartmann* (2005), for example, show that an increase in the meridional temperature gradient (due to tropical upper tropospheric warming or polar lower stratospheric cooling) could lead to enhanced baroclinicity in the midlatitudes and enhanced baroclinic wave generation. An increase of the wave flux out of the troposphere could increase the Brewer-Dobson overturning circulation in the stratosphere (*Butchart and Scaife*, 2001; *Eichelberger and Hartmann*, 2005), leading to increased adiabatic warming of the polar lower stratosphere.

To examine the extent to which the wave forcing can explain the PV response, the area-weighted averaged 100 hPa monthly eddy heat flux between 40° and 80° is shown in Fig. 6.3. Additionally, the ERA-Interim 100 hPa heat flux is given in Fig. 6.4. The heat flux derived from the monthly mean data is lower than the monthly averages of the heat flux derived from daily data (Fig. 6.4), but the seasonal cycle is similar. This indicates that the monthly mean data is suitable to obtain an estimate of the seasonal cycle of the heat flux.

The NH winter heat flux is somewhat higher for the ECHAM model than for the UM model. Interestingly, this is consistent with the ECHAM polar cap PV being somewhat lower than the UM polar cap PV. CO_2 doubling hardly affects the SH heat flux in the UM model, and leads to a slight decrease in the SH flux in autumn and spring in the ECHAM model. The NH heat flux, on the other hand, increases in both models, especially in winter. The largest increase is found in December and January in the UM model, and in January and February in the ECHAM model. An increase in the NH upward flux of wave activity from the troposphere due to an increase in greenhouse gas concentrations is also found by, for example, *Butchart et al.* (2000), *Schnadt et al.* (2002) and *Shepherd* (2008). *Haklander et al.* (2008) studied changes in the NH upward wave flux in the same ECHAM model runs in more detail, and found an increase of about 12% in the January-February mean 100 hPa heat flux due to CO_2 doubling. They state that this can mainly be attributed to changes in stationary wave-1, related to an increase in the meridional temperature gradient, and suggest that at least part of the increase is due to more stationary wave-1 generation at midlatitudes in the troposphere. *Sigmond et al.* (2004) show that tropospheric CO_2 doubling alone results in a warming of the lower polar stratosphere in the NH winter. This warming is likely related to the wave forcing (through an increase in the Brewer-Dobson circulation), suggesting that the heat flux increase in the NH is related to the CO_2 doubling in the troposphere. Changes initially made to the troposphere (increase in CO_2) could thus affect the stratospheric PV through wave forcing. These stratospheric

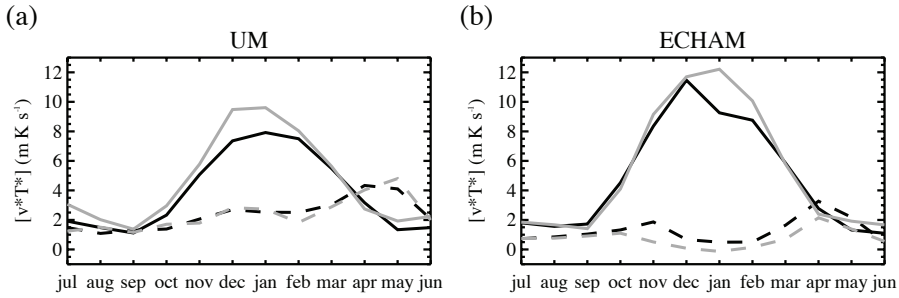

Figure 6.3: *Monthly climatological heat flux $[v^\star T^\star]$ at 100 hPa (area-weighted average between 40° and 80°, in m K s^{-1}) for the control run (black lines) and for the doubled CO_2 run (grey lines), for the NH (solid) and minus SH (dashed), for (a) the UM model and (b) the ECHAM model, as a function of time (months). Months noted on the horizontal axis are for the NH, and the SH values are shifted by 6 months compared to this axis.*

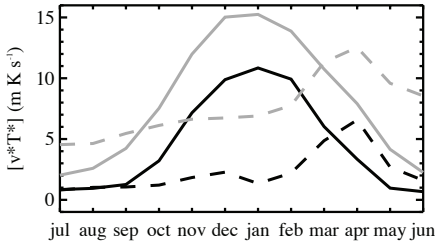

Figure 6.4: *ERA-Interim climatological 100 hPa heat flux (area-weighted average between 40° and 80°, in m K s^{-1}), derived from monthly mean data ($[\overline{v}^\star \overline{T}^\star]$, with an overbar representing the time mean, black lines) and monthly means of the heat flux derived from daily data ($\overline{[v^\star T^\star]}$, grey lines), for the NH (solid) and minus the SH (dashed). Months noted on the horizontal axis are for the NH, and the SH values are shifted by 6 months compared to this axis.*

PV changes can again feed back on the tropospheric winds, as the troposphere adjusts to the stratospheric changes.

A stronger winter wave forcing is related to lower polar cap PV anomaly values and higher midlatitude PV anomaly values (see chapter 3), similar to what is found for a CO_2 doubling in the NH (Fig. 6.2). The increase in midlatitude winter stratospheric PV in the SH ECHAM model is likely related to the polar cooling and the accompanying increase in polar PV, extending further equatorward than in the control run, thereby also affecting the midlatitude PV. If this effect plays a role, it is expected to do so in late winter, when the vortex attains its maximum size at the 600 K level. For the ECHAM model, the decrease in SH midlatitude PV in autumn and spring could be related to the decrease in wave forcing (Fig. 6.3b), but this decrease in wave forcing

is absent in the UM model, indicating that other processes must play a role as well. Other processes may incorporate changes in the propagation and absorption of waves within the stratosphere. Several studies have shown that waves tend to propagate more toward the equator for stronger westerly winds in the lower stratosphere (*Hartmann et al.*, 2000; *Shindell et al.*, 2001; *Perlwitz and Harnik*, 2003; *Kushner and Polvani*, 2004; *Sigmond and Scinocca*, 2010). Planetary wave refraction is influenced by wind shear. Waves propagating upward from the troposphere are refracted equatorward by the increased vertical wind shear in the lower stratosphere when the vortex is strong (*Shindell et al.*, 2001). This provides a positive feedback, where a stronger vortex is less disturbed by waves. A strengthening of the SH vortex due to CO_2 doubling might thus lead to more equatorward refraction of waves, an increase in the polar cap PV anomaly and a decrease in the PV anomaly at lower latitudes, since less polar PV is transported off the pole.

6.4 Stratospheric influence on the troposphere

Figures 6.1 and 6.2 displayed that a CO_2 doubling affects the stratospheric PV distribution. To investigate the impact on the tropospheric circulation, PV inversion is applied to the monthly PV values between 400 K and 1250 K. The formation of the polar vortex starts in the upper stratosphere in autumn, reaching the lower stratosphere in winter (Fig. 6.1). Since it is mainly the lower stratosphere that influences the tropospheric winds, the late winter season is examined: February in the NH and August in the SH.

Since we consider climate change experiments, difficulties arise with interpreting the wind response in isentropic coordinates. Globally averaged, a tropospheric warming response of about 3 K is found, indicating a shift of the atmosphere relative to the potential temperature axis. A certain isentropic level in the troposphere will therefore be closer to the surface for the doubled CO_2 run than for the control run. This means that the wind response in isentropic coordinates mainly shows the tropospheric vertical wind shear, and not the change in winds due to climate change. Therefore it is decided to interpolate the results back to pressure levels, to facilitate a fair comparison of the wind response in the model runs and in the inversion results. Due to the interpolations and due to the way we define the lower boundary in isentropic coordinates (see section 6.2), no results are available at the lowermost pressure levels. This, however, still allows us to examine the influence of the stratosphere on the middle troposphere, which is suitable for the purpose of the present study.

Figure 6.5 shows the NH February mean PV anomaly and zonal mean zonal wind field for the UM control run (top row, left and middle column) and the response to CO_2 doubling (lower row). The potential temperature varies with pressure from about 300 K at 500 hPa, to 400 K at 100 hPa, 850 K at 10 hPa, and 1200 K at 5 hPa. It should

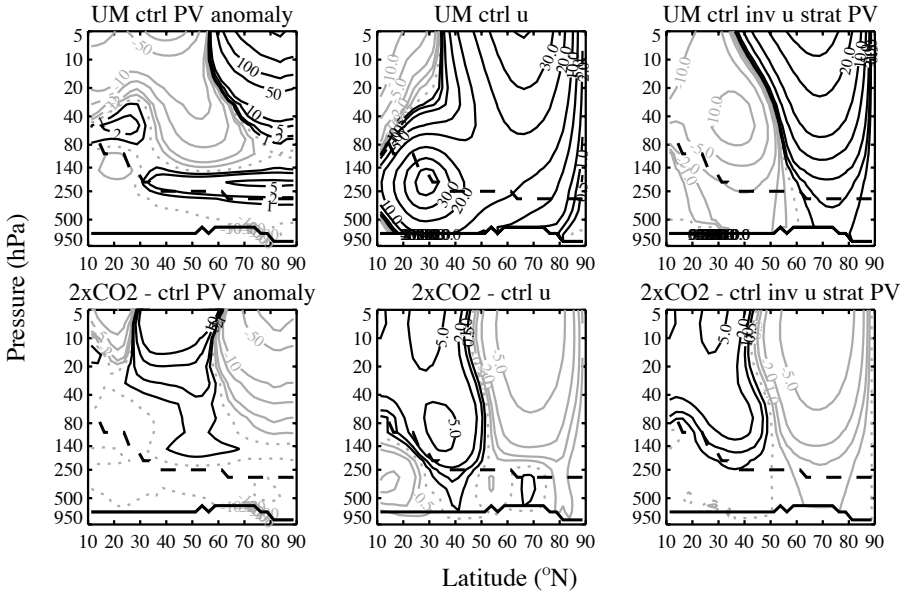

Figure 6.5: *February mean, zonal mean monthly PV anomaly (in PVU, left column), UM zonal wind (in m s^{-1}, middle column) and zonal wind obtained from inverting the stratospheric PV between 400 K and 1250 K (in m s^{-1}, right column), for the UM control run (top row), and the difference between the UM doubled CO_2 run minus the UM control run (bottom row), for the NH as a function of pressure (hPa) and latitude (°N). The position of the control run tropopause (as measured by the 2 PVU isopleth) is indicated by the thick dashed line, while the thick solid line near the bottom of each figure represents the lower boundary of the inversion domain (interpolated back to pressure coordinates). Contours for the PV anomaly are as in Fig. 6.1 with the ± 1 PVU contour added, contours for the wind fields are every 10 m s^{-1} with the ± 0.5, 1, 2 and 5 m s^{-1} contours added. Negative values are represented by grey lines and the zero contours by grey dotted lines.*

be noted that the potential temperature strongly varies with latitude in the troposphere, at 500 hPa from about 280 K at the pole to 320 K in the tropics. The tropopause has a potential temperature of about 300 K at the pole and 380 K at 10° in winter, so the PV anomaly above 400 K is indeed a stratospheric PV anomaly.

In the UM model, CO_2 doubling results in a clear decrease in the PV anomaly over the pole, while the midlatitude PV anomaly increases. Accompanying these PV changes, a decrease in the magnitude of the westerly polar jet is found in the stratosphere. However, the wind speed on the equatorward side of the jet increases, indicating an equatorward shift of the stratospheric jet. The wind field that is obtained from inversion of the stratospheric PV above 400 K is shown in the right column of Fig. 6.5. The stratospheric PV changes induce stratospheric wind changes, but also affect the high latitude tropospheric winds (lower right panel in Fig. 6.5). The tropospheric wind response related to the stratospheric PV changes is small (of the order of 0.5 m s^{-1}),

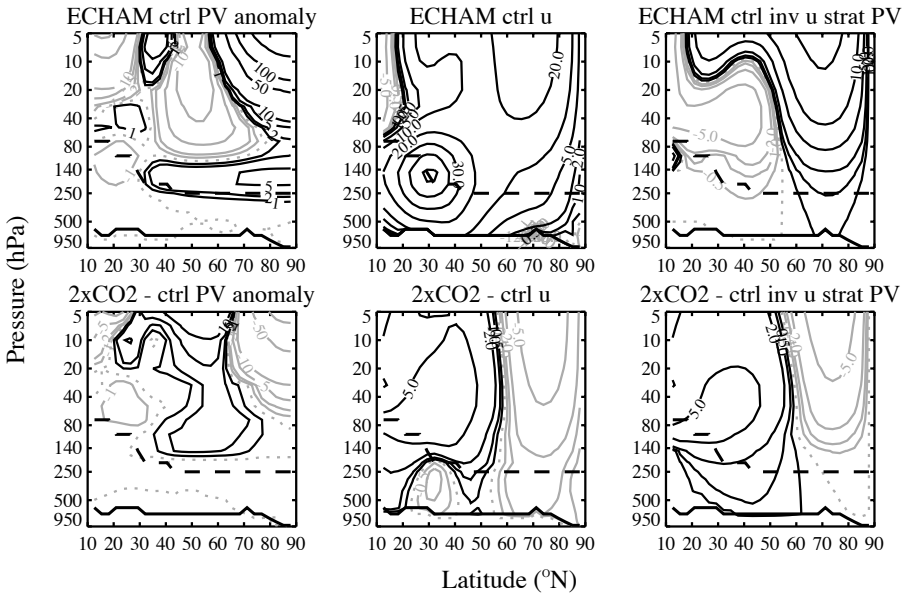

Figure 6.6: *Same as Fig. 6.5 but for the ECHAM model.*

but of the same order of magnitude as the total response in model zonal wind (lower middle panel in Fig. 6.5). This indicates that the influence of the stratosphere is relevant for the tropospheric response, and that it results in a weaker westerly wind in the high latitude troposphere in the NH winter.

The results for the ECHAM model are presented in Fig. 6.6. The models agree on the large scale response to CO_2 doubling. Both show a decrease in the polar stratospheric PV, a decrease in the high latitude winds and an equatorward shift of the stratospheric polar jet. However, for the ECHAM model, the decrease in westerly winds in the stratospheric inversions is restricted to the higher latitude stratosphere (lower right panel in Fig. 6.6), while an increased westerly influence (of 0.5 to 1 m s^{-1}) of the stratosphere on the midlatitude tropospheric winds is found. Decreased PV anomaly values are indeed restricted to somewhat higher latitudes and levels in the ECHAM model than in the UM model, while an increase in the mid- to high latitude PV anomaly is found in the lower stratosphere in the ECHAM model (compare the lower left panels of Figs. 6.5 and 6.6). These figures illustrate that a slight shift in the location of a PV anomaly (in altitude or latitude) can change the tropospheric response to stratospheric PV changes.

The SH August mean PV anomaly, wind field and inverted wind field from the stratospheric PV are shown in Fig. 6.7 and 6.8 for the UM model and the ECHAM

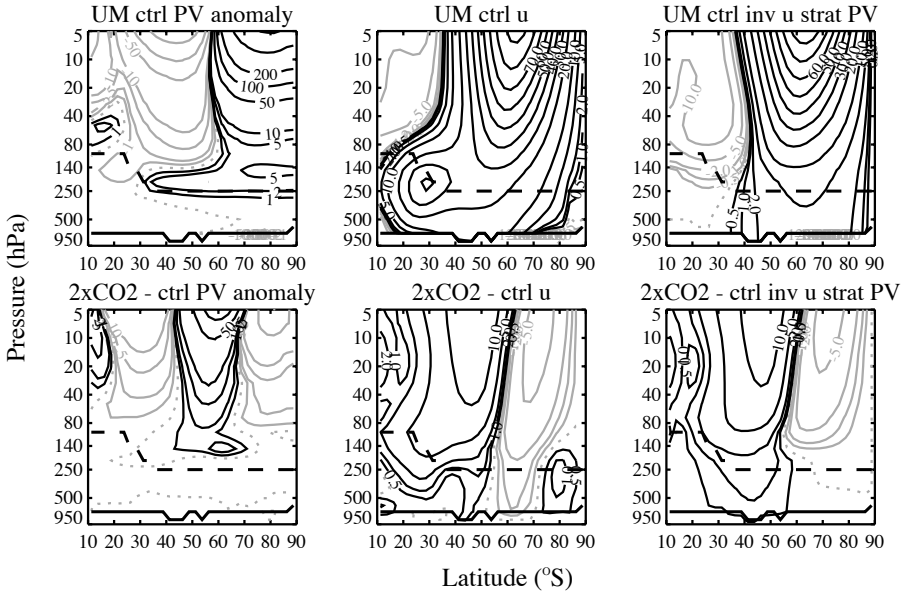

Figure 6.7: *Same as Fig. 6.5 but for August in the SH (minus the PV anomaly values are shown).*

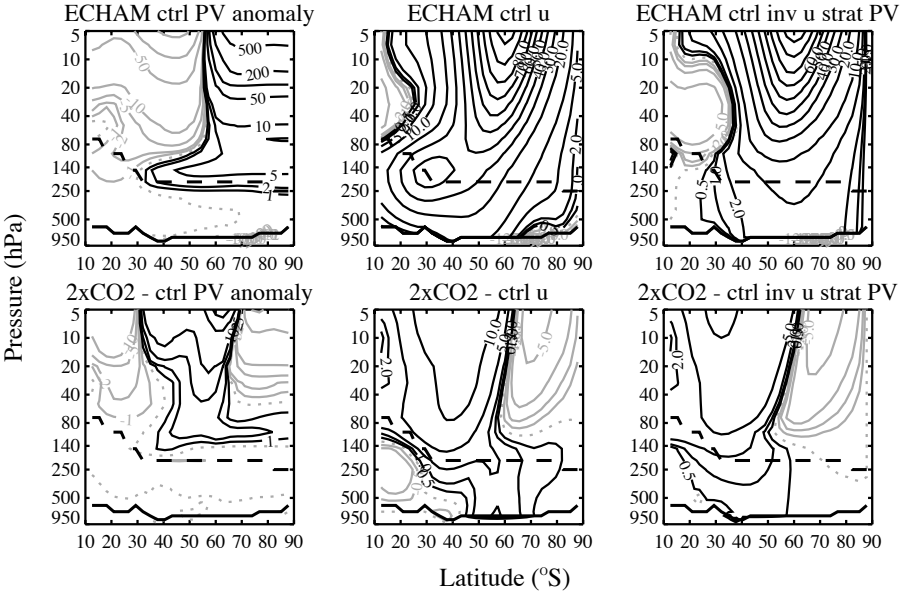

Figure 6.8: *Same as Fig. 6.6 but for August in the SH (minus the PV anomaly values are shown).*

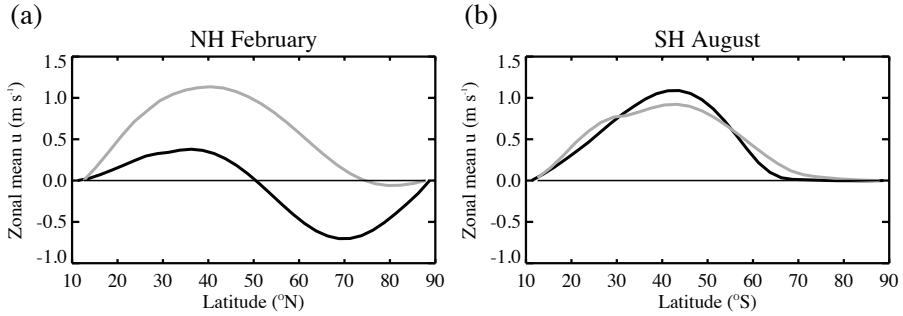

Figure 6.9: *Zonal mean zonal wind response to CO_2 doubling (doubled CO_2 run minus the control run), obtained from inverting the stratospheric PV between 400 K and 1250 K (in m s^{-1}) for the UM model (black lines) and the ECHAM model (grey lines) at 400 hPa as a function of latitude, for (a) February in the NH and (b) August in the SH.*

model, respectively. Similar to Fig. 6.5, results are presented for the control run and the difference between the doubled CO_2 run and the control run. In the SH, both models show an increase in the stratospheric PV anomaly around 55°, while the low latitude and polar PV anomaly values decrease. In both models the stratospheric PV differences have a westerly influence on the midlatitude tropospheric winds (lower right panels in Figs. 6.7 and 6.8). The influence of the stratosphere on the troposphere is of the same order as in the NH in the ECHAM model, but a larger increase of the middle stratospheric jet is found in the SH. Similar to the NH, an equatorward shift of the polar jet is also seen in the SH response.

It should be noted that the PV anomalies shown in Figs. 6.5 to 6.8 are the isentropic PV values interpolated to pressure coordinates. In general the same features are observed in both coordinate systems, but an exception is the polar stratospheric PV anomaly in the SH, which shows a decrease due to CO_2 doubling at pressure levels in August (Fig. 6.7 and 6.8), while an increase was observed at isentropic levels (Fig. 6.2a and b). This is related to a decrease in pressure at isentropic levels over the south pole due to CO_2 doubling, while CO_2 doubling hardly affects the pressure over the north pole (in February at 600 K). The stratospheric polar PV response in the NH is therefore similar at pressure levels and at isentropic levels.

In the previous section, the interpretation of the PV response to CO_2 doubling was given at isentropic levels, since we consider the isentropic PV. It should however be kept in mind that the interpretation of a response to climate change depends on the coordinate system that is used.

The tropospheric response related to changes in the stratospheric PV is summarized in Fig. 6.9, which shows the wind response in the middle troposphere, at 400 hPa, for February in the NH (Fig. 6.9a) and for August in the SH (Fig. 6.9b). In the UM

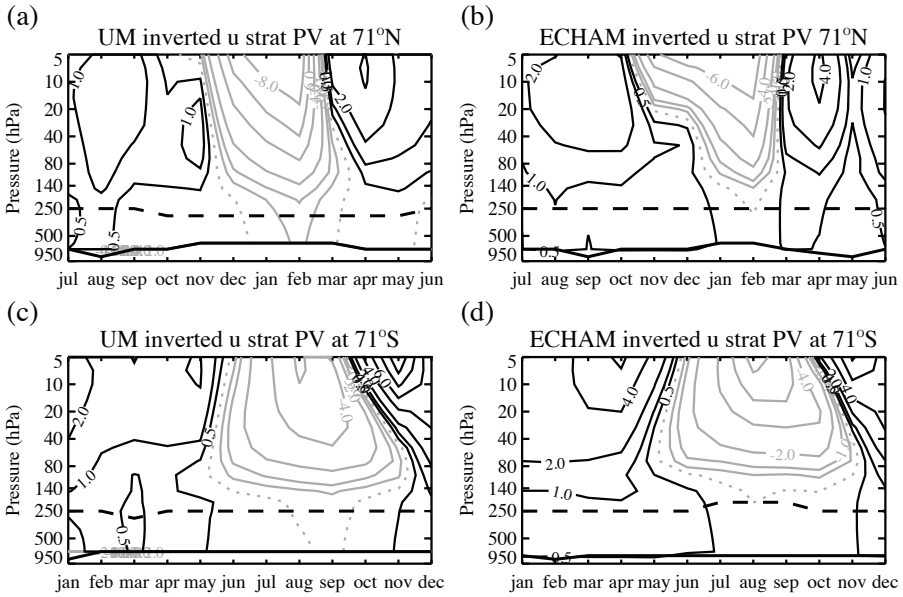

Figure 6.10: *Monthly zonal mean zonal wind response to CO_2 doubling, obtained from inverting the stratospheric PV between 400 K and 1250 K (in m s^{-1}), (a) at 71°N for the UM model, (b) at 71°N for the ECHAM model, (c) at 71°S for the UM model, and (d) at 71°S for the ECHAM model, as a function of time and pressure. Contours every 2 m s^{-1} with the ± 0.5 and 1 m s^{-1} contours added, with negative values represented by grey lines and zero contours by grey dotted lines.*

model, there is an easterly response on the tropospheric winds north of 50°N, while the response is westerly at low northern latitudes. The ECHAM model gives a westerly response south of 70°N and hardly any response in the high northern latitudes. In the SH, both models give a similar westerly response equatorward of about 65°S, maximizing at 1 m s^{-1} around 40°S.

The previous results were for the late winter season. Figure 6.10 indicates how the wind response, obtained from inverting the stratospheric PV, changes throughout the year, as a function of pressure, at 71°.

In the UM model, the NH tropospheric wind response to the stratospheric PV changes is small throughout the year, with a slightly decreased westerly influence in late winter and a slightly increased westerly influence in summer. For the NH response in the ECHAM model, CO_2 doubling increases the westerly influence of the stratosphere on the high latitude tropospheric winds from summer to early winter and in early spring, while a decreased westerly influence is found in late winter.

A slight decrease in the westerly influence is found in the winter season in the SH as well. The SH response to CO_2 doubling is an increased westerly influence of the stratosphere on the midlatitude tropospheric winds of the order of 0.5 to 1 m s^{-1}

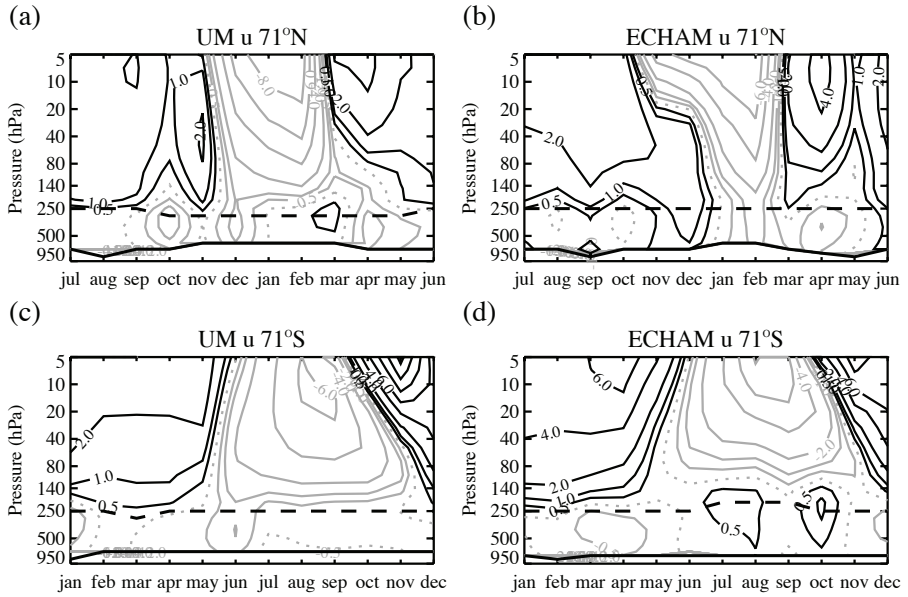

Figure 6.11: *Same as Fig. 6.10 but for the model wind response.*

throughout the year (not shown), but at the high latitudes this increased westerly influence is restricted to the summer and autumn seasons (Figs. 6.10c and d).

For comparison, Fig. 6.11 shows the total wind response in the model runs, again at 71°. The figures presented in this section show that the tropospheric wind response due to changes in the stratospheric PV is small, of the order of 0.5 to 1 m s^{-1}, but also indicate that the total wind response in the model is of the same order of magnitude. The stratospheric influence is therefore not negligible. The tropospheric response in the models is sometimes of opposite sign as the response to stratospheric PV changes, indicating that tropospheric processes can modify and mask the stratospheric influence.

6.5 Conclusions

We examined the influence of a CO_2 doubling on the zonal mean stratospheric PV distribution for the UM model (based on the Hadley Centre Atmosphere Model coupled to a thermodynamic slab ocean model) and the middle-atmosphere version of the ECHAM4 climate model. Subsequently, we investigated the tropospheric wind response to changes in the stratospheric PV, by inverting the stratospheric PV.

An increase in greenhouse gases enhances the stratospheric emission of longwave

radiation and the cooling to space. Based on these radiative arguments, an increase in the stratospheric PV is expected. This is indeed found in the SH winter, but not in the NH, indicating that other processes are of importance as well. Inspection of the 100 hPa eddy heat flux, used as a measure of the wave forcing from the troposphere to the stratosphere, shows an increased winter flux in the NH due to CO_2 doubling. The PV response is thus strongly coupled to the change in the heat flux, where an increased heat flux is associated with a reduced polar cap PV anomaly and an enhanced midlatitude PV anomaly. In autumn and spring the change in heat flux is small and the NH polar PV slightly increases, likely related to the cooling effect of the increased CO_2 concentrations. In the SH, a CO_2 doubling hardly affects the 100 hPa heat flux, and the radiative effect dominates, leading to an increase in the polar PV at isentropic levels.

The influence of the stratospheric PV on the tropospheric wind depends on the PV in the lower stratosphere. Due to CO_2 doubling, the SH lower stratospheric PV increases in late winter. An increased westerly influence of the stratosphere on the tropospheric midlatitude winds is therefore found in August, in both models. The largest PV increases are found in midlatitudes, at the edge of the SH vortex. The horizontal gradient in PV thus increases in the midlatitudes, leading to increased westerlies, but the horizontal PV gradient decreases at high latitudes, leading to somewhat decreased westerlies there, mainly in the stratosphere. In the NH, CO_2 doubling is associated with a decrease in the stratospheric PV in late winter, resulting in a reduced westerly influence of the stratospheric PV on the high latitude tropospheric winds. In the ECHAM model, the decrease in stratospheric PV is, however, restricted to higher altitudes than in the UM model, and an increased westerly influence is found in the low to midlatitudes, related to the increase in midlatitude PV in the lower stratosphere.

The tropospheric response in zonal wind due to stratospheric PV changes is of the order of 0.5 to 1 m s^{-1}. The tropospheric wind response obtained from the stratospheric inversions differs in structure from the total tropospheric wind response, but is of similar magnitude, indicating that changes in the stratosphere can certainly modify the tropospheric wind response to CO_2 doubling in the models studied here.

The present study shows that although radiative effects of greenhouse gases are important in determining the stratospheric PV distribution, it can not simply be assumed that the stratospheric PV increases with increasing greenhouse gas concentrations, since the wave forcing of the stratosphere might also change due to increases in CO_2. The results presented here indicate that, in the NH, the wave effect might dominate over the radiative effect, leading to a decrease in the polar stratospheric PV anomaly. The influence of the stratosphere on the tropospheric response to climate change depends very sensitive on the radiatively and dynamically induced PV changes in the lower stratosphere. This is consistent with the studies of *Sigmond et al.* (2008) and *Sigmond and Scinocca* (2010), who found that the state of the lower stratosphere in-

fluences the tropospheric response to climate change, and that a low model top, in the middle stratosphere, is sufficient to capture the stratospheric influence.

Acknowledgements

The ECMWF ERA-Interim data used in this study have been provided by ECMWF. The ECHAM model data were made available by Alwin Haklander at KNMI, and Michael Sigmond at the University of Toronto.

7

General conclusions and outlook

The stratospheric potential vorticity field in the current climate, its variations around the occurrence of a sudden stratospheric warming, and its possible changes in the future have been examined in this thesis. Subsequently, the impact of changes in the stratosphere on tropospheric climate has been studied. The results indicate that the influence of large-scale variations in the stratosphere is seen in the tropospheric zonal winds. For the monthly mean climatology, the influence of the stratosphere on the tropospheric winds is only small, but for individual winters the influence can be substantial, on monthly as well as daily timescales. The stratospheric changes that accompanied the major sudden stratospheric warming in January 2009, for example, resulted in an easterly wind forcing of about 5 m s^{-1} on the tropospheric winds. Furthermore, the influence of the stratosphere on the tropospheric winds was felt until months after the sudden warming event, indicating that inclusion of stratospheric processes in models might improve extended range weather forecasts. The stratospheric changes that result from CO_2 doubling in a climate model were also found to have an influence on the tropospheric winds. Although the magnitude of the tropospheric response related to stratospheric changes is small, it is of the same order of magnitude as the total tropospheric response, indicating that changes in the stratosphere can certainly modify the tropospheric response to climate change.

7.1 General conclusions

The current and future stratosphere-troposphere coupling have been studied on the basis of five research questions that were posed in section 1.3 in the introduction chapter. In this section, the research described in chapters 2 to 6 is used to (partially) answer these questions. Remarks that follow from combining the results of different chapters are presented in the next section, while some remaining questions are outlined in section 7.3.

How does the stratosphere affect the tropospheric winds under different conditions of the Arctic Oscillation?

There is a clear connection between the average Arctic Oscillation (AO) index in January and the January average zonal mean potential vorticity (PV) distribution in the Northern Hemisphere stratosphere. The polar stratospheric PV attains much higher values during January months with a positive AO index than during January months with a negative AO index.

Using nonlinear PV inversion, the large-scale zonal mean adjustment to amplitude variations in the monthly average zonal mean PV that are associated with the Arctic Oscillation was determined. In general, the January mean stratospheric PV has a westerly influence on the zonal mean mid- to high latitude tropospheric winds. However, during January months with a negative AO index, this westerly influence is reduced, while it is enhanced when the AO index is positive. Although the influence on the wind of the stratospheric PV is largest in the stratosphere, it can also explain a part ($\sim 20\%$) of the difference in mid- to high latitude tropospheric winds between January months with a positive AO index and January months with a negative AO index.

What are the seasonal cycle and interhemispheric differences in the climatological stratospheric potential vorticity distribution?

The seasonal cycle of the stratospheric polar cap PV anomaly (the PV anomaly is defined as that part of the PV that induces a wind field according to the PV inversion equation) is strongly related to radiative effects. A positive polar PV anomaly forms in autumn and winter due to radiative cooling in the polar night, and vanishes in spring due to absorption of solar radiation by ozone. The polar PV anomaly is negative in summer.

A semi-annual cycle is found in the midlatitude PV anomaly in the mid- to high stratosphere, with maxima in autumn and spring. Radiative effects cause the formation of the polar vortex and the maximum PV anomaly values in autumn. Wave breaking at the edge of the vortex causes the vortex boundary to retreat to higher latitudes, and

results in a midlatitude PV minimum in winter. Transport and mixing during the break up of the polar vortex cause the PV anomaly maximum in spring.

The formation of the vortex in autumn is similar for the Northern Hemisphere (NH) and the Southern Hemisphere (SH), but waves affect the NH stratosphere throughout winter, weakening the vortex compared to the less disturbed SH vortex. Since distortion of the polar vortex by waves presents a source of midlatitude PV in the NH, the winter minimum in the midlatitude PV anomaly is more clear in the SH. Wave breaking events thus cause the polar cap PV anomaly to be lower in the NH than in the SH, while they cause the midlatitude PV anomaly to be higher in the NH than in the SH. The stronger and colder SH vortex allows for (more) ozone depletion in spring. Lower ozone concentrations in the polar area for the SH compared to the NH result in a delayed break up of the SH vortex, especially in the lower stratosphere.

In summer, the easterly stratospheric flow prohibits wave propagation from the troposphere to the stratosphere in both the NH and SH, leading to small interhemispheric differences during this season.

What determines the interannual variability of the winter stratosphere?

The stratospheric polar cap PV anomaly is strongly related to the preceding 100 hPa heat flux. It was found that, on average, about 50% of the interannual variability in the state of the stratosphere that is observed in the Northern Hemisphere can be explained by the interannual variations in the 100 hPa heat flux. For severe events, like the major sudden stratospheric warming (SSW) in the winter of 2008/2009, the fraction of the variability explained by the 100 hPa heat flux can be even larger ($\sim 80\%$).

The variability in the 100 hPa heat flux is related to wave forcing from the troposphere to the stratosphere, but can also be affected by the state of the lower stratosphere, which determines the amount of wave forcing that can propagate into the stratosphere.

What was the influence of the 2009 major sudden stratospheric warming on the tropospheric winds?

The January 2009 major SSW had a strong influence on the stratospheric PV anomaly over the pole, with positive values before the SSW, and negative values after the SSW, especially in the lower to middle stratosphere. Accordingly, the influence of the stratosphere on the tropospheric winds, derived from PV inversion, was westerly before the SSW, while it was easterly afterwards. The change in stratospheric influence resulted in changes up to 5 m s^{-1} in the mid- to high latitude tropospheric winds within a few weeks. These changes were found to be a substantial contribution to the observed wind difference, indicating that the stratosphere influenced the tropospheric conditions, leading to a weakening of the westerlies or even a switch to easterlies after the

occurrence of the January 2009 SSW.

Comparison of 2008/2009 to an undisturbed winter (1996/1997) indicated that the effect of the SSW in the troposphere and lower stratosphere is felt for months after the occurrence of the SSW. In March 2009, an easterly influence of about 2 m s^{-1} was found, while a westerly influence of the same order of magnitude was found in absence of an SSW in March 1997.

To what extent does the stratosphere influence the tropospheric zonal wind response to CO_2 doubling?

Due to CO_2 doubling, the SH lower stratospheric PV increases in late winter, related to enhanced stratospheric emission of longwave radiation and the cooling to space. The largest PV increases are found in midlatitudes, at the edge of the vortex. An increased westerly influence of the stratosphere on the tropospheric midlatitude winds is therefore found in August, in both climate models that are considered.

In the NH, CO_2 doubling is associated with a decrease in the stratospheric polar PV in late winter, related to an increase in wave forcing of the stratosphere. This PV decrease results in a reduced westerly influence of the stratospheric PV on the high latitude tropospheric winds. In one model, the decrease in stratospheric PV is, however, restricted to higher altitudes than in the other model, and an increased westerly influence is found in the low to midlatitude troposphere, related to the increase in midlatitude PV in the lower stratosphere. This indicates that the influence of the stratosphere on the tropospheric response to climate change is very sensitive to the radiatively and dynamically induced PV changes in the lower stratosphere.

The tropospheric response in zonal wind due to stratospheric PV changes is of the order of 0.5 to 1 m s^{-1}. The tropospheric wind response obtained from the stratospheric inversions differs in structure from the total tropospheric wind response, but is of similar magnitude. This indicates that changes in the stratosphere can certainly modify the tropospheric wind response to CO_2 doubling and that it is therefore important to correctly capture the stratospheric changes in climate models.

7.2 Connection between the chapters

Each research question discussed in the previous section was mainly the subject of a separate chapter. However, some additional remarks can be made from combining the results from different chapters.

The results of chapter 5 can be connected to those of chapter 2. Chapter 5 showed that the stratospheric changes that accompany an SSW exert an easterly influence on the tropospheric winds, which is visible on monthly timescales. Winters with a negative AO index often correspond to winters with SSWs (*Hartmann et al.*, 2000).

On the basis of these considerations, an easterly tropospheric wind difference related to stratospheric changes between winters with a negative AO index and winters with a positive AO index is expected. Chapter 2 indeed shows that the westerly influence of the stratosphere on the tropospheric winds is weaker for a negative AO index than for a positive AO index.

The figures representing the wind response to CO_2 doubling (lower middle panels in Figs. 6.5 to 6.8) differ from the figure showing the wind difference between January months with a positive AO index and months with a negative AO index (Fig. 2.9a). Comparison of the results in chapters 2 and 6 therefore does not directly indicate that an increase in greenhouse gas concentrations results in a trend in the AO index. Based on these results it is uncertain whether Western Europe will experience more mild winters in the future (as indicated in the ECHAM model by the increase in westerly winds around 50°N in February), or that winters might get colder (as indicated in the UM model by the slight decrease in westerly winds around 50°N in February). However, in both cases the changes in the lower stratosphere seem to be of importance in determining the tropospheric response.

Chapters 3, 4 and 6 all indicate that the state of the stratosphere is strongly influenced by wave forcing from below. The wave forcing can be used to explain large parts of the interannual, intra-annual and interhemispheric differences in stratospheric PV. The interhemispheric differences in the current climate showed that a weaker wave forcing in the SH is related to higher stratospheric PV anomaly values in winter in the SH than in the NH (chapter 3). Chapter 6 further showed that interhemispheric differences in the response to CO_2 doubling can, at least partly, be explained by the change in wave forcing, with an enhanced 100 hPa heat flux in the NH, while the SH 100 hPa heat flux is hardly affected by CO_2 doubling. Chapter 4 provided evidence that the interannual variability in the polar stratospheric PV is strongly related to the wave forcing from below, and also that the large-scale stratospheric PV differences within a single winter can be explained from the variability in the 100 hPa heat flux (at least for the winter of 2008/2009).

Chapters 4 and 5 both discuss an aspect of the major SSW in January 2009. Chapter 4 focusses on the forcing of the SSW from below, showing that the changes in the polar PV that accompany the SSW are strongly related to the preceding 100 hPa heat flux. Chapter 5, on the other hand, focusses on the coupling of the stratosphere back to the troposphere, by examining the influence of changes in the stratosphere on the tropospheric winds, once these stratospheric changes are present. Together, these chapters provide a view of the stratosphere-troposphere coupling in the winter of 2008/2009.

The studies of *Charlton-Perez et al.* (2008) and *Bell et al.* (2010) indicate that the number of SSWs might increase due to climate change. Combining this with the results of chapter 5, an increased easterly influence of the stratosphere on the high

latitude tropospheric winds might thus be expected due to an increase in greenhouse gas concentrations, which is indeed consistent with the results of chapter 6. As *Bell et al.* (2010) already notes, this indicates that the climate response to CO_2 increases is likely partly associated with a change of the mean state of the atmosphere, and partly associated with a change in the variability (measured by the number of SSWs).

Chapter 3 illustrated that higher winter PV anomaly values are found in the cold, strong SH polar vortex than in the warmer and weaker NH polar vortex. Based on these results, a strengthening of the polar vortex and an increase in the PV anomaly values might be expected as a response to an increased emission of longwave radiation to space and cooling of the stratosphere due to an increase in greenhouse gas concentrations. Chapter 6, however, shows that the actual response to CO_2 doubling in a climate model is more subtle, and that, beside radiative effects, dynamical effects also play a role, especially in the NH.

7.3 Remaining questions

Although the research presented in this thesis sheds some light on the role of the stratosphere in climate and the coupling between the stratosphere and the troposphere, many questions still remain, some of which are outlined here.

- The seasonal cycle of the stratospheric PV anomaly can be clearly related to radiative and wave effects, but the processes that determine the PV anomaly in the upper troposphere/lower stratosphere (UTLS) are less clear. The strong coupling between the UTLS PV anomaly and the surface in the PV inversion indicates that the UTLS PV anomaly is likely related to tropospheric processes. This also indicates that separation of the tropospheric and stratospheric PV exactly at the tropopause might not be the correct way to examine the influence of the stratospheric PV on the troposphere, since the UTLS PV anomaly lies mainly in the stratosphere, but it is strongly coupled to the troposphere. The present research indicates that the UTLS PV anomaly is likely related to the amount of tropical convection/precipitation and the accompanying strength of the Hadley circulation. Differences in PV between years with high and low tropical precipitation are, however, small in the ECMWF ERA-Interim dataset. A possible way to examine the relation between the UTLS PV anomaly and the tropical convection/precipitation in more detail, is by performing model experiments with a simple climate model in which the tropical convection can be imposed as an external forcing, and varied in strength.

- The relation between the polar PV and the 100 hPa heat flux derived in chapter 4 is for the Northern Hemisphere, it would also be interesting to study if a similar PV-flux relation is valid in the Southern Hemisphere. The variability in the

100 hPa heat flux is smaller in the SH than in the NH, since there is less wave generation in the SH troposphere, but in September 2002 an SSW did occur in the SH. An interesting test case would be to examine if the variability in the polar PV for this spring could be predicted from the 100 hPa flux, like for the 2009 SSW in the NH.

- The PV-flux relation showed a large scatter of the data around the linear fit that was used. This indicates that, although the mean PV-flux relation gives a good predication of the polar PV for the winter of 2008/2009 from the 100 hPa flux, this might not be the case for other years. It would therefore be interesting to apply this PV-flux relation to other years as well. Furthermore, it is interesting to study the form of the relation between the 100 hPa flux and the polar PV for separate years, to examine, for example, if the slope of the fit depends on the state (wind or wind shear) of the lower stratosphere. Since the state of the lower stratosphere determines the wave propagation in this region, it is possible that the 100 hPa flux affects the polar PV more under certain stratospheric circumstances. A possible way to test this, would be to group years according to their lower stratospheric wind or wind shear, and compare the relation between the polar PV and 100 hPa flux for the two groups.

- Another aspect that deserves more attention in future research is the cause of SSWs. Chapter 4 shows that the occurrence of the 2009 major SSW is strongly related to the preceding 100 hPa heat flux, but the origin of the variability in the 100 hPa flux is not studied. Part of this variability will be of tropospheric origin, related to the generation of waves. The occurrence of El Niño events, with tropical sea surface temperature anomalies in the Pacific, can, for example, affect the generation and propagation of waves (*Manzini et al.*, 2006). The relation between tropospheric wave generation and the 100 hPa flux might, for example, be examined in a conceptual model study, in which the land-sea temperature contrast is enhanced, to enhance the wave generation.

  The 100 hPa flux can also be affected by the state of the lower stratosphere (*Scott and Polvani*, 2004). This could be examined by comparing the heat flux at 100 hPa between years with high and years with low wind (shear) in the lower stratosphere. The difficulty with examining tropospheric and stratospheric influences on the 100 hPa flux is, however, that there is a two-way coupling between the heat flux and wind field. A possible way to try to uncouple these effects is by examining time-series. By comparing years with and without SSWs it might then be possible to study whether the lower stratospheric wind (shear) shows exceptional values before the occurrence of SSWs, allowing the 100 hPa flux to increase in magnitude at these times.

Beside wave forcing at 100 hPa, the occurrence of an SSW also depends on the wave propagation within the stratosphere. In the PV-flux relation this is not explicitly taken into account, but the relation between the 100 hPa heat flux and the polar PV indicates that a certain part of the wave activity affects the polar cap. The fraction of the waves that propagate poleward in the stratosphere can, however, vary from year to year. This can be affected by the state of the stratosphere, which is for example influenced by the phase of the Quasi Biennial Oscillation (QBO). The phase of the QBO is a measure of the zonal wind direction in the equatorial stratosphere, which affects the region of wave breaking. Since planetary waves can not propagate into a region of easterlies, more poleward wave propagation is found when the QBO is in its easterly phase (*Baldwin et al.*, 2001). A difference in the PV-flux relation between years with an easterly and years with a westerly QBO phase might therefore be expected. This could, for example, be studied by grouping winters according to their phase of the QBO in early winter.

- Chapter 6 illustrates the influence of CO_2 doubling on the stratospheric PV distribution. This could be elaborated on by considering transient model runs, in which the CO_2 concentration varies with time. Furthermore, the expected recovery of ozone concentrations in the coming century (due to the ban of CFCs) will also affect the stratospheric PV. This aspect has not been studied here, although the results of chapter 3 suggested that recovery of the ozone hole will decrease the SH lower stratospheric polar PV anomaly in spring, and lead to an earlier vortex break up. This could be studied in more detail in a climate model run with varying ozone concentrations.

Chapter 5 showed that the stratospheric variability associated with an SSW influences the tropospheric zonal winds, up to several weeks after the sudden warming event. As previous studies indicate that the number of SSWs might increase in the future (*Charlton-Perez et al.*, 2008; *Bell et al.*, 2010), it will be even more important to take these kind of stratospheric variations into account in weather and climate predictions. If the state of the stratosphere also plays a role in determining the occurrence of SSWs, by influencing the amount of wave propagation into the stratosphere, the role of the stratosphere in climate is even larger. This thesis contributes to the understanding of the stratosphere and its role in climate, which is of importance to improve model simulations of the stratospheric climate and future climate predictions.

Bibliography

Ambaum, M. H. P., and B. J. Hoskins, The NAO troposphere-stratosphere connection, *Journal of Climate*, *15*, 1969–1978, 2002.

Andrews, D. G., J. R. Holton, and C. B. Leovy, *Middle atmosphere dynamics*, 489 pp., Academic Press, San Diego, 1987.

Austin, J., et al., Uncertainties and assessments of chemistry-climate models of the stratosphere, *Atmospheric Chemistry and Physics*, *3*(1), 1–27, 2003.

Baldwin, M. P., and T. J. Dunkerton, Biennial, quasi-biennial, and decadal oscillations of the potential vorticity in the northern stratosphere, *Journal of Geophysical Research*, *103*(D4), 3919–3928, 1998.

Baldwin, M. P., and T. J. Dunkerton, Propagation of the Arctic Oscillation from the stratosphere to the troposphere, *Journal of Geophysical Research*, *104*(D24), 30,937–30,946, 1999.

Baldwin, M. P., and T. J. Dunkerton, Stratospheric harbingers of anomalous weather regimes, *Science*, *294*, 581–584, 2001.

Baldwin, M. P., and J. R. Holton, Climatology of the stratospheric polar vortex and planetary wave breaking, *Journal of Atmospheric Sciences*, *45*(7), 1123–1142, 1988.

Baldwin, M. P., D. B. Stephenson, D. W. J. Thompson, T. J. Dunkerton, A. J. Charlton, and A. O'Neill, Stratospheric memory and skill of extended-range weather forecasts, *Science*, *301*, 636–640, 2003.

Baldwin, M. P., M. Dameris, and T. G. Shepherd, How will the stratosphere affect climate change?, *Science*, *316*, 1576–1577, 2007.

Baldwin, M. P., et al., The Quasi-Biennial Oscillation, *Reviews of Geophysics*, *39*(2), 179–229, 2001.

Bell, C. J., The role of stratospheric variability in climate, Ph.D. thesis, University of Reading, UK, 2009.

Bell, C. J., L. J. Gray, A. J. Charlton-Perez, M. M. Joshi, and A. A. Scaife, Stratospheric communication of El Niño teleconnections to European winter, *Journal of Climate*, *22*, 4083–4096, 2009.

Bell, C. J., L. J. Gray, and J. Kettleborough, Changes in Northern Hemisphere stratospheric variability under increased CO_2 concentrations, *Quarterly Journal of the Royal Meteorological Society*, *136*, 1181–1190, 2010.

Black, R. X., Stratospheric forcing of surface climate in the Arctic Oscillation, *Journal of Climate*, *15*, 268–277, 2002.

Black, R. X., and B. A. McDaniel, Diagnostic case studies of the Northern Annular Mode, *Journal of Climate*, *17*(20), 3990–4004, 2004.

Boville, B. A., The influence of the polar night jet on the tropospheric circulation in a GCM, *Journal of the Atmospheric Sciences*, *41*(7), 1132–1142, 1984.

Brune, W. H., J. G. Anderson, D. W. Toohey, D. W. Fahey, S. R. Kawa, R. L. Jones, D. S. McKenna, and L. R. Poole, The potential for ozone depletion in the Arctic polar stratosphere, *Science*, *252*(5010), 1260–1266, 1991.

Brunet, G., R. Vautard, B. Legras, and S. Edouard, Potential vorticity on isentropic surfaces: climatology and diagnostics, *Monthly Weather Review*, *123*, 1037–1058, 1995.

Butchart, N., and A. A. Scaife, Removal of chlorofluorocarbons by increased mass exchange between the stratosphere and troposphere in a changing climate, *Nature*, *410*, 799–802, 2001.

Butchart, N., J. Austin, J. R. Knight, A. A. Scaife, and M. L. Gallani, The response of the stratospheric climate to projected changes in the concentrations of well-mixed greenhouse gases from 1992 to 2051, *Journal of Climate*, *13*, 2142–2159, 2000.

Cagnazzo, C., C. Claud, and S. Hare, Aspects of stratospheric long-term changes induced by ozone depletion, *Climate Dynamics*, *27*, 101–111, doi:10.1007/s00382-006-0120-1, 2006.

Charlton, A. J., and L. M. Polvani, A new look at Stratospheric Sudden Warmings. Part I: Climatology and modeling benchmarks, *Journal of Climate*, *20*, 449–469, 2007.

Charlton, A. J., A. O'Neill, W. A. Lahoz, and A. C. Massacand, Sensitivity of tropospheric forecasts to stratospheric initial conditions, *Quarterly Journal of the Royal Meteorological Society*, *130*, 1771–1792, 2004.

Charlton, A. J., A. O'Neill, P. Berrisford, and W. A. Lahoz, Can the dynamical impact of the stratosphere on the troposphere be described by large-scale adjustment to the stratospheric PV distribution?, *Quarterly Journal of the Royal Meteorological Society*, *131*, 525–543, 2005a.

Charlton, A. J., A. O'Neill, W. A. Lahoz, and P. Berrisford, The splitting of the stratospheric polar vortex in the southern hemisphere, September 2002: Dynamical evolution, *Journal of Atmospheric Sciences*, *62*, 590–602, 2005b.

Charlton, A. J., L. M. Polvani, J. Perlwitz, F. Sassi, E. Manzini, K. Shibata, S. Pawson, J. E. Nielsen, and D. Rind, A new look at stratospheric sudden warmings. Part II: Evaluation of numerical model simulations, *Journal of Climate*, *20*, 470–488, 2007.

Charlton-Perez, A. J., L. M. Polvani, J. Austin, and F. Li, The frequency and dynamics of stratospheric sudden warmings in the 21st century, *Journal of Geophysical Research*, *113*(D16116), doi:10.1029/2007JD009571, 2008.

Charney, J. G., and P. G. Drazin, Propagation of planetary-scale disturbances from the lower into the upper atmosphere, *Journal of Geophysical Research*, *66*(1), 83–109, 1961.

Christiansen, B., Downward propagation of zonal mean zonal wind anomalies from the stratosphere to the troposphere: Model and reanalysis, *Journal of Geophysical Research*, *106*(D21), 27,307–27,322, 2001.

Coy, L., E. R. Nash, and P. A. Newman, Meteorology of the polar vortex: Spring 1997, *Geophysical Research Letters*, *24*(22), 2693–2696, 1997.

Davis, C. A., Piecewise potential vorticity inversion, *Journal of Atmospheric Sciences*, *49*, 1397–1411, 1992.

Dickinson, R. E., Method of parameterization for infrared cooling between altitudes of 30 and 70 kilometers, *Journal of Geophysical Research*, *78*, 4451–4457, doi:10.1029/JC078i021p04451, 1973.

Edouard, S., R. Vautard, and G. Brunet, On the maintenance of potential vorticity in isentropic coordinates, *Quarterly Journal of the Royal Meteorological Society*, *123*, 2069–2094, 1997.

Eichelberger, S. J., and D. L. Hartmann, Changes in the strength of the Brewer-Dobson circulation in a simple AGCM, *Geophysical Research Letters*, *32*(L15807), doi:10.1029/2005GL022924, 2005.

Fels, S. B., J. D. Mahlman, M. D. Schwarzkopf, and R. W. Sinclair, Stratospheric sensitivity to perturbations in ozone and carbon dioxide: Radiative and dynamical response, *Journal of the Atmospheric Sciences*, *37*, 2265–2297, 1980.

Fueglistaler, S., B. Legras, A. Beljaars, J. J. Morcrette, A. Simmons, A. M. Tompkins, and S. Uppala, The diabatic heat budget of the upper troposphere and lower/mid stratosphere in ECMWF reanalyses, *Quarterly Journal of the Royal Meteorological Society*, *135*, 21–37, 2009.

Fyfe, J. C., G. J. Boer, and G. M. Flato, The Arctic and Antarctic Oscillations and their projected changes under global warming, *Geophysical Research Letters*, *26*(11), 1601–1604, 1999.

Gerber, E. P., and L. M. Polvani, Stratosphere-troposphere coupling in a relatively simple AGCM: The importance of stratospheric variability, *Journal of Climate*, *22*, 1920–1933, 2009.

Gerber, E. P., C. Orbe, and L. M. Polvani, Stratospheric influence on the tropospheric circulation revealed by idealized ensemble forecasts, *Geophysical Research Letters*, *36*(L24801), doi:10.1029/2009GL040913, 2009.

Gille, J. C., and L. V. Lyjak, Radiative heating and cooling rates in the middle atmosphere, *Journal of the Atmospheric Sciences*, *43*(20), 2215–2229, 1986.

Gillett, N. P., M. R. Allen, R. E. McDonald, C. A. Senior, D. T. Shindell, and G. A. Schmidt, How linear is the Arctic Oscillation response to greenhouse gases?, *Journal of Geophysical Research*, *107*(D3), doi:10.1029/2001JD000589, 2002.

Gillett, N. P., M. R. Allen, and K. D. Williams, Modelling the atmospheric response to doubled CO_2 and depleted stratospheric ozone using a stratosphere-resolving coupled GCM, *Quarterly Journal of the Royal Meteorological Society*, *129*, 947–966, doi:10.1256/qj.02.102, 2003.

Graf, H.-F., I. Kirchner, and J. Perlwitz, Changing lower stratospheric circulation: The role of ozone and greenhouse gases, *Journal of Geophysical Research*, *103*(D10), 11,251–11,261, 1998.

Greatbatch, R. J., The North Atlantic Oscillation, *Stochastic Environmental Research and Risk Assessment*, *14*, 213–242, 2000.

Haklander, A. J., P. C. Siegmund, and H. M. Kelder, Interannual variability of the stratospheric wave driving during northern winter, *Atmospheric Chemistry and Physics*, *7*, 2575–2584, 2007.

Haklander, A. J., P. C. Siegmund, M. Sigmond, and H. M. Kelder, How does the northern-winter wave driving of the Brewer-Dobson circulation increase in an enhanced-CO_2 climate simulation?, *Geophysical Research Letters*, *35*(L07702), doi:10.1029/2007GL033054, 2008.

Harnik, N., The evolution of a stratospheric wave packet, *Journal of the Atmospheric Sciences*, *59*, 202–217, 2002.

Hartley, D. E., J. T. Villarin, R. X. Black, and C. A. Davis, A new perspective on the dynamical link between the stratosphere and troposphere, *Nature*, *391*, 471–474, 1998.

Hartmann, D. L., The structure of the stratosphere in the southern hemisphere during late winter 1973 as observed by satellite, *Journal of Atmospheric Sciences*, *33*, 1141–1154, 1976.

Hartmann, D. L., J. M. Wallace, V. Limpasuvan, D. W. J. Thompson, and J. R. Holton, Can ozone depletion and global warming interact to produce rapid climate change?, *Proceedings of the National Academy of Sciences*, *97*(4), 1412–1417, 2000.

Harvey, V. L., and M. H. Hitchman, A climatology of the Aleutian high, *Journal of Atmospheric Sciences*, *53*(14), 2088–2101, 1996.

Harvey, V. L., R. B. Pierce, T. D. Fairlie, and M. H. Hitchman, A climatology of stratospheric polar vortices and anticyclones, *Journal of Geophysical Research*, *107*(D20, 4442), doi:10.1029/2001JD001471, 2002.

Haynes, P., Stratospheric dynamics, *Annual Review of Fluid Mechanics*, *37*, 263–293, doi:10.1146/annurev.fluid.37.061903.175710, 2005.

Holton, J. R., The dynamics of sudden stratospheric warmings, *Annual Review of Earth and Planetary Sciences*, *8*, 169–190, 1980.

Holton, J. R., and C. Mass, Stratospheric vacillation cycles, *Journal of Atmospheric Sciences*, *33*, 2218–2225, doi:10.1175/1520-0469(1976)033, 1976.

Hoskins, B. J., and P. J. Valdes, On the existence of storm-tracks, *Journal of Atmospheric Sciences*, *47*(15), 1854–1864, 1990.

Hoskins, B. J., M. E. McIntyre, and A. W. Robertson, On the use and significance of isentropic potential vorticity maps, *Quarterly Journal of the Royal Meteorological Society*, *111*, 877–946, 1985.

Hurrell, J. W., Decadal trends in the North Atlantic Oscillation: Regional temperatures and precipitation, *Science*, *269*(5224), 676–679, 1995.

Hurrell, J. W., Y. Kushnir, and M. Visbeck, The North Atlantic Oscillation, *Science*, *291*(5504), 603–605, 2001.

James, I. N., *Introduction to circulating atmospheres*, 444 pp., Cambridge University Press, Cambridge, UK, 1995.

Kiehl, J. T., and S. Solomon, On the radiative balance of the stratosphere, *Journal of the Atmospheric Sciences*, *43*(14), 1525–1534, 1986.

Kinnersley, J. S., Interannual variability of stratospheric zonal wind forced by the northern lower-stratospheric large-scale waves, *Journal of Atmospheric Sciences*, *55*, 2270–2283, 1998.

Kleinschmidt, E., Über aufbau und entstehung von zyklonen, *Meteorologische Rundschau*, *3*(1/2), 1–6, 1950.

Kodera, K., K. Yamazaki, M. Chiba, and K. Shibata, Downward propagation of upper stratospheric mean zonal wind perturbation to the troposphere, *Geophysical Research Letters*, *17*(9), 1263–1266, 1990.

Kodera, K., H. Koide, and H. Yoshimura, Northern Hemisphere winter circulation associated with the North Atlantic Oscillation and stratospheric polar-night jet, *Geophysical Research Letters*, *26*(4), 443–446, 1999.

Kushner, P. J., and L. M. Polvani, Stratosphere-troposphere coupling in a relatively simple AGCM: The role of eddies, *Journal of Climate*, *17*, 629–639, 2004.

Labitzke, K., The amplification of height wave 1 in January 1979: A characteristic precondition for the major warming in February, *Monthly Weather Review*, *109*, 983–989, 1981.

Labitzke, K., and M. Kunze, On the remarkable Arctic winter in 2008/2009, *Journal of Geophysical Research*, *114*(D00102), doi:10.1029/2009JD012273, 2009.

Lahoz, W. A., et al., Vortex dynamics and the evolution of water vapour in the stratosphere of the southern hemisphere, *Quarterly Journal of the Royal Meteorological Society*, *122*, 423–450, 1996.

Lait, L. R., An alternative form for potential vorticity, *Journal of Atmospheric Sciences*, *51*(12), 1754–1759, 1994.

Langematz, U., and M. Kunze, An update on dynamical changes in the Arctic and Antarctic stratospheric polar vortices, *Climate Dynamics*, *27*, 647–660, 2006.

Langematz, U., M. Kunze, K. Krüger, and K. Labitzke, Thermal and dynamical changes of the stratosphere since 1979 and their link to ozone and CO_2 changes, *Journal of Geophysical Research*, *108*(D1, 4027), doi:10.1029/2002JD002069, 2003.

Li, F., J. Austin, and J. Wilson, The strength of the Brewer-Dobson circulation in a changing climate: coupled chemistry-climate model simulations, *Journal of Climate*, *21*, 40–57, doi:10.1175/2007JCLI1663.1, 2008.

Limpasuvan, V., D. W. J. Thompson, and D. L. Hartmann, The life cycle of the northern hemisphere sudden stratospheric warmings, *Journal of Climate*, *17*, 2584–2596, 2004.

Lin, P., Q. Fu, S. Solomon, and J. M. Wallace, Temperature trend patterns in southern hemisphere high latitudes: Novel indications of stratospheric change, *Journal of Climate*, *22*, 6325–6341, doi:10.1175/2009JCLI2971.1, 2009.

Luterbacher, J., et al., Extending North Atlantic Oscillation reconstructions back to 1500, *Atmospheric Science Letters*, doi:10.1006/asle.2001.0044, 2002.

Manney, G. L., K. Krüger, J. L. Sabutis, S. A. Sena, and S. Pawson, The remarkable 2003-2004 winter and other recent warm winters in the Arctic stratosphere since the late 1990s, *Journal of Geophysical Research*, *110*(D04107), doi:10.1029/2004JD005367, 2005.

Manney, G. L., M. J. Schwartz, K. Krüger, M. L. Santee, S. Pawson, J. N. Lee, W. H. Daffer, R. A. Fuller, and N. J. Livesey, Aura Microwave Limb Sounder observations of dynamics and transport during the record-breaking 2009 Arctic stratospheric major warming, *Geophysical Research Letters*, *36*(L12815), doi:10.1029/2009GL038586, 2009.

Manzini, E., B. Steil, C. Brühl, M. A. Giorgetta, and K. Krüger, A new interactive chemistry-climate model: 2. Sensitivity of the middle atmosphere to ozone depletion and increase in greenhouse gases and implications for recent stratospheric cooling, *Journal of Geophysical Research*, *108*(D14, 4429), doi:10.1029/2002JD002977, 2003.

Manzini, E., M. A. Giorgetta, M. Esch, L. Kornblueh, and E. Roeckner, The influence of sea surface temperatures on the northern winter stratosphere: Ensemble simulations with the MAECHAM5 model, *Journal of Climate*, *19*, 3863–3881, 2006.

Matsuno, T., A dynamical model of the stratospheric sudden warming, *Journal of the Atmospheric Sciences*, *28*, 1479–1494, 1971.

Matthewman, N. J., J. G. Esler, A. J. Charlton-Perez, and L. M. Polvani, A new look at Stratospheric Sudden Warmings. Part III: Polar vortex evolution and vertical structure, *Journal of Climate*, *22*, 1566–1585, 2009.

Maycock, A. C., S. P. E. Keeley, A. J. Charlton-Perez, and F. J. Doblas-Reyes, Stratospheric circulation in seasonal forecasting models: Implications for seasonal prediction, *Climate Dynamics*, *In press*, doi:10.1007/s00382-009-0665-x, 2009.

McIntyre, M. E., and T. N. Palmer, Breaking planetary waves in the stratosphere, *Nature*, *305*, 593–600, 1983.

McIntyre, M. E., and T. N. Palmer, The 'surf zone' in the stratosphere, *Journal of Atmospheric and Terrestrial Physics*, *46*(9), 825–849, 1984.

Mechoso, C. R., A. O'Neill, V. D. Pope, and J. D. Farrara, A study of the stratospheric final warming of 1982 in the southern hemisphere, *Quarterly Journal of the Royal Meteorological Society*, *144*, 1365–1384, 1988.

Mlynczak, M. G., C. J. Mertens, R. R. Garcia, and R. W. Portmann, A detailed evaluation of the stratospheric heat budget 2. Global radiation balance and diabatic circulations, *Journal of Geophysical Research*, *104*(D6), 6039–6066, 1999.

Moritz, R. E., C. M. Bitz, and E. J. Steig, Dynamics of recent climate change in the Arctic, *Science*, *297*, 1497–1502, 2002.

Newman, P. A., and E. R. Nash, Quantifying the wave driving of the stratosphere, *Journal of Geophysical Research*, *105*(D10), 12,485–12,497, 2000.

Newman, P. A., E. R. Nash, and J. E. Rosenfield, What controls the temperature of the Arctic stratosphere during the spring?, *Journal of Geophysical Research*, *106*(D17), 19,999–20,010, 2001.

Norton, W. A., Sensitivity of northern hemisphere surface climate to simulation of the stratospheric polar vortex, *Geophysical Research Letters*, *30*(12), doi:10.1029/2003GL016958, 2003.

Osborn, T. J., Simulating the winter North Atlantic Oscillation: the roles of internal variability and greenhouse gas forcing, *Climate Dynamics*, *22*, 605–623, 2004.

Osborn, T. J., Recent variations in the winter North Atlantic Oscillation, *Weather*, *61*(12), 353–355, 2006.

Overland, J. E., and M. Wang, The Arctic climate paradox: The recent decrease of the Arctic Oscillation, *Geophysical Research Letters*, *32*(L06701), doi:10.1029/2004GL021752, 2005.

Perlwitz, J., and H.-F. Graf, The statistical connection between tropospheric and stratospheric circulation of the northern hemisphere in winter, *Journal of Climate*, *8*, 2281–2295, 1995.

Perlwitz, J., and H.-F. Graf, Troposphere-stratosphere dynamic coupling under strong and weak polar vortex conditions, *Geophysical Research Letters*, *28*(2), 271–274, 2001.

Perlwitz, J., and N. Harnik, Observational evidence of a stratospheric influence on the troposphere by planetary wave reflection, *Journal of Climate*, *16*, 3011–3026, 2003.

Perlwitz, J., and N. Harnik, Downward coupling between the stratosphere and troposphere: The relative roles of wave and zonal mean processes, *Journal of Climate*, *17*, 4902–4909, 2004.

Polvani, L. M., and P. J. Kushner, Tropospheric response to stratospheric perturbations in a relatively simple general circulation model, *Geophysical Research Letters*, *29*(7), doi:10.1029/2001GL014284, 2002.

Polvani, L. M., and R. Saravanan, The three-dimensional structure of breaking rossby waves in the polar wintertime stratosphere, *Journal of the Atmospheric Sciences*, *57*, 3663–3685, 2000.

Polvani, L. M., and D. W. Waugh, Upward wave activity flux as a precursor to extreme stratospheric events and subsequent anomalous surface weather regimes, *Journal of Climate*, *17*, 3548–3554, 2004.

Randel, W. J., The seasonal evolution of planetary waves in the southern hemisphere stratosphere and troposphere, *Quarterly Journal of the Royal Meteorological Society*, *114*, 1385–1409, 1988.

Randel, W. J., and F. Wu, Cooling of the Arctic and Antarctic polar stratospheres due to ozone depletion, *Journal of Climate*, *12*, 1467–1479, 1999.

Rind, D., D. Shindell, P. Lonergan, and N. K. Balachandran, Climate change and the middle atmosphere. Part III: The doubled CO_2 climate revisited, *Journal of Climate*, *11*, 876–894, 1998.

Rind, D., J. Perlwitz, and P. Lonergan, AO/NAO response to climate change: 1. Respective influences of stratospheric and tropospheric climate changes, *Journal of Geophysical Research*, *110*(D12107), doi:10.1029/2004JD005103, 2005.

Roff, G., D. W. J. Thompson, and H. Hendon, Does increasing model stratospheric resolution improve extended-range forecast skill?, *Geophysical Research Letters*, *submitted*, 2010.

Rosenfield, J. E., P. A. Newman, and M. R. Schoeberl, Computations of diabatic descent in the stratospheric polar vortex, *Journal of Geophysical Research*, *99*(D8), 16,677–16,689, 1994.

Scaife, A. A., J. R. Knight, G. K. Vallis, and C. K. Folland, A stratospheric influence on the winter NAO and North Atlantic surface climate, *Geophysical Research Letters*, *32*(L18715), doi:10.1029/2005GL023226, 2005.

Schnadt, C., M. Dameris, M. Ponater, R. Hein, V. Grewe, and B. Steil, Interaction of atmospheric chemistry and climate and its impact on stratospheric ozone, *Climate Dynamics*, *18*, 501–517, 2002.

Schoeberl, M. R., and D. L. Hartmann, The dynamics of the stratospheric polar vortex and its relation to springtime ozone depletions, *Science*, *251*(4989), 46–52, 1991.

Scott, R. K., and L. M. Polvani, Stratospheric control of upward wave flux near the tropopause, *Geophysical Research Letters*, *31*(L02115), doi:10.1029/2003GL017965, 2004.

Scott, R. K., D. G. Dritschel, L. M. Polvani, and D. W. Waugh, Enhancement of rossby wave breaking by steep potential vorticity gradients in the winter stratosphere, *Journal of the Atmospheric Sciences*, *61*, 904–918, 2004.

Semenov, V. A., M. Latif, J. H. Jungclaus, and W. Park, Is the observed NAO variability during the instrumental record unusual?, *Geophysical Research Letters*, *35*(L11701), doi:10.1029/2008GL033273, 2008.

Shaw, T. A., and T. G. Shepherd, Raising the roof, *Nature Geoscience*, *1*, 12–13, 2008.

Shaw, T. A., J. Perlwitz, and N. Harnik, Downward wave coupling between the stratosphere and troposphere: The importance of meridional wave guiding and comparison with zonal-mean coupling, *Journal of Climate*, *In press*, doi:10.1175/2010JCLI3804.1, 2010.

Shepherd, T. G., The middle atmosphere, *Journal of Atmospheric and Solar-Terrestrial Physics*, *62*, 1587–1601, 2000.

Shepherd, T. G., Issues in stratosphere-troposphere coupling, *Journal of the Meteorological Society of Japan*, *80*(4B), 769–792, 2002.

Shepherd, T. G., Dynamics, stratospheric ozone, and climate change, *Atmosphere-Ocean*, *46*(1), 117–138, doi:10.3137/ao.460106, 2008.

Shindell, D. T., R. L. Miller, G. A. Schmidt, and L. Pandolfo, Simulation of recent northern winter climate trends by greenhouse-gas forcing, *Nature*, *399*, 452–455, 1999.

Shindell, D. T., G. A. Schmidt, R. L. Miller, and D. Rind, Northern Hemisphere winter climate response to greenhouse gas, ozone, solar, and volcanic forcing, *Journal of Geophysical Research*, *106*(D7), 7193–7210, 2001.

Shine, K. P., The middle atmosphere in the absence of dynamical heat fluxes, *Quarterly Journal of the Royal Meteorological Society*, *113*, 603–633, 1987.

Sickmöller, M., R. Blender, and K. Fraedrich, Observed winter cyclone tracks in the northern hemisphere in re-analysed ECMWF data, *Quarterly Journal of the Royal Meteorological Society*, *126*, 591–620, 2000.

Siegmund, P., Stratospheric polar cap mean height and temperature as extended-range weather predictors, *Monthly Weather Review*, *133*, 2436–2448, 2005.

Sigmond, M., and J. F. Scinocca, The influence of the basic state on the northern hemisphere circulation response to climate change, *Journal of Climate*, *23*, 1434–1446, doi:10.1175/2009JCLI3167.1, 2010.

Sigmond, M., P. C. Siegmund, E. Manzini, and H. Kelder, A simulation of the separate climate effects of middle-atmospheric and tropospheric CO_2 doubling, *Journal of Climate*, *17*, 2352–2367, 2004.

Sigmond, M., J. F. Scinocca, and P. J. Kushner, Impact of the stratosphere on tropospheric climate change, *Geophysical Research Letters*, *35*(L12706), doi:10.1029/2008GL033573, 2008.

Simpson, I. R., M. Blackburn, and J. D. Haigh, The role of eddies in driving the tropospheric response to stratospheric heating perturbations, *Journal of the Atmospheric Sciences*, *66*, 1347–1365, doi:10.1175/2008JAS2758.1, 2009.

Solomon, S., Stratospheric ozone depletion: a review of concepts and history, *Reviews of Geophysics*, *37*(3), 275–316, 1999.

Song, Y., and W. A. Robinson, Dynamical mechanisms for stratospheric influences on the troposphere, *Journal of the Atmospheric Sciences*, *61*, 1711–1725, 2004.

Stolarski, R. S., A. R. Douglass, P. A. Newman, S. Pawson, and M. R. Schoeberl, Relative contribution of greenhouse gases and ozone-depleting substances to temperature trends in the stratosphere: A chemistry-climate model study, *Journal of Climate*, *23*, 28–42, doi:10.1175/2009JCLI2955.1, 2010.

Thompson, D. W. J., and S. Solomon, Understanding recent stratospheric climate change, *Journal of Climate*, *22*, 1934–1943, doi:10.1175/2008JCLI2482.1, 2009.

Thompson, D. W. J., and J. M. Wallace, The Arctic Oscillation signature in the wintertime geopotential height and temperature fields, *Geophysical Research Letters*, *25*(9), 1297–1300, 1998.

Thompson, D. W. J., and J. M. Wallace, Annular modes in the extratropical circulation. Part I: Month-to-month variability, *Journal of Climate*, *13*, 1000–1016, 2000.

Thompson, D. W. J., J. M. Wallace, and G. C. Hegerl, Annular modes in the extratropical circulation. Part II: Trends, *Journal of Climate*, *13*, 1018–1036, 2000.

Thompson, D. W. J., M. P. Baldwin, and J. M. Wallace, Stratospheric connection to northern hemisphere wintertime weather: Implications for prediction, *Journal of Climate*, *15*, 1421–1428, 2002.

Thompson, D. W. J., S. Lee, and M. P. Baldwin, Atmospheric processes governing the Northern hemisphere Annular Mode/North Atlantic Oscillation. In: Hurrell JW, Kushnir Y, Ottersen G, Visbeck M (eds) The North Atlantic Oscillation: climatic significance and environmental impact, *Geophysical Monograph*, *134*, 81–112, 2003.

Thompson, D. W. J., M. P. Baldwin, and S. Solomon, Stratosphere-troposphere coupling in the southern hemisphere, *Journal of Atmospheric Sciences*, *62*, 708–715, 2005.

Thorpe, A. J., Diagnosis of balanced vortex structure using potential vorticity, *Journal of the Atmospheric Sciences*, *42*(4), 397–406, 1985.

Thorpe, A. J., Synoptic scale disturbances with circular symmetry, *Monthly Weather Review*, *114*, 1384–1389, 1986.

Uppenbrink, J., The North Atlantic Oscillation, *Science*, *283*(5404), 948–949, 1999.

Visbeck, M. H., J. W. Hurrell, L. Polvani, and H. M. Cullen, The North Atlantic Oscillation: Past, present, and future, *Proceedings of the National Academy of Sciences of the USA*, *98*(23), 12,876–12,877, 2001.

Waugh, D. W., and W. J. Randel, Climatology of Arctic and Antarctic polar vortices using elliptical diagnostics, *Journal of Atmospheric Sciences*, *56*, 1594–1613, 1999.

Waugh, D. W., W. J. Randel, S. Pawson, P. A. Newman, and E. R. Nash, Persistence of the lower stratospheric polar vortices, *Journal of Geophysical Research*, *104*(D22), 27,191–27,201, 1999.

Wittman, M. A. H., A. J. Charlton, and L. M. Polvani, The effect of lower stratospheric shear on baroclinic instability, *Journal of Atmospheric Sciences*, *64*, 479–496, doi:10.1175/JAS3828.1, 2007.

Yoden, S., T. Yamaga, S. Pawson, and U. Langematz, A composite analysis of the stratospheric sudden warmings simulated in a perpetual January integration of the Berlin TSM GCM, *Journal of the Meteorological Society of Japan*, *77*(2), 431–445, 1999.

Zhou, S., M. E. Gelman, A. J. Miller, and J. P. McCormack, An inter-hemisphere comparison of the persistent stratospheric polar vortex, *Geophysical Research Letters*, *27*(8), 1123–1126, 2000.

Bedankt - Thank you

Op deze plek wil ik de mensen bedanken die elk op hun eigen manier een bijdrage hebben geleverd aan het totstandkomen van dit proefschrift.

Allereerst mijn begeleiders Aarnout en Theo, die me de kans hebben gegeven dit onderzoek te doen. Bedankt voor jullie geduld en het blijven stimuleren om mijn eigen weg te zoeken in het stratosferische onderzoek. Daarnaast wil ik Wouter de Geus bedanken voor zijn voorbereidende werk tijdens zijn masteronderzoek.

Alle collega's op het IMAU hebben er voor gezorgd dat het IMAU een fijne plek was om te werken de afgelopen vier jaar. Bedankt voor de gezelligheid tijdens de thee en lunch pauzes en alle hulp bij onderzoeks-, data, computer en administratieve zaken. Erik, bedankt voor je gezelligheid als kamergenoot en voor het luisteren naar alles wat ik kwijt wou. Christiana, thank you for your company during the last year, when you joined our room. Verder wil ik mijn tijdelijke kamergenoten Selma, Leela, Dewi en Matthijs bedanken: ik had niet verwacht dat het tijdens de verbouwing van het IMAU zo gezellig zou zijn!

Ook buiten het werk was het vaak erg gezellig met collega's. Willem Jan, Jojanneke, Erik, Petra, Guy en Arjen bedankt voor de leuke etentjes, verjaardagen en spelletjesavonden. Petra, bedankt voor je vriendschap en je hulp als ik iets wilde weten over proefschriften of promoveren, je bent een gezellige onderbuurvrouw in de torenflat in Zeist!

Het was ook altijd fijn om even bij te kletsen met mijn studiegenoten. Bas, Niels, Arjan, naast studiegenoten inmiddels ook collega's, bedankt voor jullie gezelschap op het IMAU, KNMI en daarbuiten. Paulien, Marijke en Tineke, de meiden-uitjes blijven gezellig!

Als het even niet zo lukt met je onderzoek is het fijn om afleiding te hebben, en die vond ik volop bij de Wageningse musical vereniging Sempre Sereno in de vorm van repetities, kroegavondjes, verjaardagen, uitstapjes en voorstellingsweken. Iedereen van Sempre heel erg bedankt voor de heerlijke tijd die ik bij jullie heb! Ook wil ik Roeland, Janneke en Jelle bedanken voor twee jaar dansen op vrijdagavond.

Janna, ook al wonen we niet meer in dezelfde plaats en gaan we niet meer naar dezelfde school, onze levens blijven elkaar raken, ook nu we allebei met ons promotieonderzoek bezig zijn. Ik ben blij dat we nog steeds vriendinnen zijn!

Een bijzonder groot dankjewel gaat naar mijn familie, die er altijd voor me zijn. Papa, mama, Suz, Lotje, Sander en Irene, bedankt voor jullie liefde, gezelschap, knuffels, interesse, steun, wijze woorden, filmavondjes, dierentuinbezoekjes, spelletjes boonanza, musicalbezoeken en andere uitstapjes!

Tenslotte bedankt aan alle collega's buiten het IMAU die ik de afgelopen jaren ben tegengekomen. Bedankt voor de fijne uren op en buiten het KNMI, Wim, Alwin, Otto, Hylke en de rest van de dynamische meteorologie seminaria groep, ik vond het leuk deel uit te maken van deze seminaria op het KNMI. Peter Siegmund bedankt voor je interesse en samenwerking het afgelopen jaar.

I would like to thank everyone that I met at conferences and during my visits to England for making these times very worthwhile, in a scientific as well as in a social way. Thank you for letting me be a part of a great stratospheric scientific community.

This thesis would not have been the same without the collaboration with the University of Reading. Thank you for many interesting, inspiring and friendly hours and emails Maarten Ambaum, Dann, Amanda, Andrew, Lesley and others at the University of Reading that I met during the last years.

A special thanks is for Christopher Bell, from the University of Reading. Thank you for your kindness, your enthusiasm, interest and nice conversations about the stratosphere. It was always a pleasure to be in your company. I'm very glad that our paths crossed, and very sad that this was only meant to last for three years. Unfortunately the two-way interaction between Heaven and Earth is not as strong as between the stratosphere and troposphere. Thank you Chris, for being such a nice colleague and friend!

- - - ⋆ - - -

It well may be, that we will never meet again in this lifetime,
so let me say before we part:
so much of me is made of what I learned from you,
you'll be with me, like a handprint on my heart,
and now whatever way our stories end,
I know you have rewritten mine
by being my friend.
(Stephen Schwartz - Wicked)

- - - ⋆ - - -

Curriculum Vitae

- ⋆ -

Yvonne Hinssen werd geboren op 17 september 1983 in Wageningen, waar ze ook opgroeide. In 2001 behaalde ze haar VWO diploma aan het Pantarijn in Wageningen. In datzelfde jaar begon ze aan de opleiding 'Meteorologie en Fysische Oceanografie' aan de Universiteit Utrecht. Van september 2005 tot juni 2006 deed Yvonne haar afstudeeronderzoek bij Wouter Knap op het Koninklijk Nederlands Meteorologisch Instituut (KNMI) in De Bilt. Tijdens dit onderzoek zijn verschillende methoden voor de bepaling van zonneschijnduur uit stralingsmetingen vergeleken. In juni 2006 studeerde Yvonne cum laude af en in september startte ze haar promotieonderzoek bij het Instituut voor Marien en Atmosferisch onderzoek Utrecht (IMAU). Onder begeleiding van Aarnout van Delden en Theo Opsteegh zijn de globale circulatie in de stratosfeer en de koppeling tussen de stratosfeer en de onderliggende troposfeer bestudeerd. De resultaten hiervan zijn in dit proefschrift beschreven.

Yvonne Hinssen was born on 17 September 1983 in Wageningen, the Netherlands. After spending her youth in Wageningen, she graduated from the VWO at the Pantarijn in Wageningen in 2001. That same year she started to study 'Meteorology and Physical Oceanography' at Utrecht University. Between September 2005 and June 2006 she did her master research with Wouter Knap at the Royal Netherlands Meteorological Institute (KNMI) in De Bilt. In this research, different methods for the determination of sunshine duration from radiation measurements were compared. Yvonne graduated in June 2006 (cum laude), and continued her atmospheric studies with a PhD project at the Institute for Marine and Atmospheric research Utrecht (IMAU) in September 2006. Under the supervision of Aarnout van Delden and Theo Opsteegh, she studied the global circulation in the stratosphere and the coupling between the stratosphere and the underlying troposphere. The obtained results are described in this thesis.

Publications

- ⋆ -

Hinssen, Y. B. L. and W. H. Knap, Comparison of pyranometric and pyrheliometric methods for the determination of sunshine duration, *Journal of Atmospheric and Oceanic Technology*, *24*(5), 835-846, 2007.

Hinssen, Y., A. van Delden, T. Opsteegh, and W. de Geus, Stratospheric impact on tropospheric winds deduced from potential vorticity inversion in relation to the Arctic Oscillation, *Quarterly Journal of the Royal Meteorological Society*, *136*, 20-29, doi:10.1002/qj.542, 2010.

Hinssen, Y., A. van Delden, T. Opsteegh, and W. de Geus, Notes and Correspondence Correction to: 'Stratospheric impact on tropospheric winds deduced from potential vorticity inversion in relation to the Arctic Oscillation' by Yvonne Hinssen, Aarnout van Delden, Theo Opsteegh and Wouter de Geus, *Quarterly Journal of the Royal Meteorological Society*, *In press*, doi:10.1002/qj.716, 2010.

Hinssen, Y., A. van Delden, and T. Opsteegh, The seasonal cycle of the potential vorticity distribution in the stratosphere, *Submitted to Quarterly Journal of the Royal Meteorological Society*, 2010.

Hinssen, Y. B. L. and M. H. P. Ambaum, Relation between the 100 hPa heat flux and stratospheric potential vorticity, *Journal of the Atmospheric Sciences*, *In press*, doi:10.1175/2010JAS3569.1, 2010.

Hinssen, Y., A. van Delden, and T. Opsteegh, Influence of sudden stratospheric warmings on tropospheric winds, *Submitted to Meteorologische Zeitschrift*, 2010.

Hinssen, Y. B. L., C. J. Bell, and P. C. Siegmund, The influence of the stratosphere on the tropospheric zonal wind response to CO_2 doubling, *Submitted to Atmospheric Chemistry and Physics*, 2010.
Published online in *Atmospheric Chemistry and Physics Discussions*, 10, 23895-23925, doi:10.5194/acpd-10-23895-2010.